Techniques and Applications of X-ray Fluorescence Microscopy in Environmental Science

Ryan Tappero

National Synchrotron Light Source-II (NSLS-II)

New York, USA

Outline

- Synchrotrons at Brookhaven National Lab
  - NSLS stats
  - NSLS-II machine status and performance
- X-ray Interactions with Matter (Image contrast mechanisms)
  - Absorption-, Fluorescence-, Diffraction-, Phase-contrast
- X-ray Fluorescence Microscopes
  - Techniques (XRF, XAS, XRD, fCMT)
  - ZP vs. KB (imaging vs. spectroscopy)
- Environmental Science Examples
- Summary

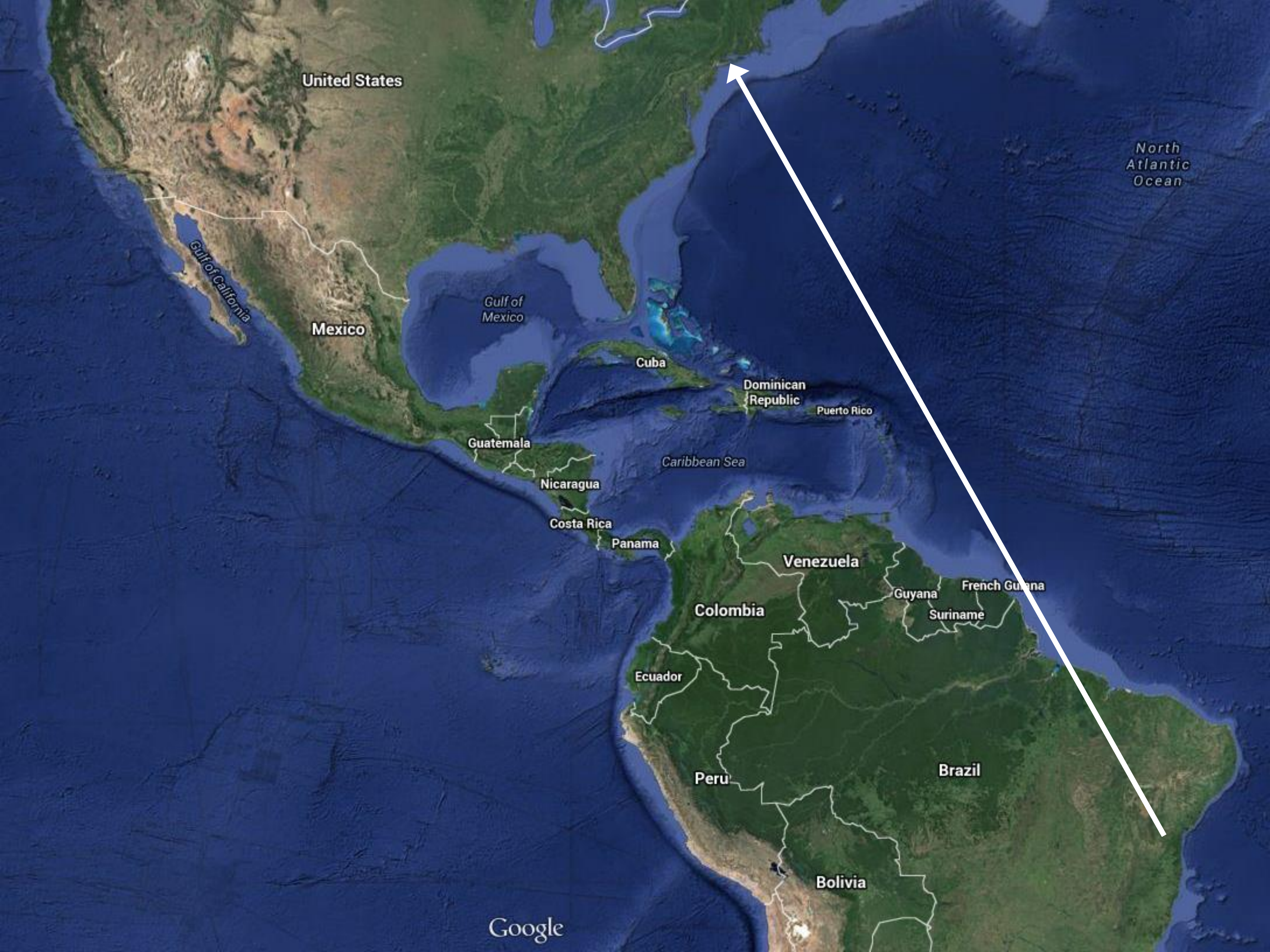
United States
North Atlantic Ocean
Gulf of California
Gulf of Mexico
Mexico
Cuba
Dominican Republic
Puerto Rico
Guatemala
Caribbean Sea
Nicaragua
Costa Rica
Panama
Venezuela
French Guiana
Guyana
Suriname
Colombia
Ecuador
Brazil
Peru
Bolivia
Google

Brookhaven National Lab

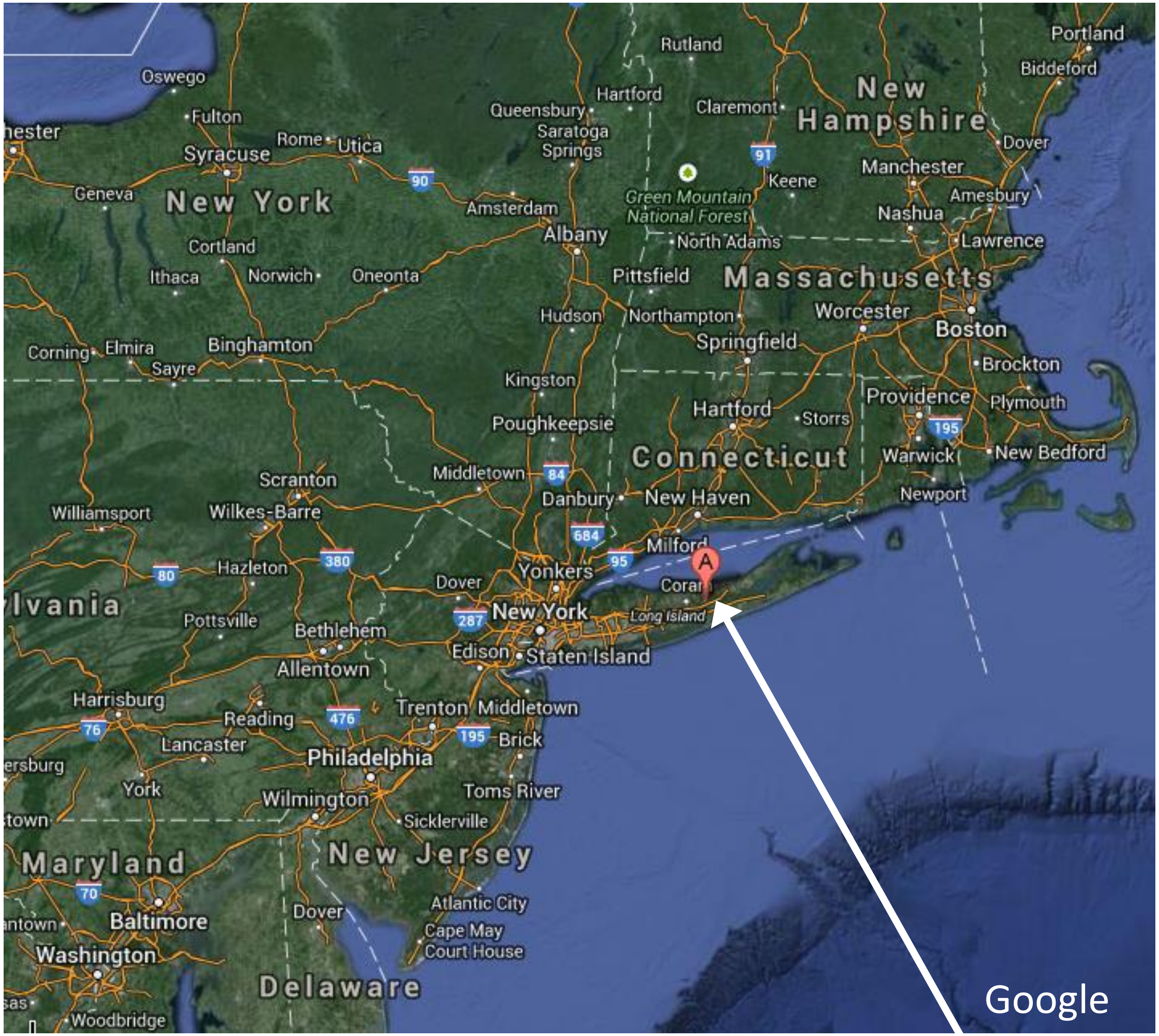

Brookhaven National Lab

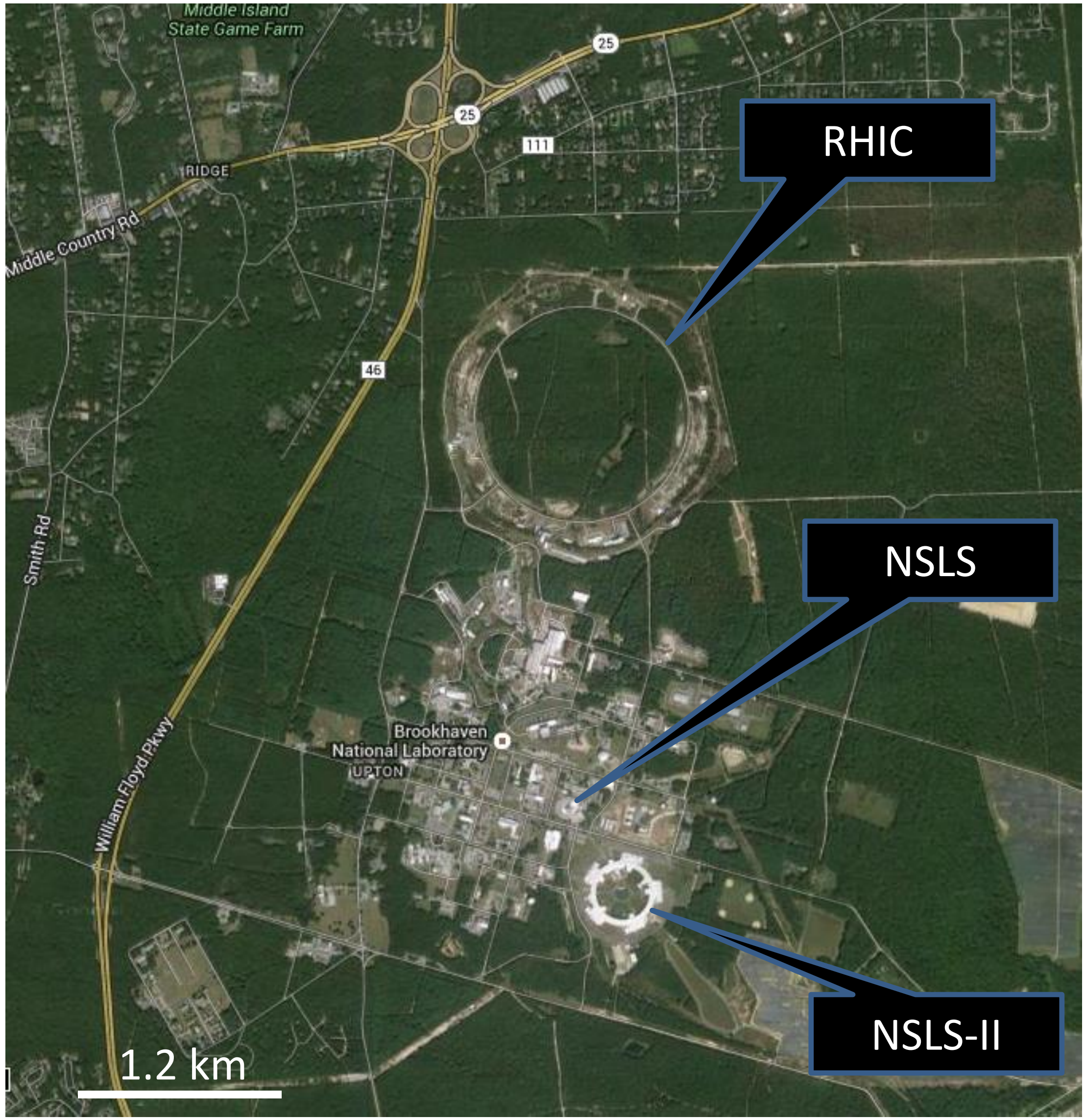

Brookhaven National Lab

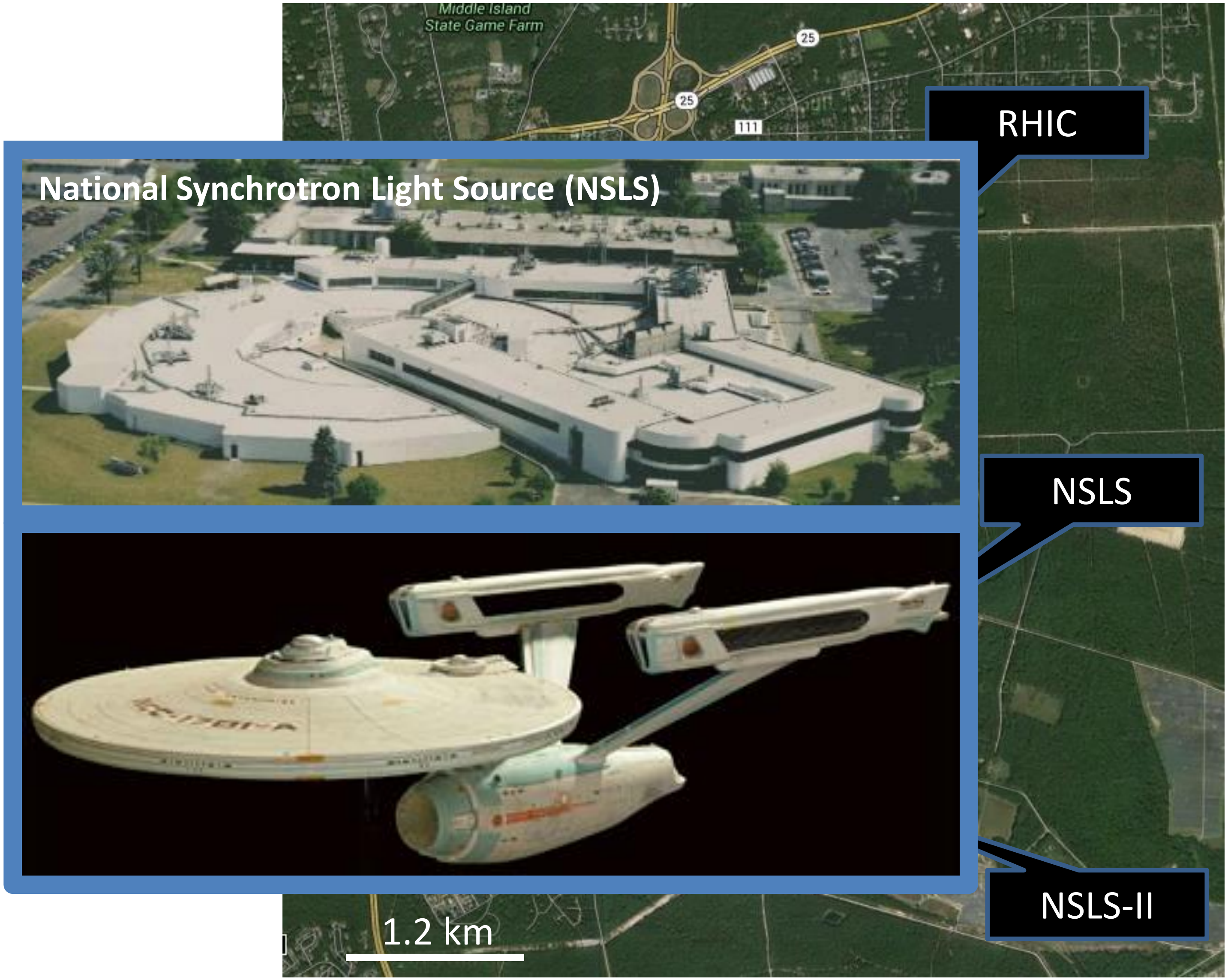

NSLS in Its Final Year of Operation as an Outstanding Scientific User Facility

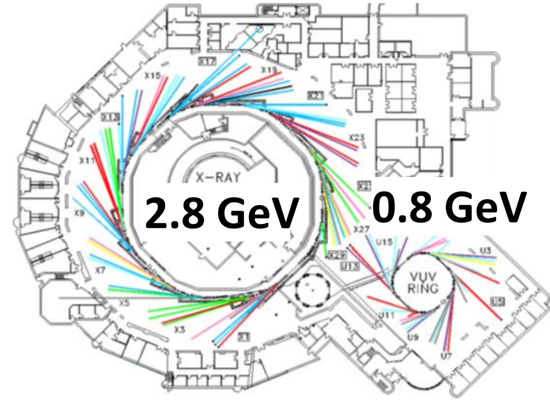

59 Beamlines

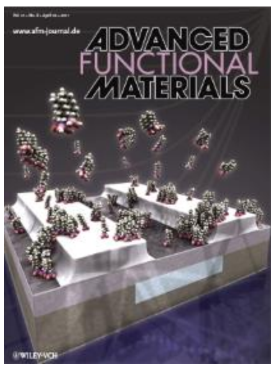

- **NSLS Tradition and Strengths:**
  Broad range of science programs
  Diverse capabilities over broad spectral range
  Highly engaged and productive user community
- **Highly Productive & High Impact**

	FY13	Since 1982
• Users	2,367	~ 57,000
• Publications	881	17,182
• Protein Databank Deposits	~ 600	7,122

  - 2 Nobel Prizes (2003, 2009)
- **Crucial Resource**
  - Universities: SBU, Columbia, MIT, Yale, Rutgers, ...
  - Industry: IBM, ExxonMobil, GE, Pharmaceuticals, ...
  - BNL: CFN, CMP, Catalysis, Struct Bio, Env Sci, ...
- **NSLS ceased ops on Sep 30, 2014**

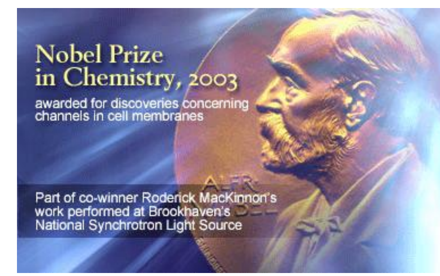

NSLS-II Project

Accelerator Systems
- Storage Ring (~ ½ mile in circumference)
- Linac and Booster Top-Off Injection System

Conventional Facilities
- Ring Building/Exp. floor (400,000 gsf)
- 5 Laboratory/Office Bldgs designed to promote interaction & collaboration among staff & users (190,000 gsf)

Experimental Facilities
- Initial suite of 6 insertion device beamlines
- Capable of hosting ~60 beamlines

Research and Developments
- High-resolution crystal optics, nano-focusing and nanopositioning, detectors developments

NSLS-II Project "Completion" Mar 2015

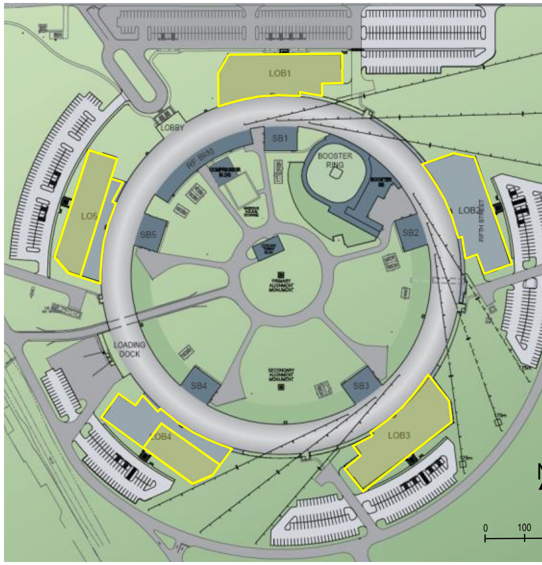

Electron storage ring at NSLS- II

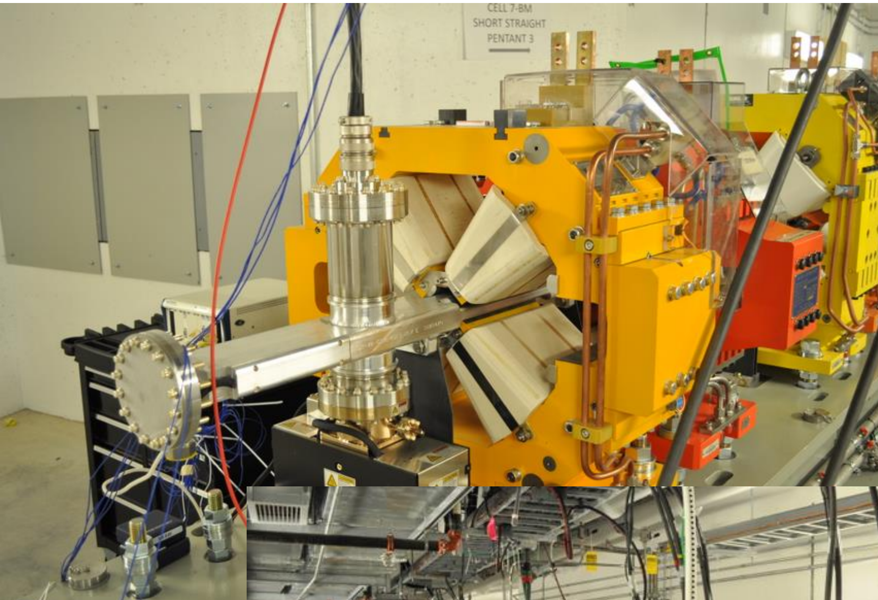

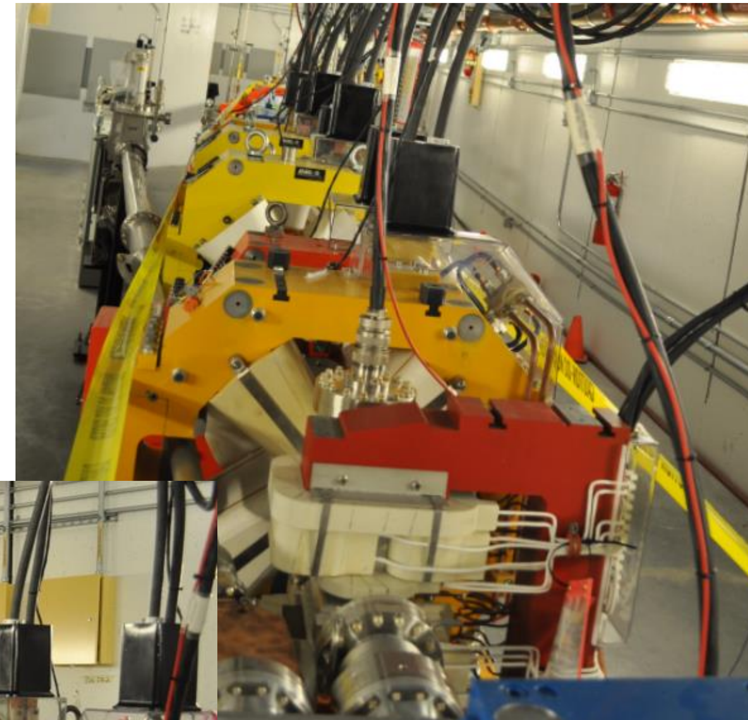

Magnet structure at NSLS-II

DBA= double-bend achromat

Particle accelerator from IKEA

Only available in Double-Bend Achromat (DBA)!

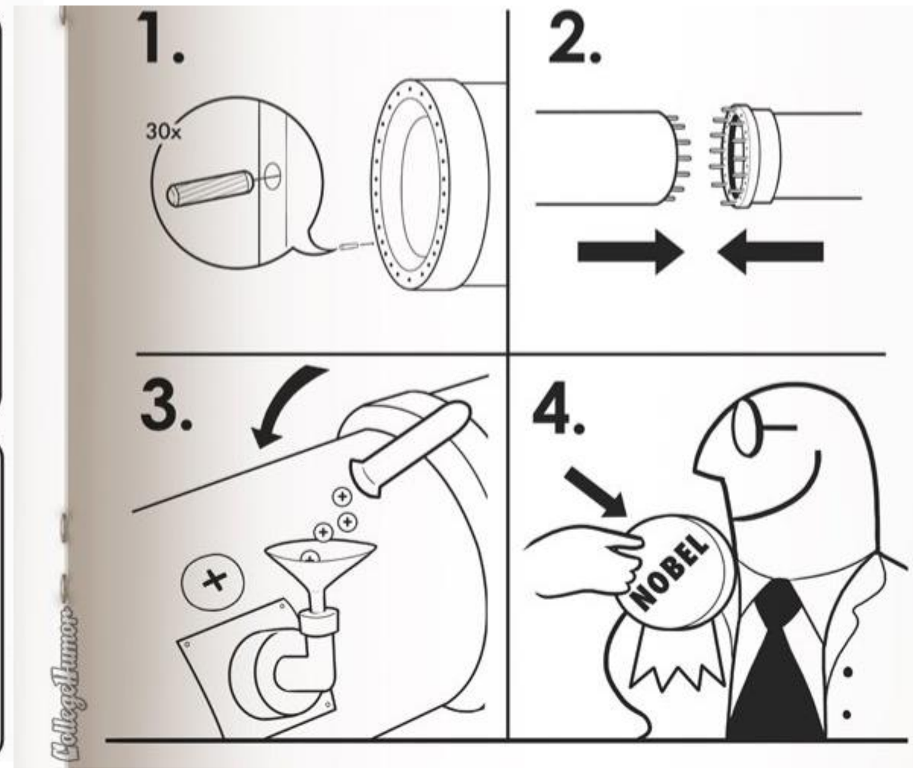

NSLS- II Accelerator Commissioning

- NSLS-II Accelerator Systems have provided >1500 hours of SR operations in FY15.
- All project BL IDs commissioned and front-ends are conditioned for 150 mA operations
- Stored 250 mA

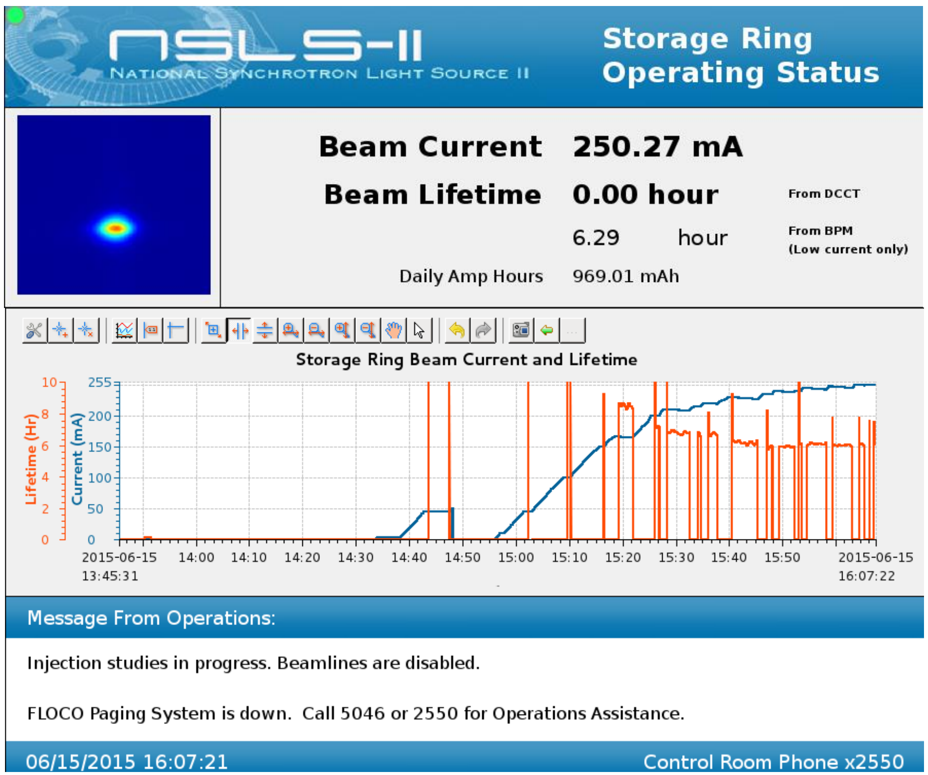

- **Stability**: Met specification:
  < 10% of source size in vertical and horizontal

- **Emittance**: Met specification
  1 nm-rad horiz
  0.006 nm-rad vert

after John Hill, NSLS-II director

CHX Beamline Commissioning

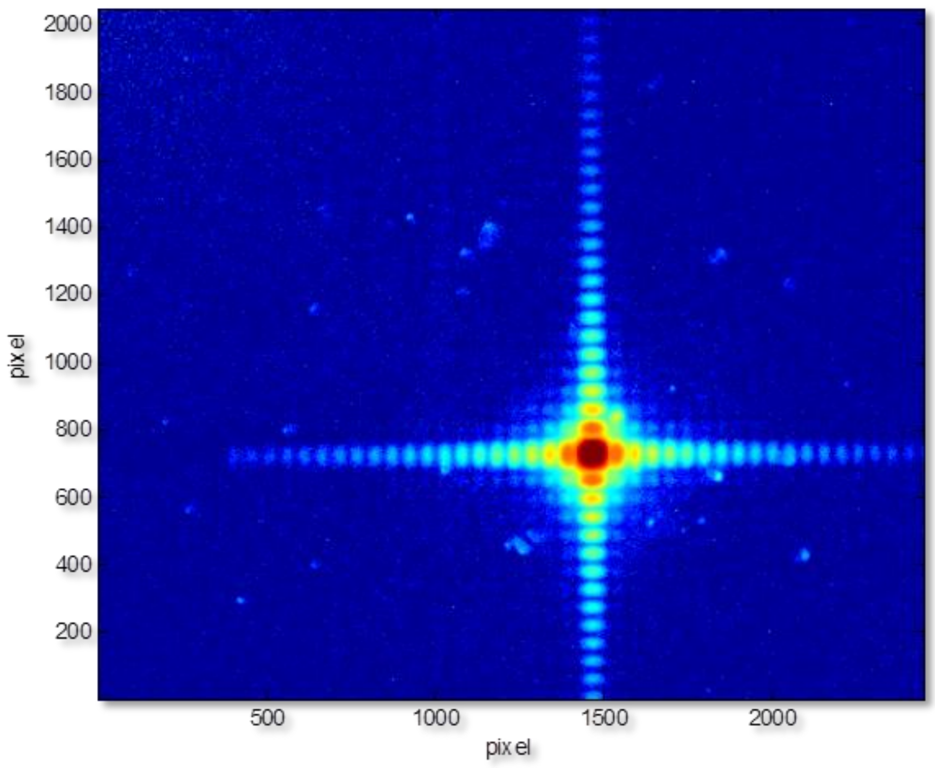

Diffraction pattern from a 20 μm square slit illustrating high **coherence in both directions**

after John Hill, NSLS-II director

Imaging data from the HXN beamline

aka “Yong’s golden donuts”

SEM image of test pattern

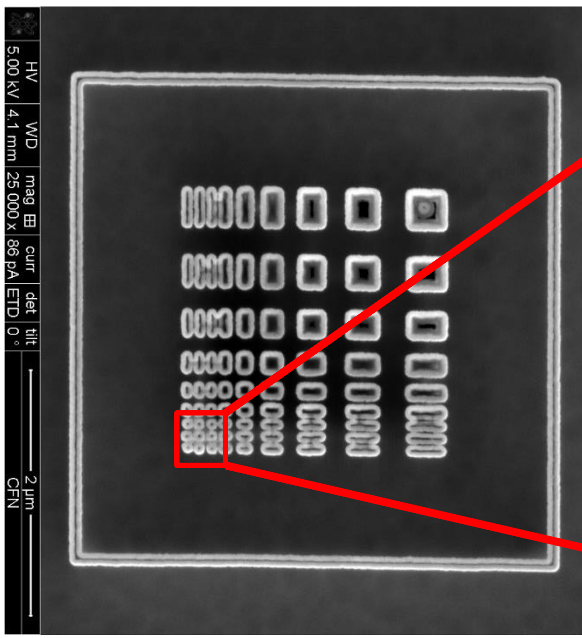

X-ray image from HXN

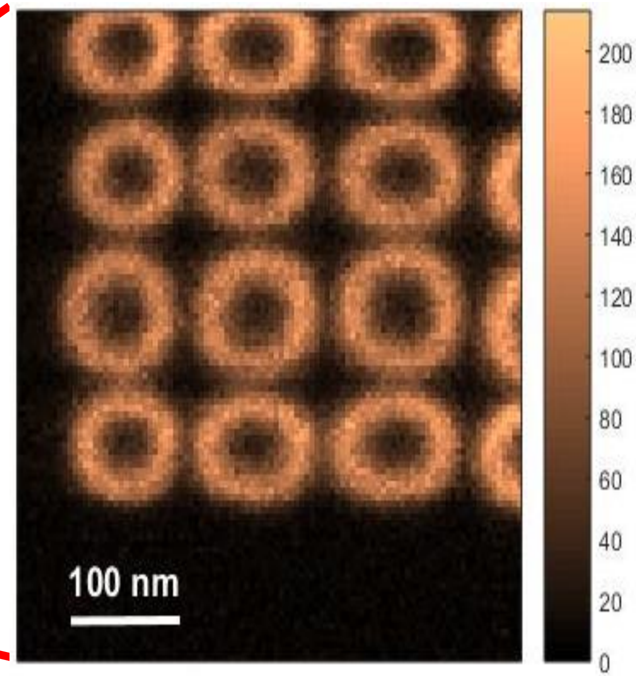

12 keV @ 50 mA current

Pt XRF fly-scan: 5nm/pixel

Dwell time: 0.5s/pixel

Data taken 4/25/15 using “fly scan” mode

~ 15 x 15 nm resolution

after John Hill, NSLS-II director

Imaging at ~15 nm resolution

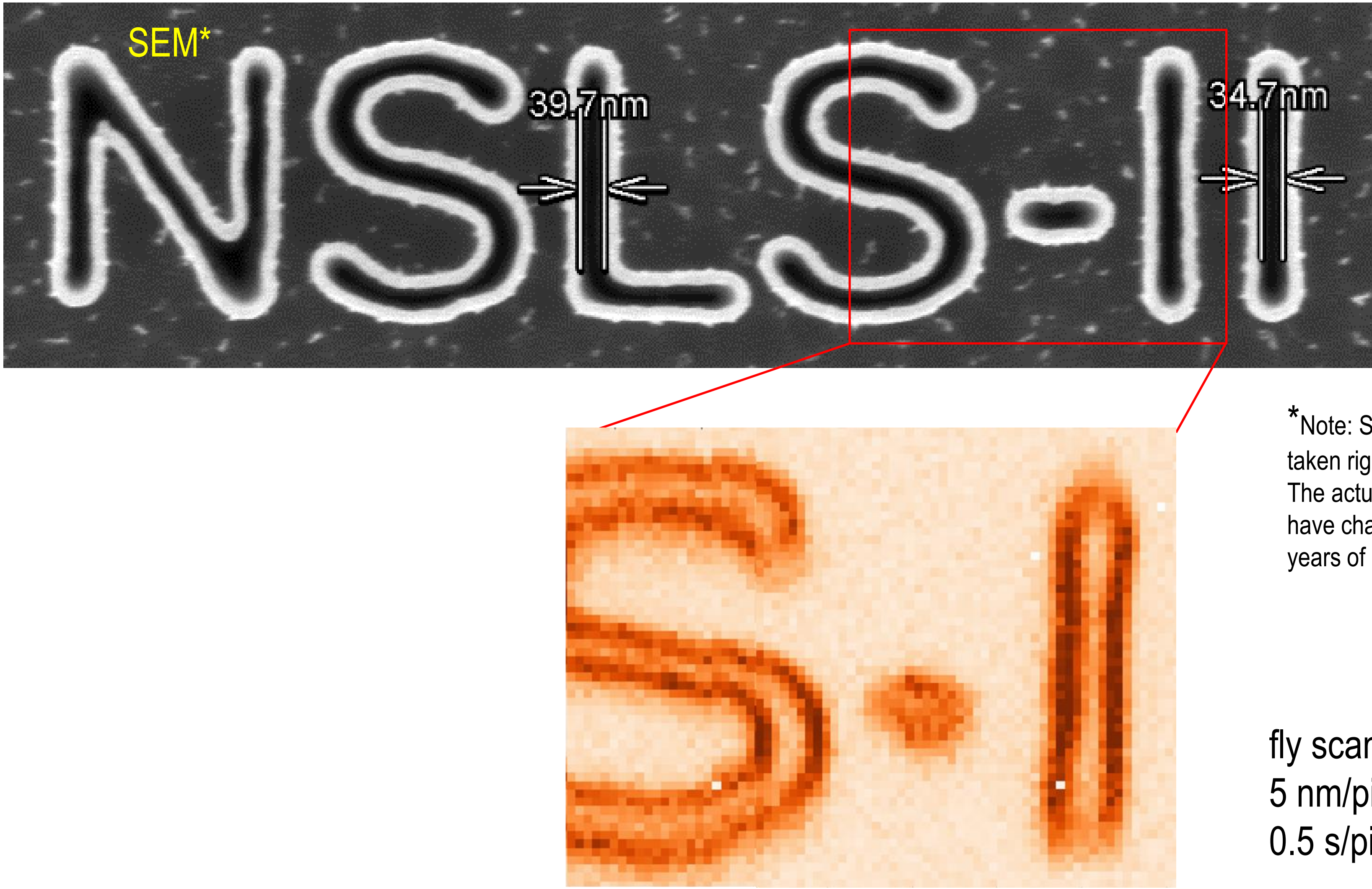

*Note: SEM image was taken right after synthesis. The actual structure may have changed after ~5 years of use

fly scan
5 nm/pixel
0.5 s/pixel

after John Hill, NSLS-II director

First Publication from NSLS-II

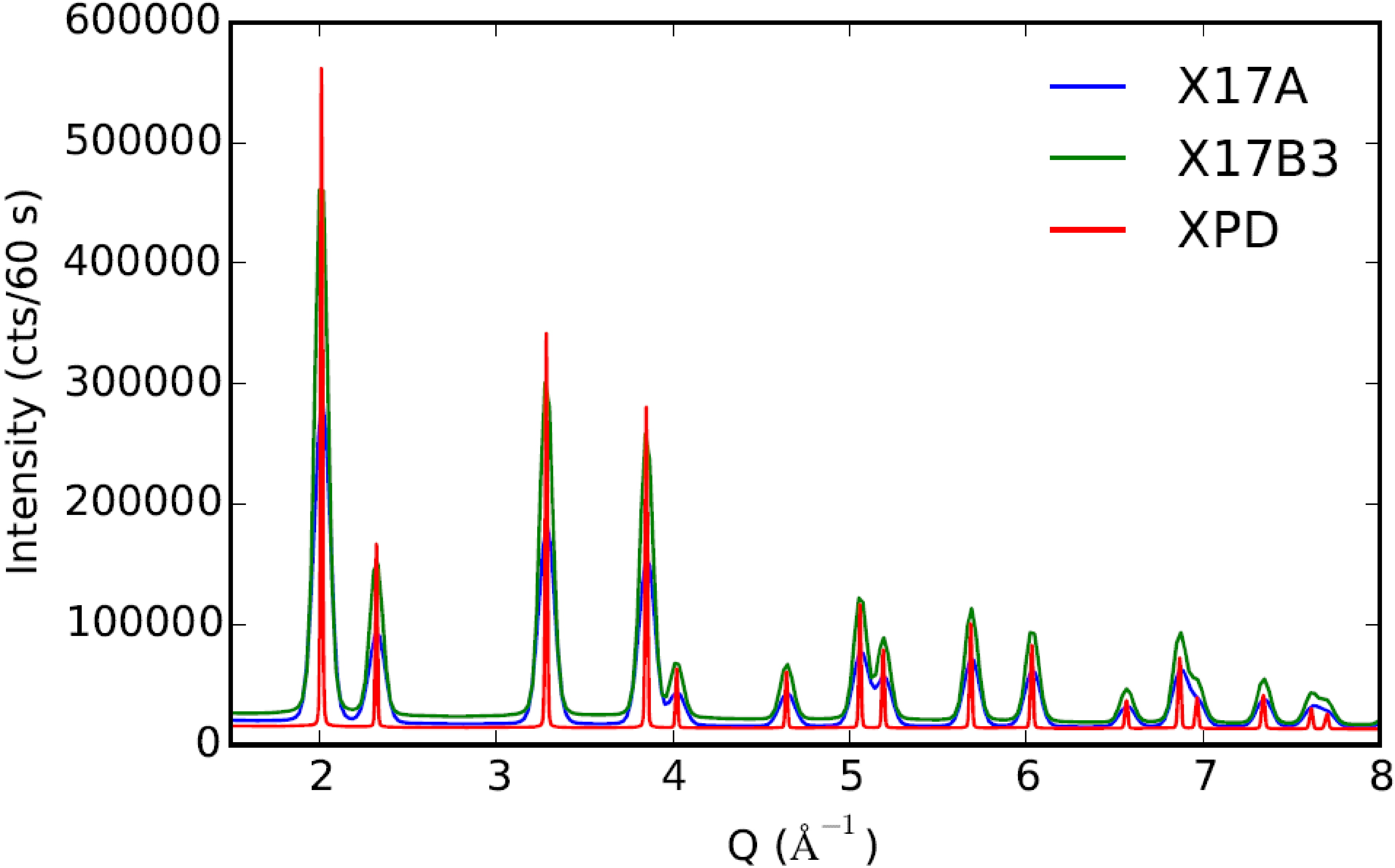

X-rays: Interaction with matter

Absorption

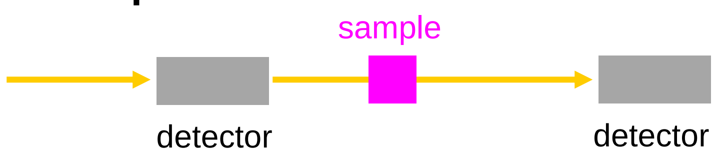

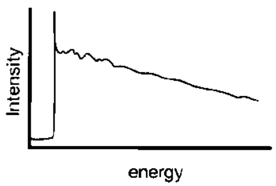

Scattering

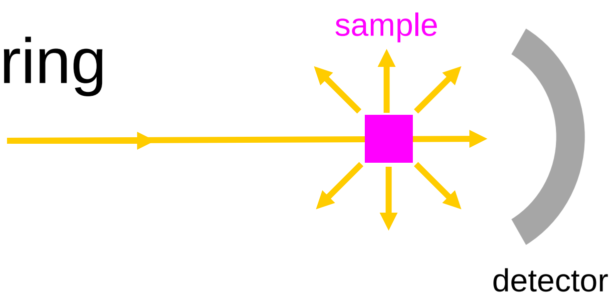

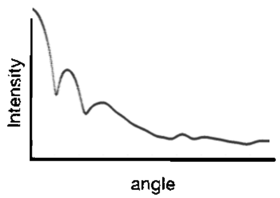

Diffraction

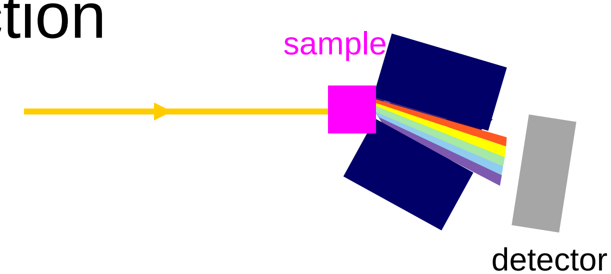

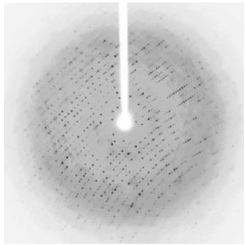

Photoabsorption

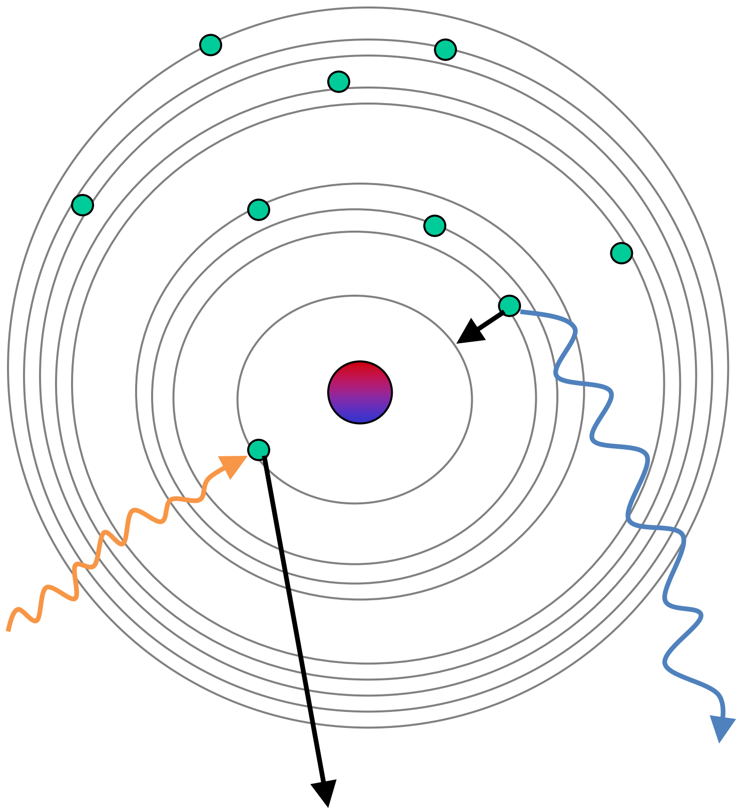

- A source X-ray strikes an inner shell electron. If at high enough energy (above *absorption edge* of element), the e^- is ejected from the atom
- Higher energy electrons cascade to fill vacancy
- Giving off characteristic fluorescent X-rays
- Characteristic X-ray: **Each element has it's own "color"!**

Anatomy of an EDX spectrum

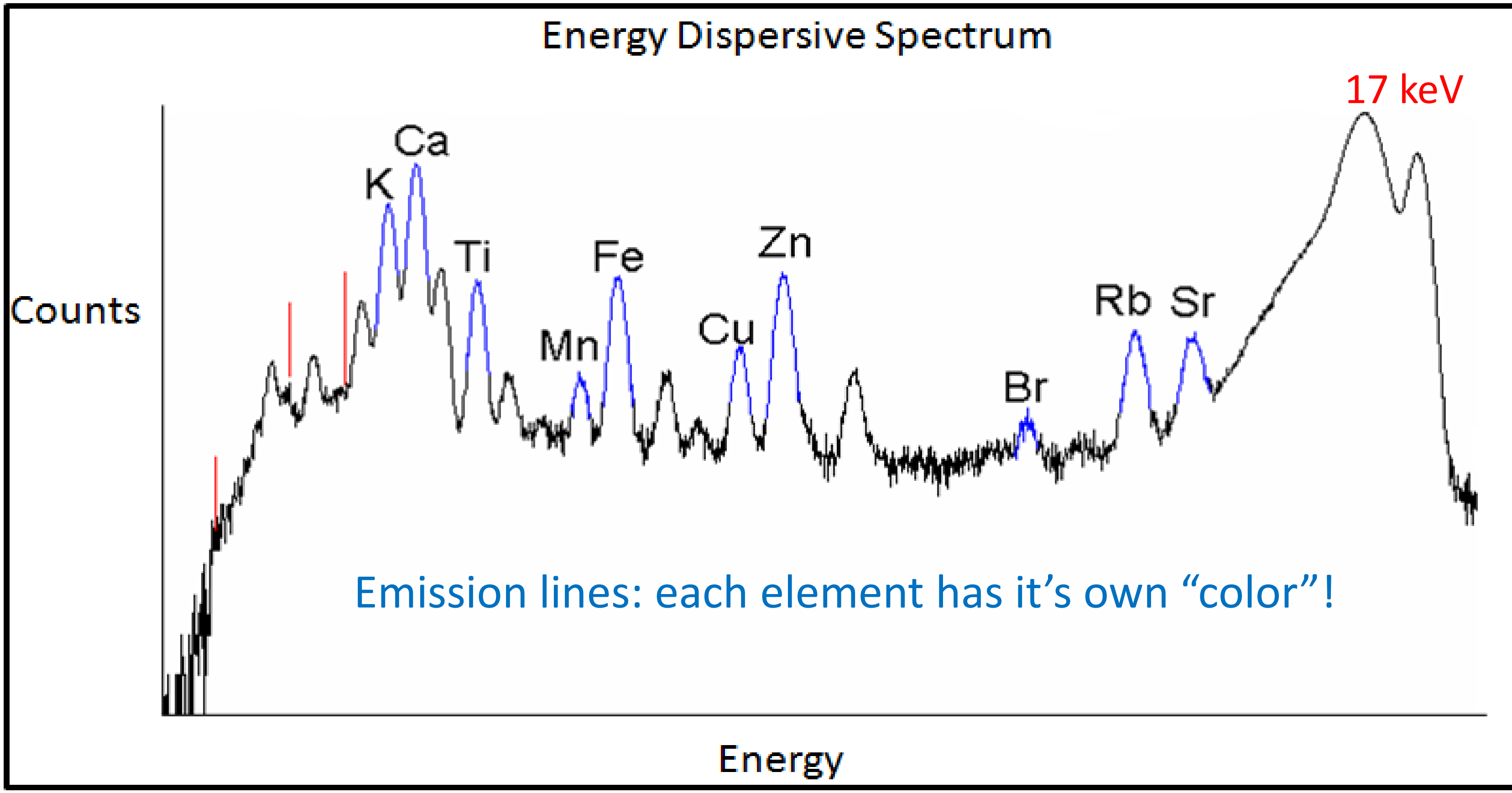

Spot XRF analysis of tumeric powder at 17 keV

Imaging or Chemical Imaging?

Dark=high absorption
Light=low absorption

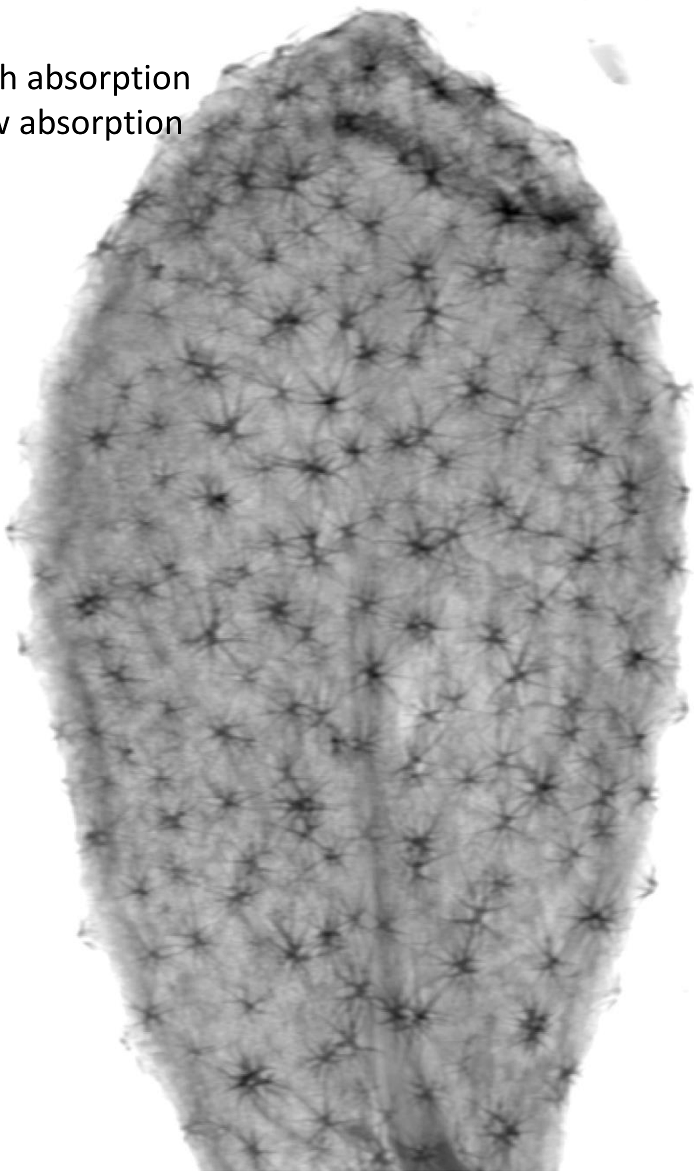

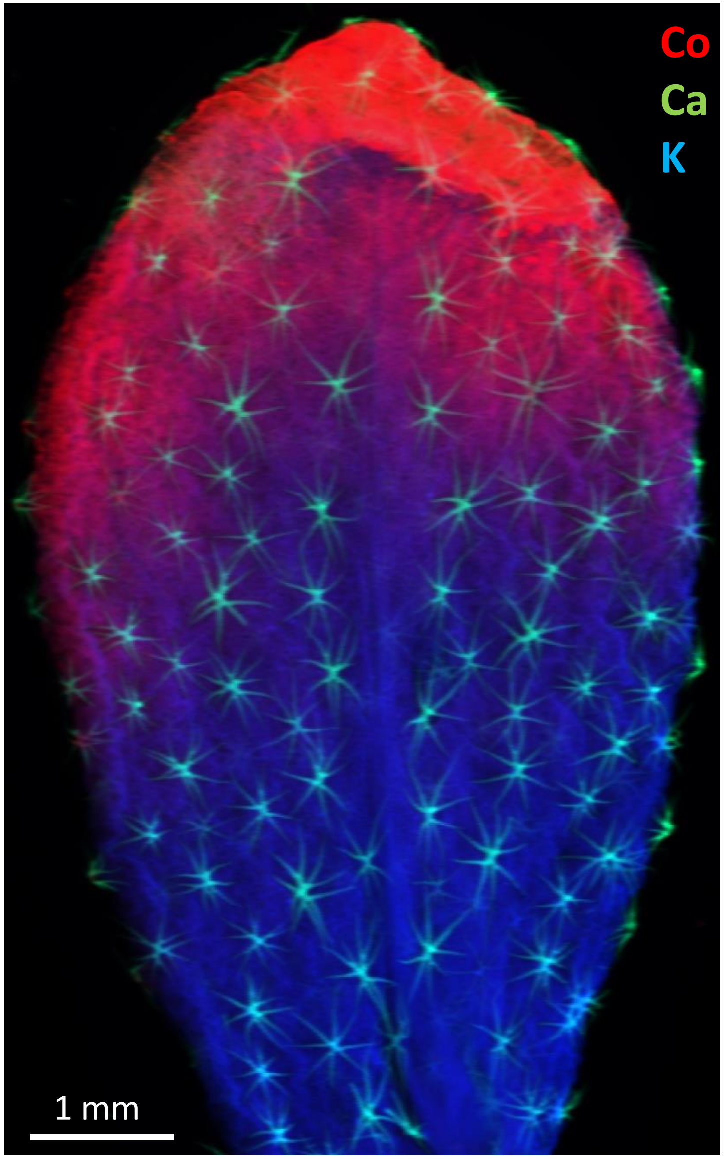

Spectroscopic "Chemical" Imaging

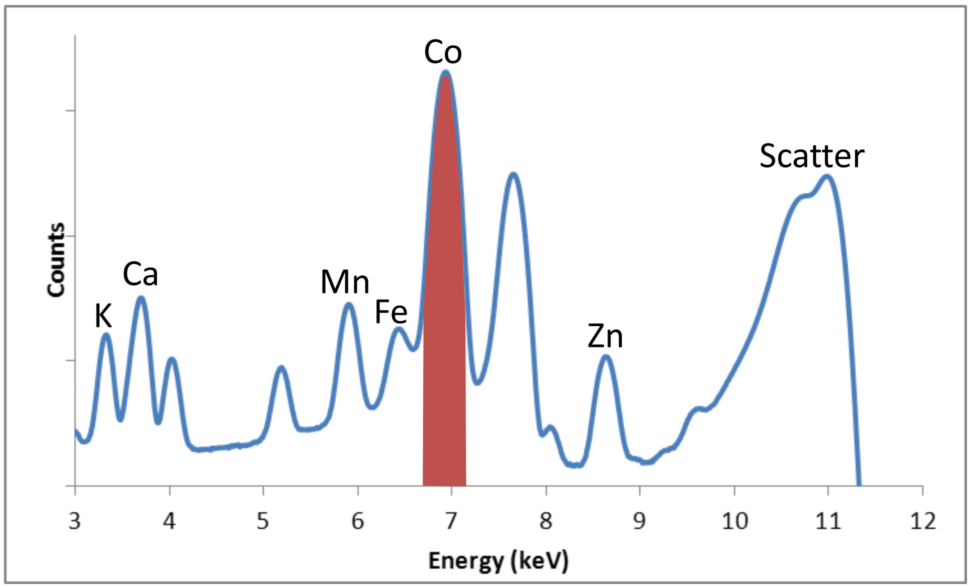

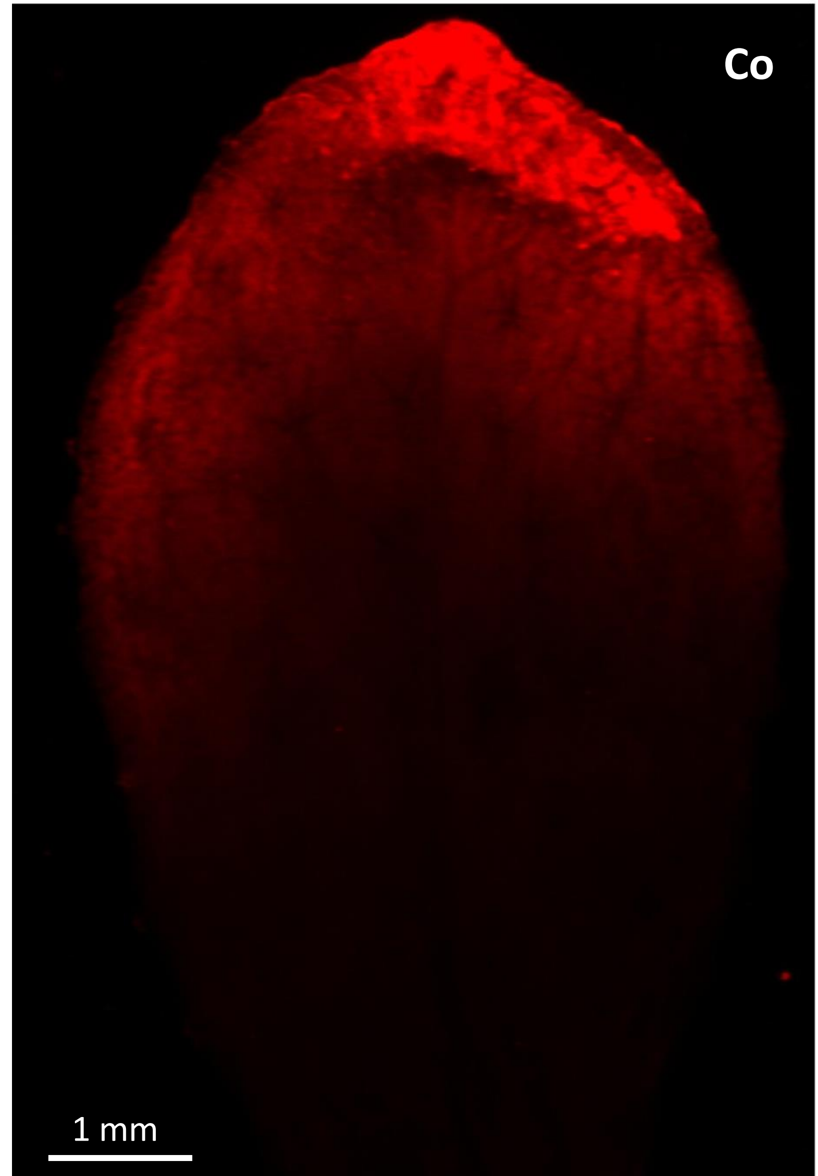

Spectroscopic “Chemical” Imaging

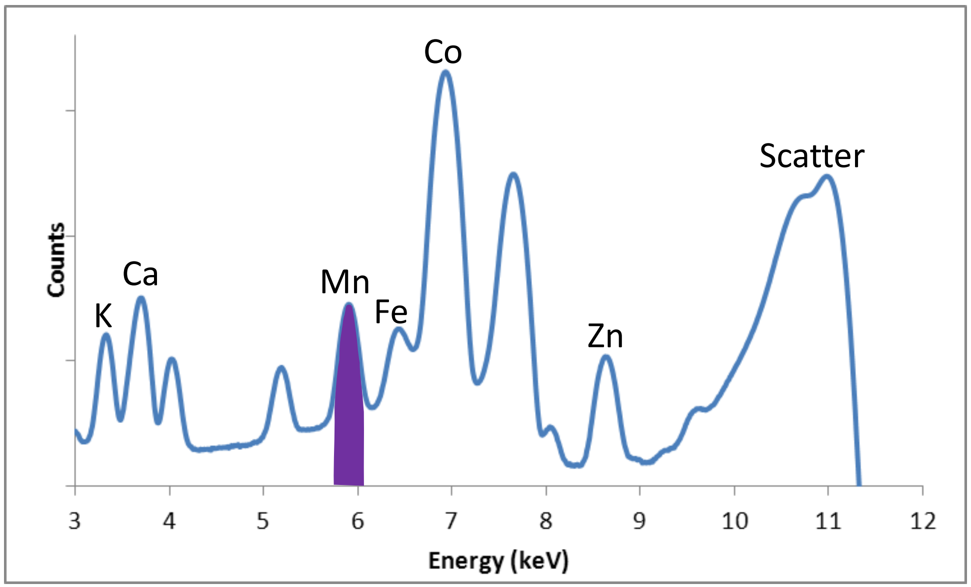

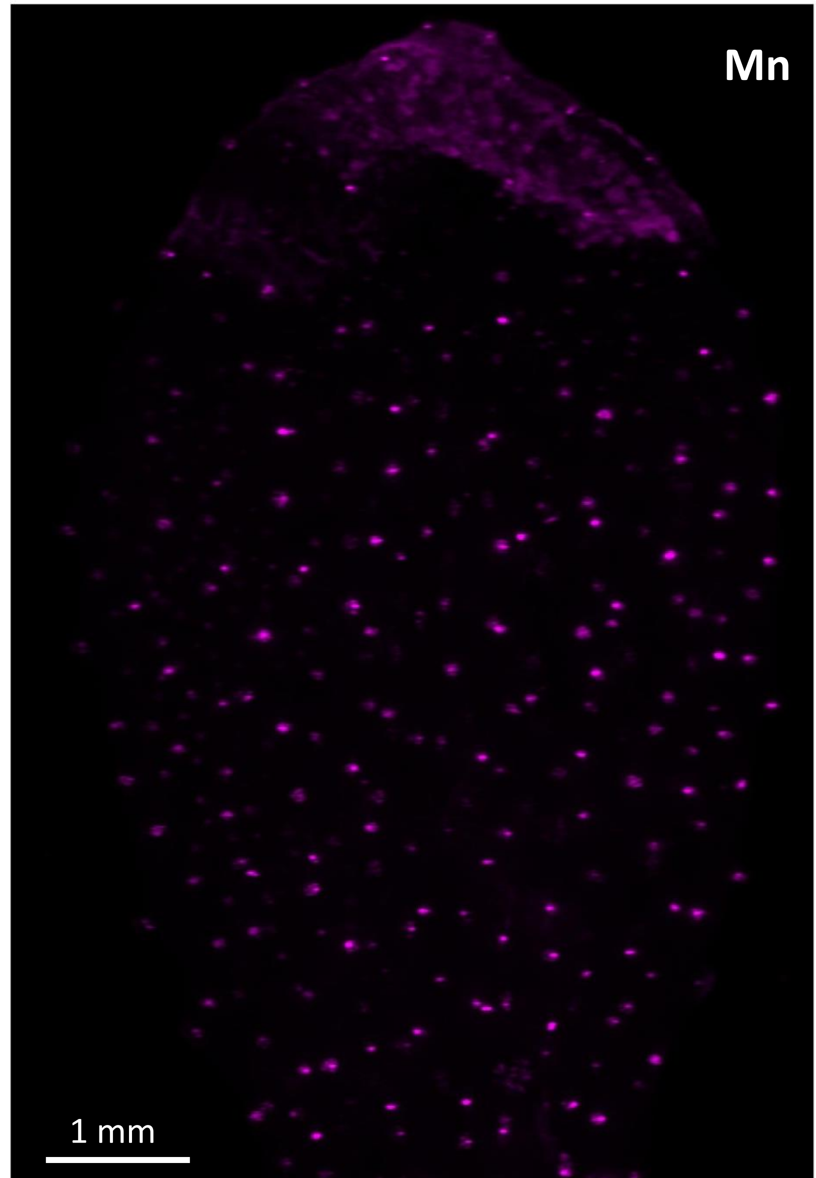

Spectroscopic “Chemical” Imaging

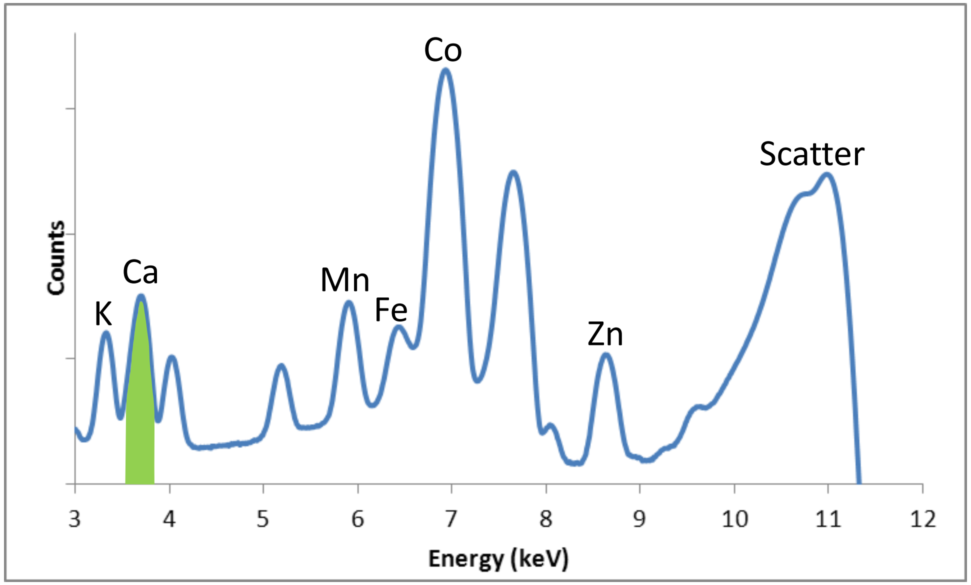

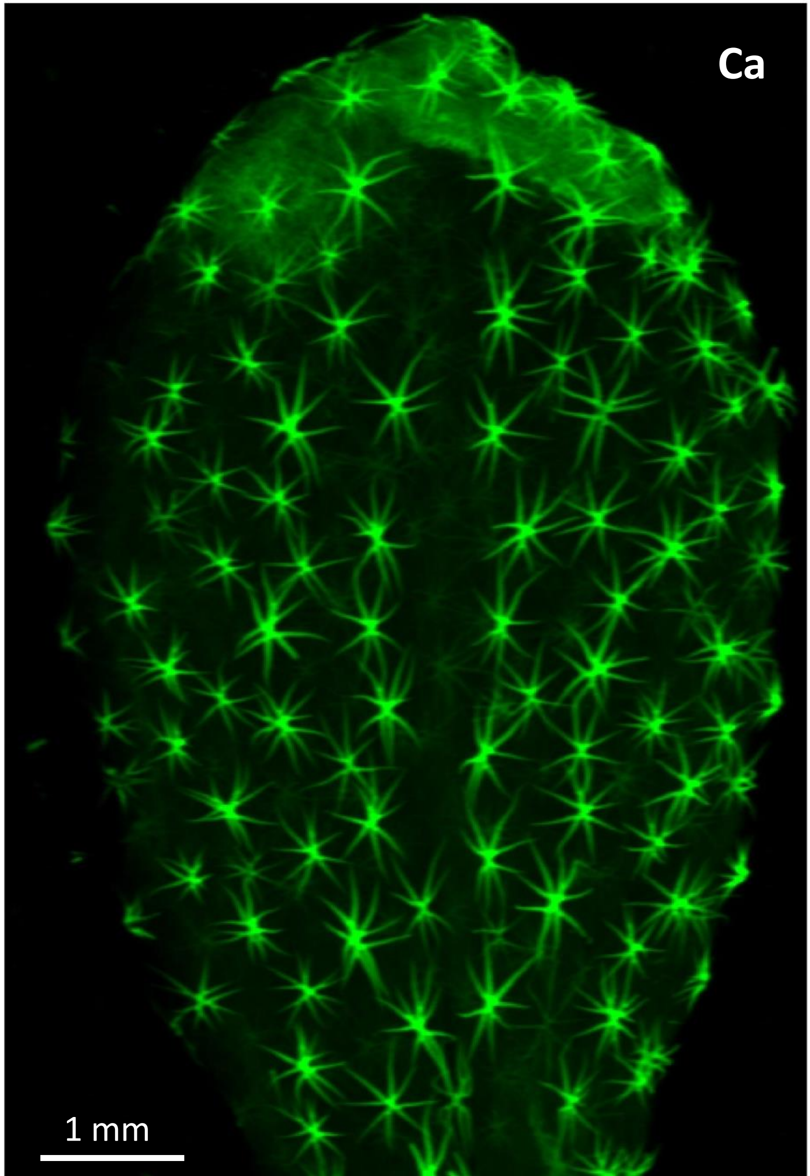

Spectroscopic "Chemical" Imaging

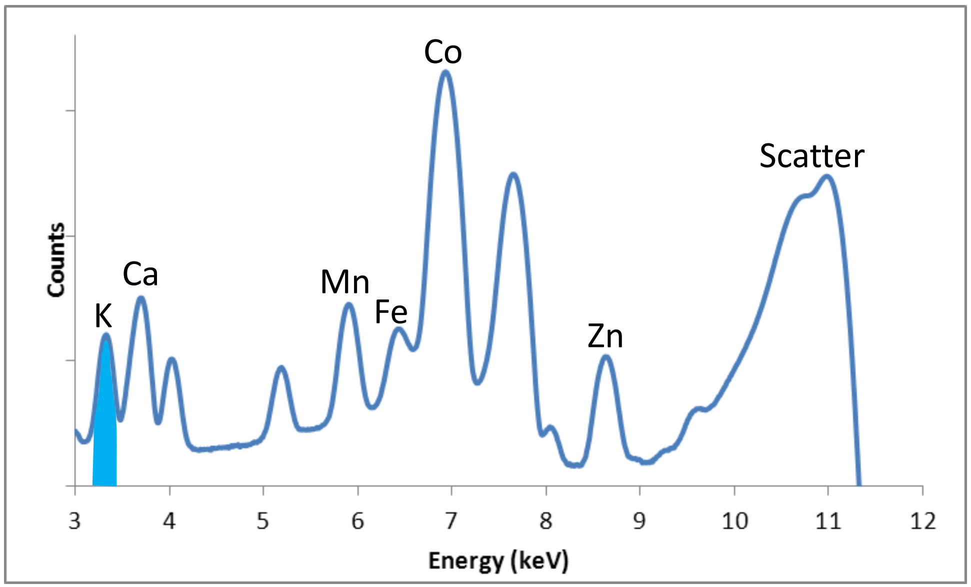

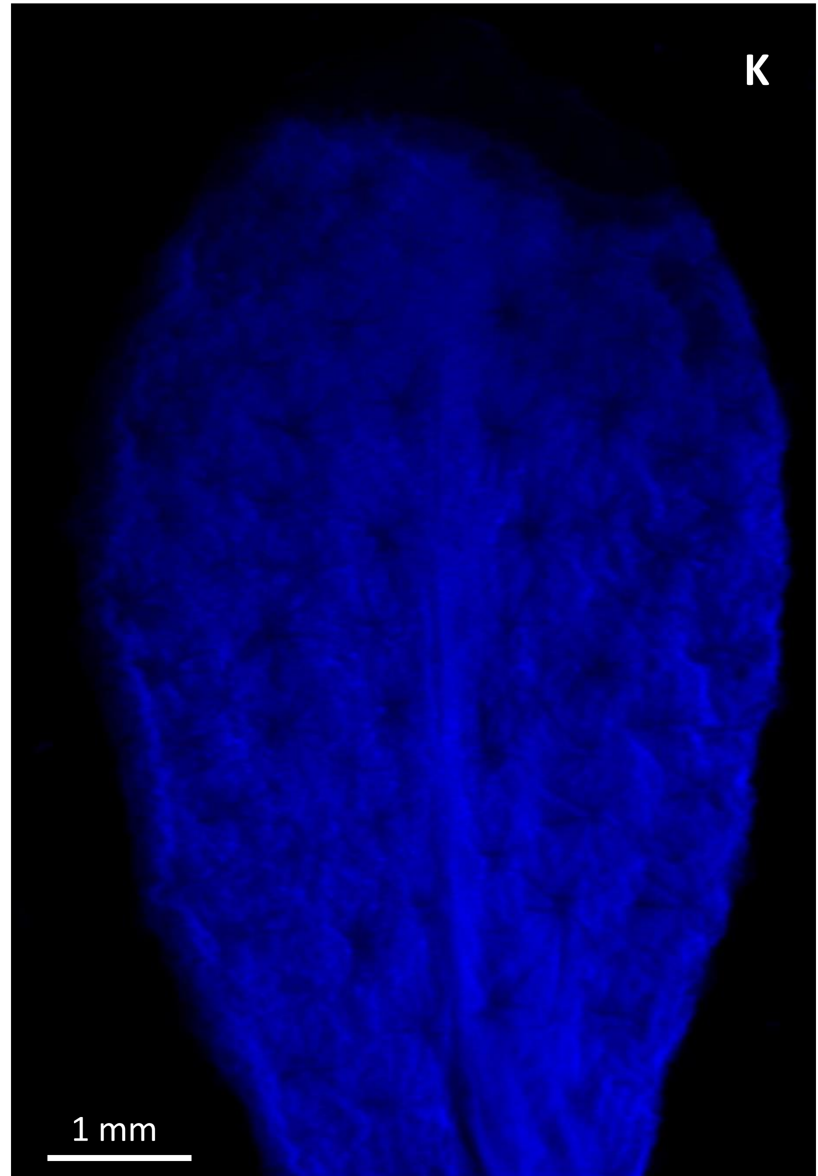

Spectroscopic "Chemical" Imaging

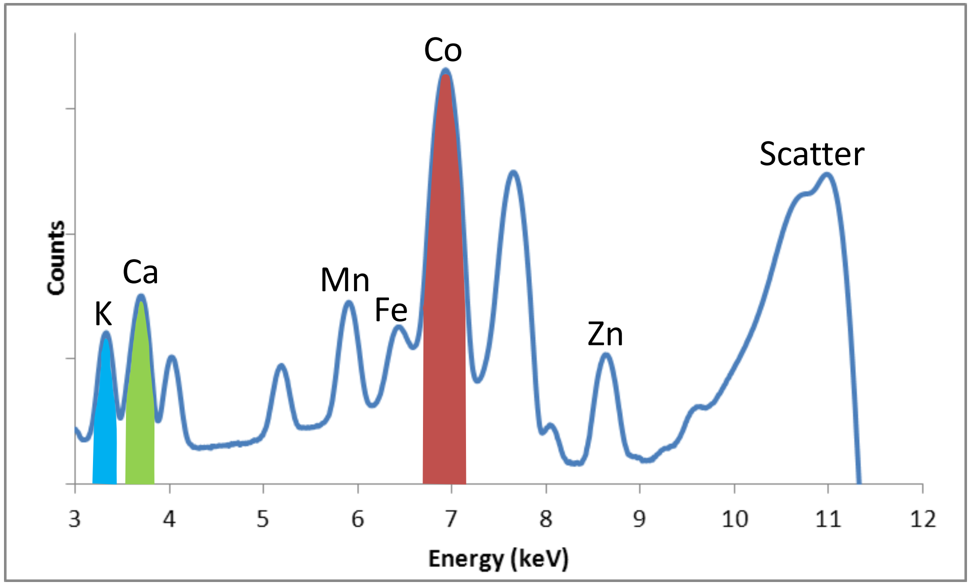

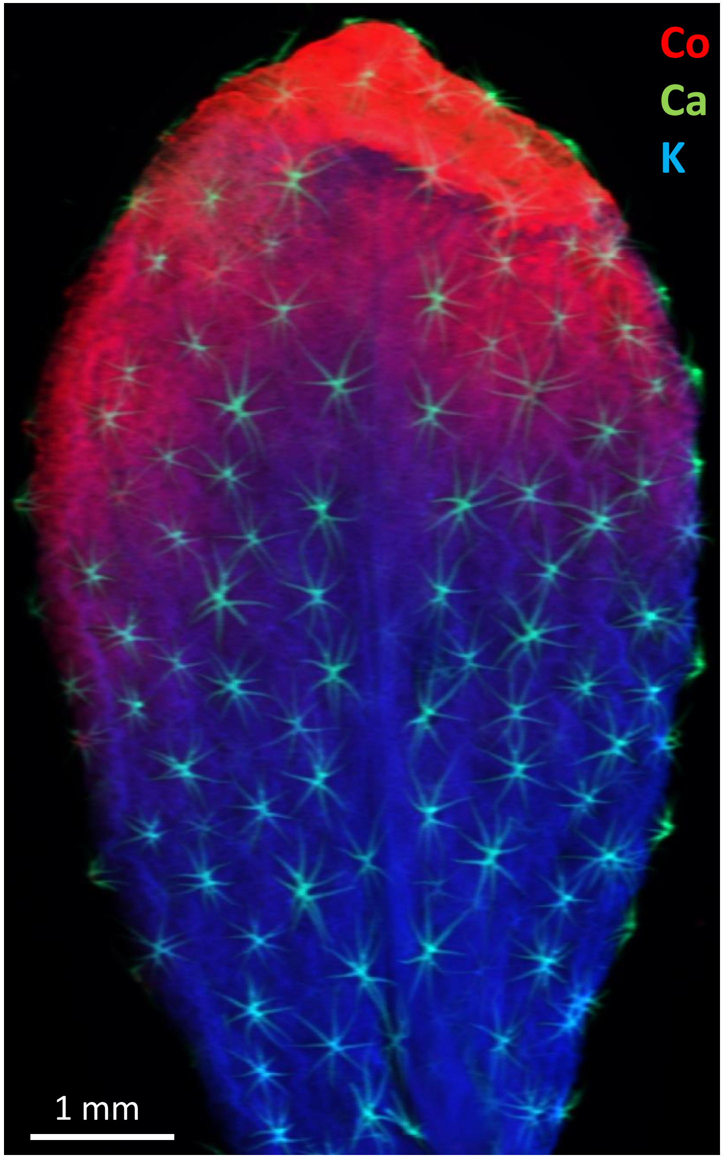

X-ray fluorescence microprobe

Purpose: spatially-resolved characterization of elemental abundances and chemical speciation in "as-is" samples that are heterogeneous at the (sub)micrometer scale.

Techniques:

- **Micro-XRF:** Spot XRF analyses of trace element composition
- **Element Mapping:** 2D composition and oxidation state imaging
- **Fluorescence Microtomography:** Internal 2D and 3D elemental imaging
- **Micro-XAS:** Spot XANES and EXAFS determinations of oxidation state and speciation
- **Micro-XRD:** phase identification and correlation with elemental and speciation information

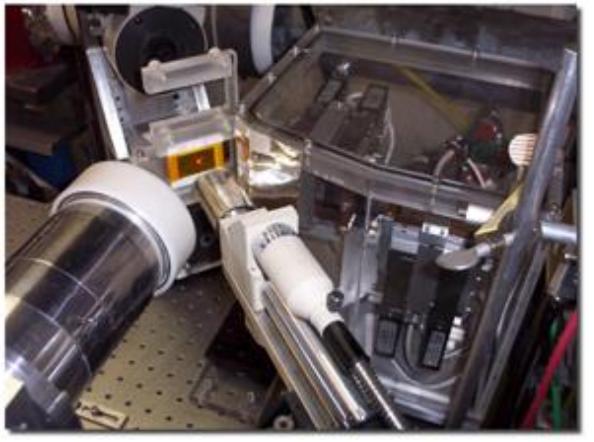

Elements with absorption edge in range for typical hard X-ray microprobe

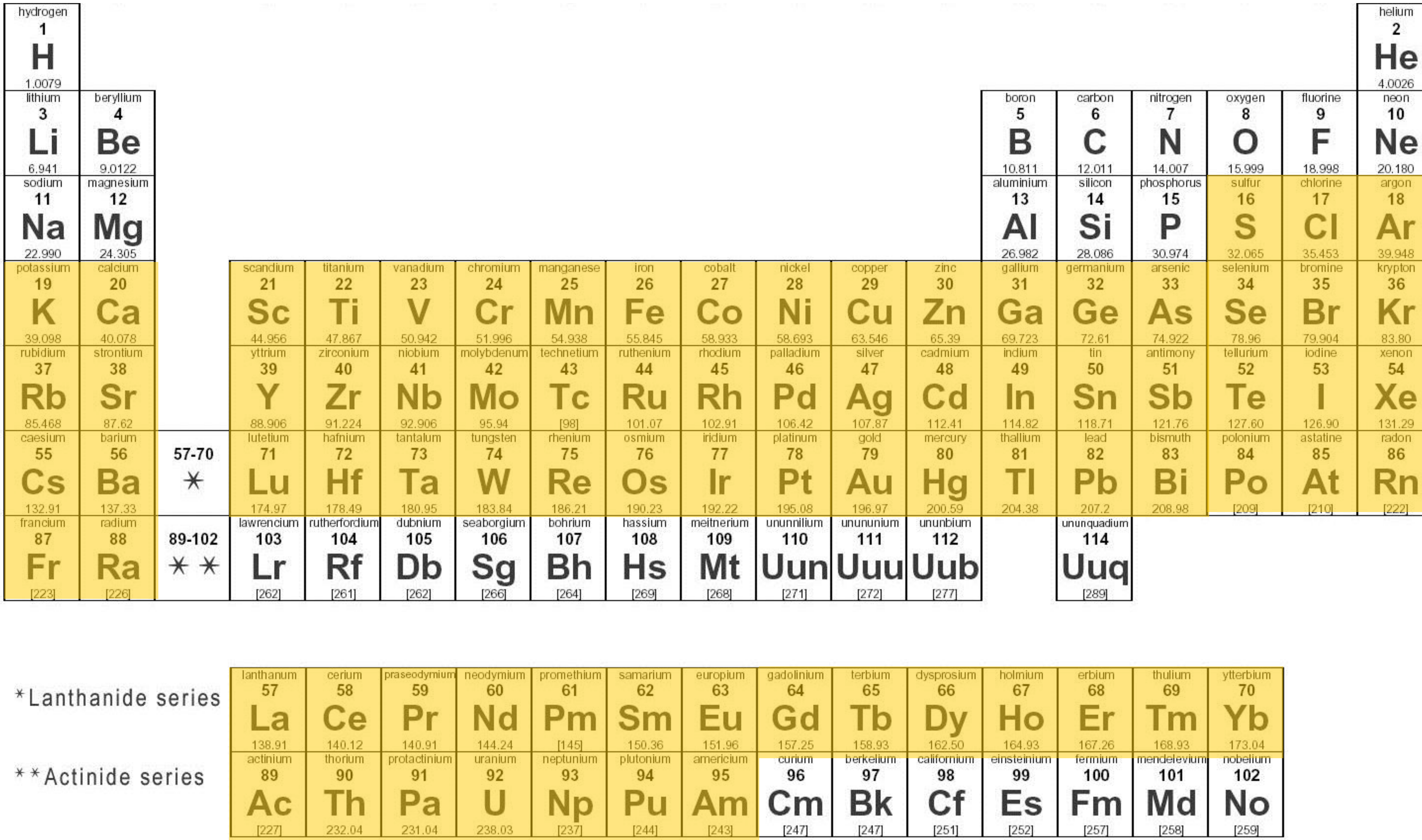

X-ray focusing– Current state-of-art

X-ray optic	Diffractive Optics	Reflective Optics	Refractive Optics
Numerical aperture	High NA possible	Limited NA	Limited NA
Resolution limit	< 1 nm?	− KB: ~ 16 nm − Wolter:~3nm	CRL: ~ 20 nm A-CRL: ~ 2 nm
Efficiency	20% - 30% (60%-80%)	70% - 90%	20% - 30%
Chromaticity	$f \sim 1/\lambda$	Non-chromatic	$f \sim 1/\lambda^2$
Features	• Monochromatic beam • On-axis geometry • Any x-ray energy	• White (pink) beam (non-ML) • Grazing inc. geometry • Any x-ray energy • KB: working distance!	• Monochromatic beam • On-axis geometry • Limited energy range • Long lenses
Limitations	•(High aspect ratio/tilt) •Positioning-alignment	Figure errors	Small working distance at high resolution

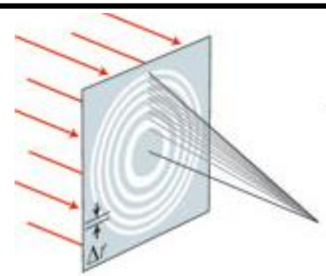

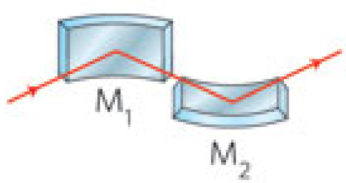

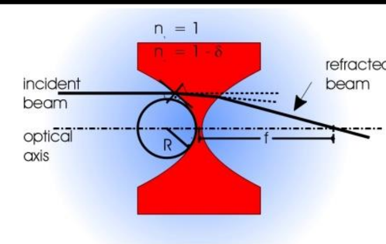

after J. Maser

X-ray Fluorescence Microscope: FZP

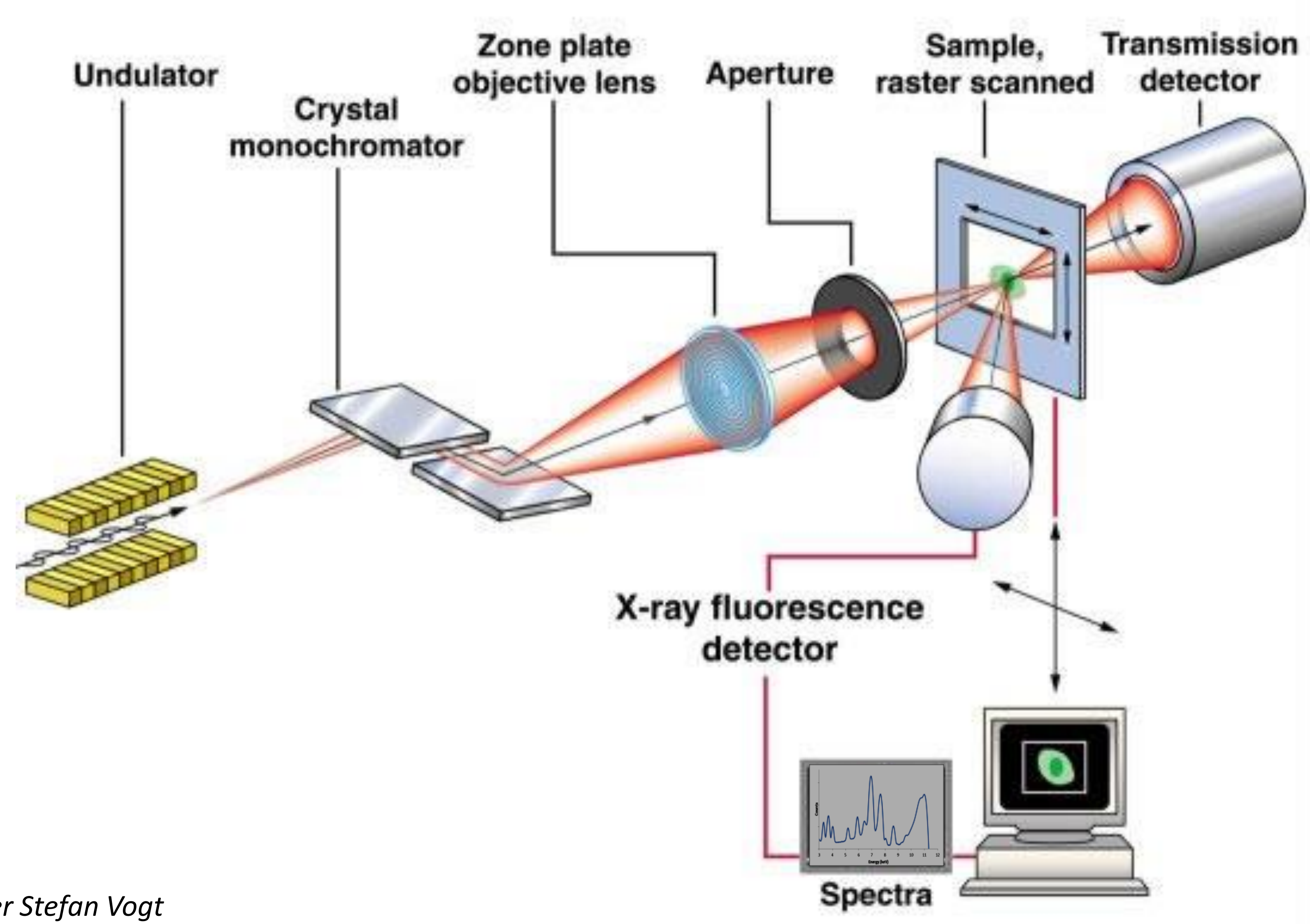

after Stefan Vogt

Why an X-ray microprobe?

- High intensity, directionality, and collimation of SR sources ideally suited for creating X-ray micro- and nano-beams.
- Very high flux density SR μ-XRF source provides extremely high *brilliance* (i.e., photons per unit source area over a unit angle of emission).
- 3rd generation facilities can deliver > 10^{12} photons s^{-1} μm^{-2} using wide bandpass X-ray focusing optics, which can yield ***ppb MDL's***.

- In-situ XRF, XAFS and XRD in heterogeneous materials, 3D chemical analysis with low power deposition.
- **No chemical pretreatment** required, samples can be analyzed in 'as collected' state. Liquids can be analyzed.

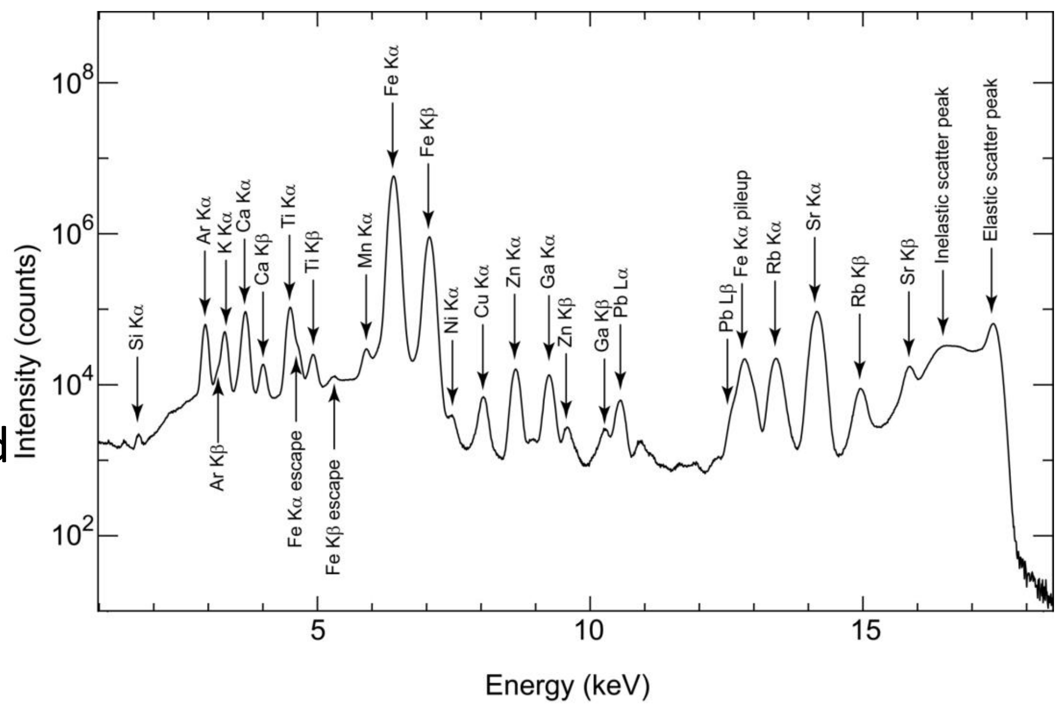

after A. Lanzirotti

SXRF Detection Limits

Probe	MDL (ppm/s)
Proton	~10-100
Electron	~ 5-30
Mono x-ray	< 1 feasible

EMPA & PIXE:

- inner shell hole production cross section low
- signal-to-background low
- PIXE flux density on the sample is low

Synchrotron X-ray microprobe with 10^{12} photons/s/mm^2 has ~10^3 lower MDL for most elements

PIXE can achieve the same MDL but with 10^4 more energy deposited in the sample.

after A. Lanzirotti

Absolute detection limits below 0.1 ag can be achieved (a few thousand of transition metal atoms) using XFM at 3rd generation sources

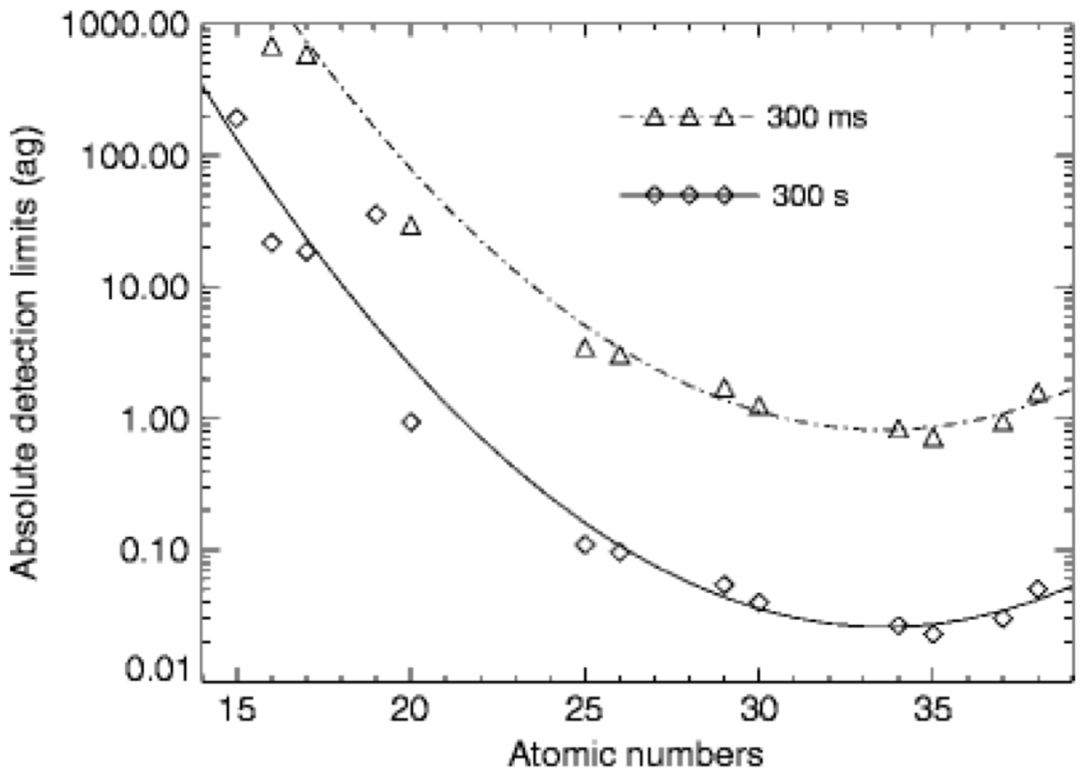

Absolute mass detection limits (NIST standard, 6 × 10^{11} photons/s) – Adams et al. (2011) in Handbook of Nuclear Chemistry, Second Edition

Anatomy of a microprobe experiment:

X-ray fluorescence imaging

"As-is" sample ⟶ 2-D μXRF "map" ⟶ 3-D fCMT
"Virtual slice"

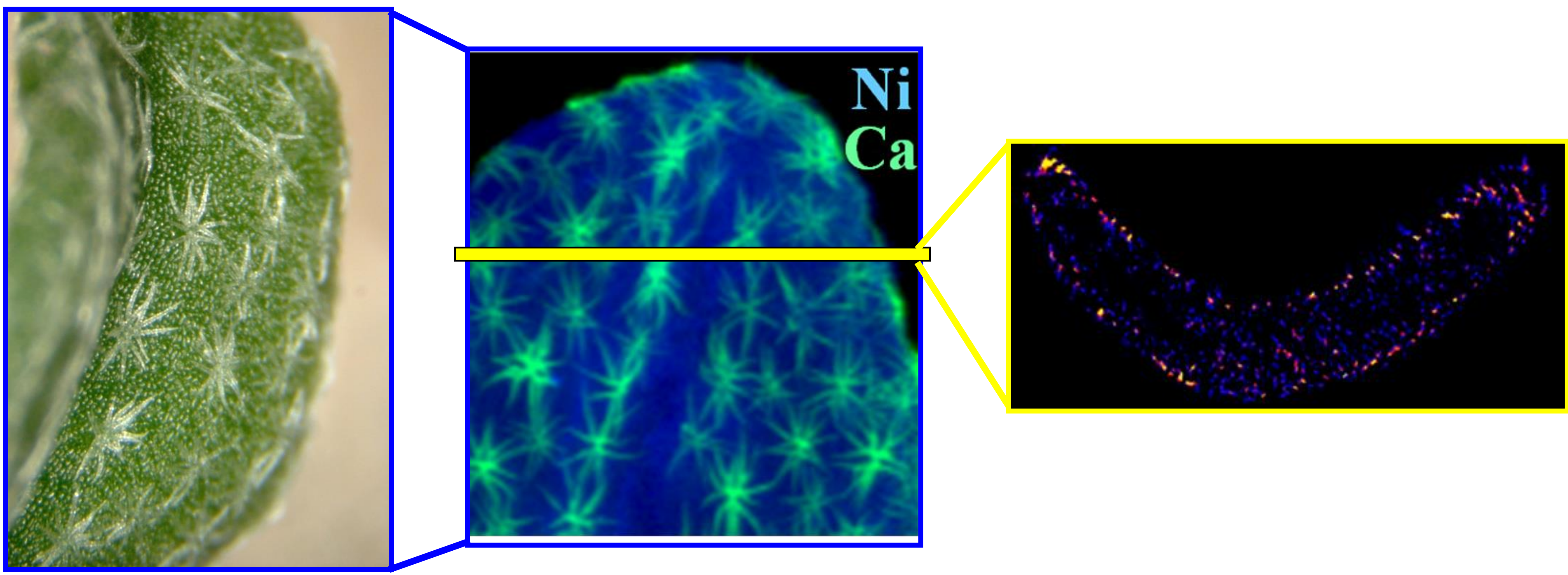

- Nickel is compartmentalized in leaf epidermal cells of hyperaccumulator *A. murale*

Anatomy of a microprobe experiment:

X-ray Absorption Spectroscopy (μXAS)

μXRF "map" ⟶ μEXAFS ⟶ Molecular speciation

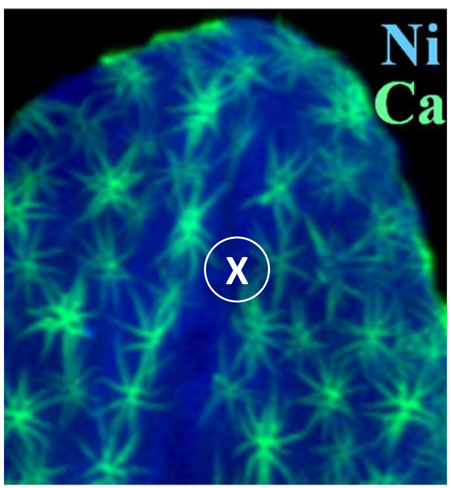

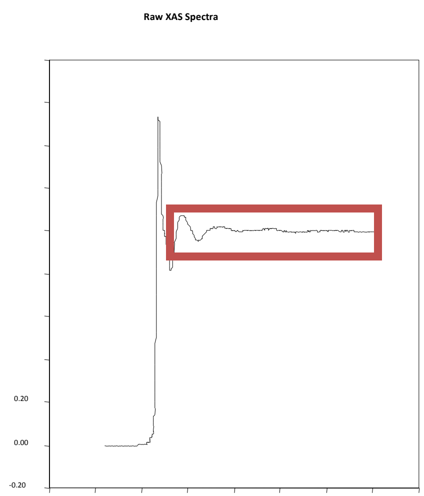

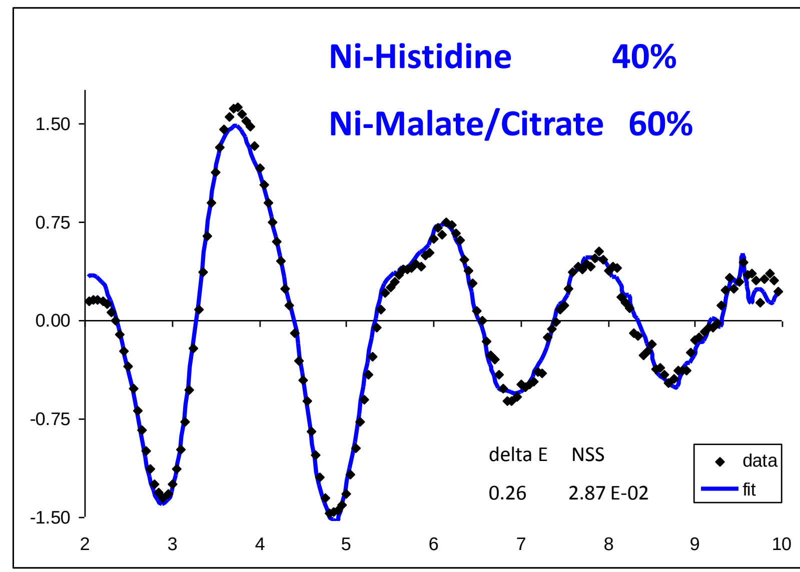

- Chemical binding (chelation) of Ni by organic and amino acids for transport in *A.m.*

Anatomy of a microprobe experiment:

X-ray microdiffraction (μXRD)

μXRF "map" ⟶ μXRD ⟶ Phase identification

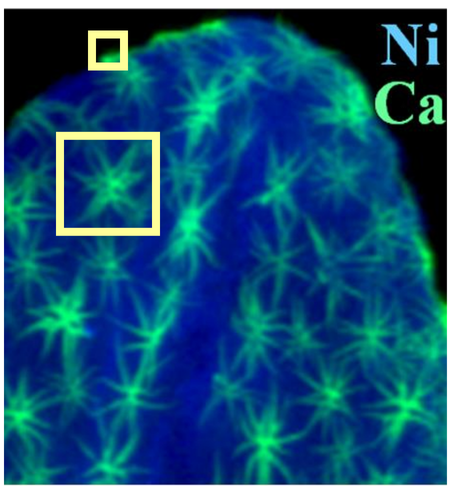

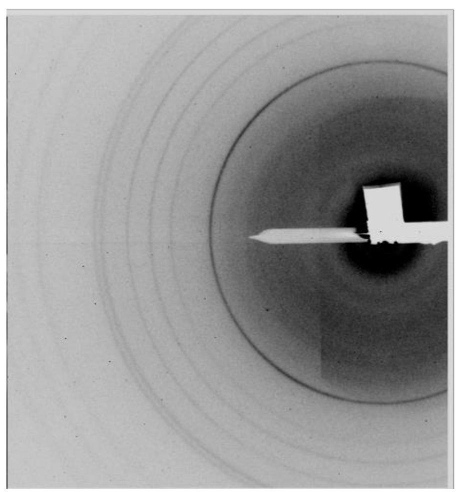

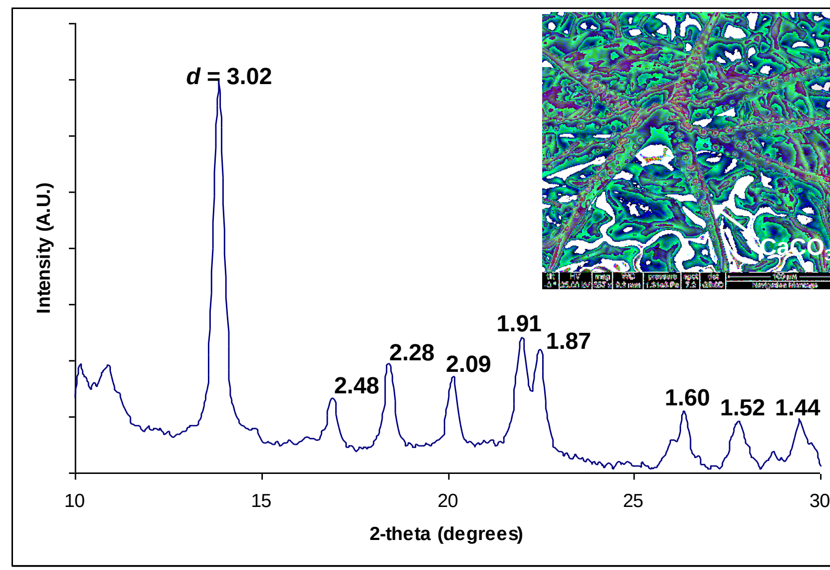

- *A. murale* trichomes (leaf hairs) are crystalline calcite ($CaCO_3$)

Science!

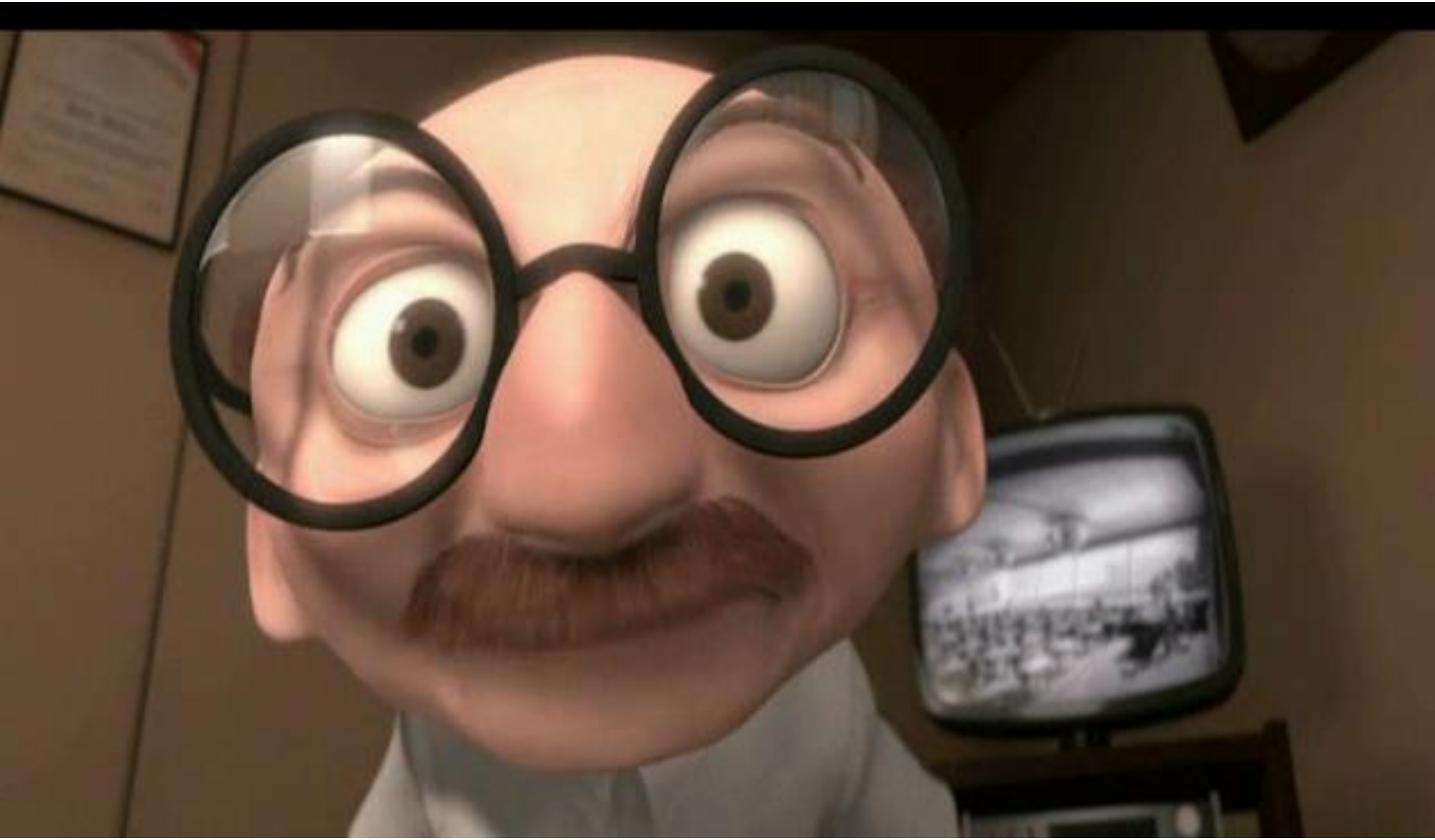

Release of metals into the Environment

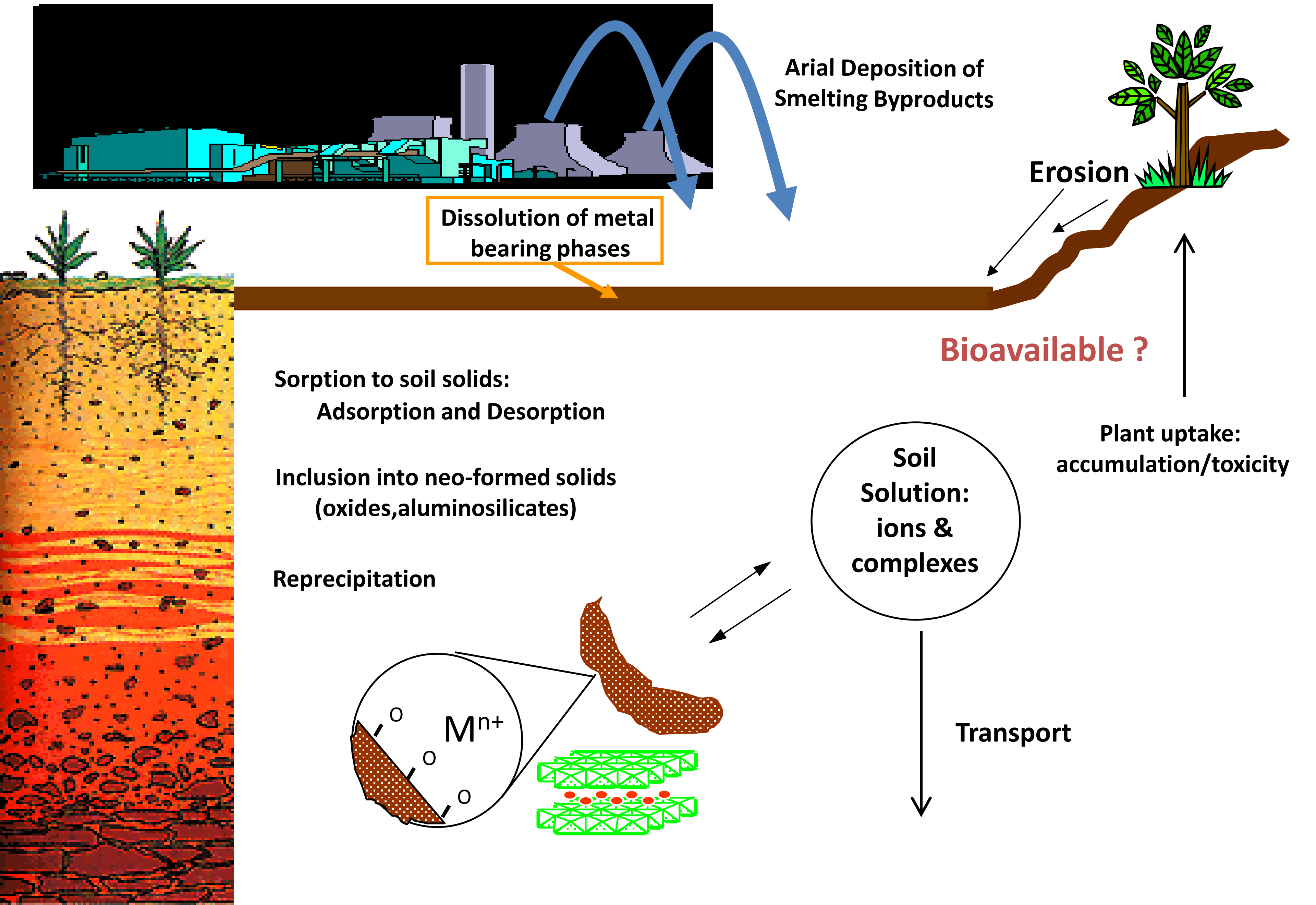

Impacts from Smelter/ Refinery Site

Phytoextraction…

relies on hyperaccumulator plants to extract metals from contaminated media

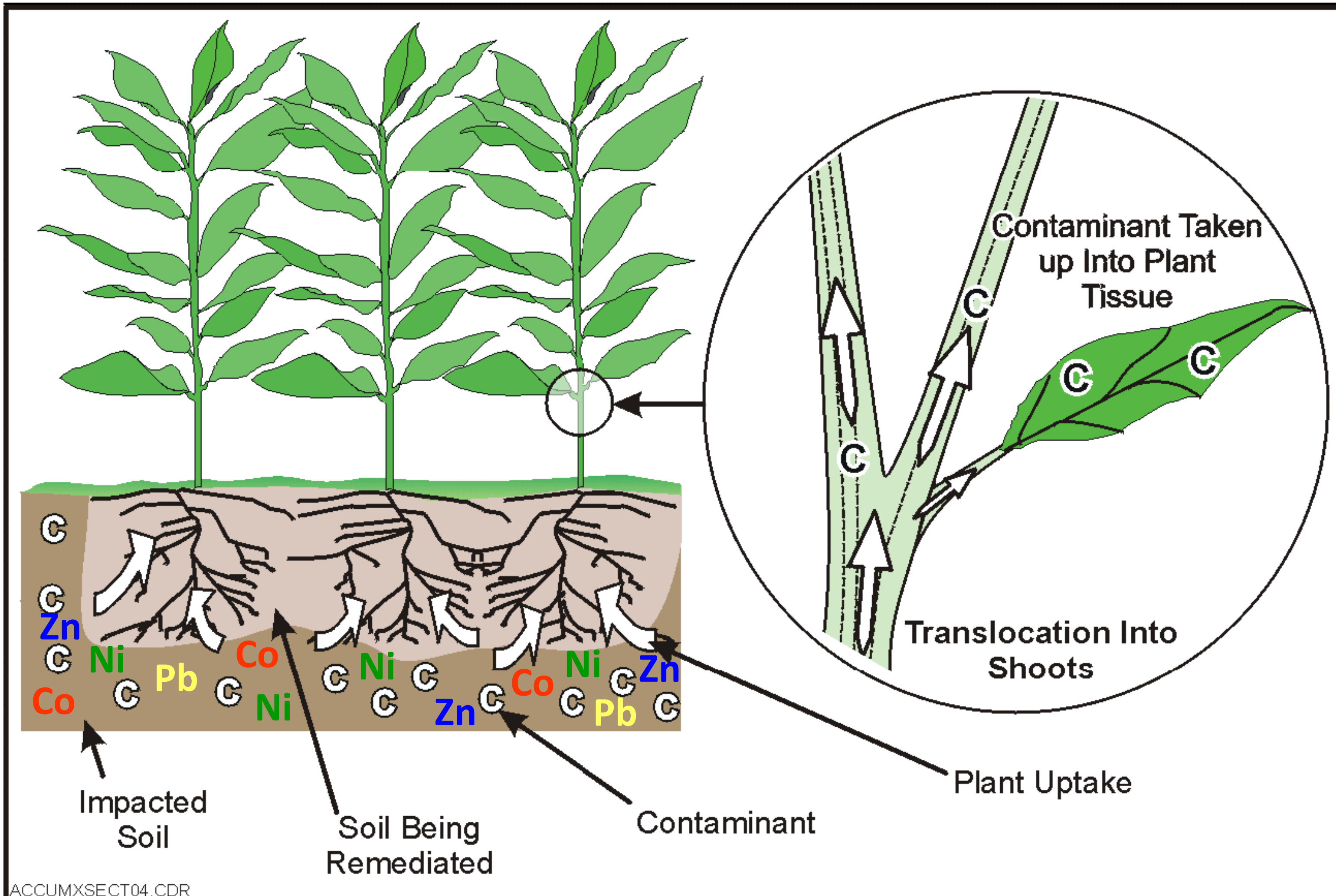

Meet nickel hyperaccumulator *Alyssum murale*

- Concentrate trace metals (weight percent) in shoot tissue as mechanism to survive metalliferous soil conditions
- Accumulators recognized for centuries and used as geobotanical indicators for mineral prospecting (Cannon 1960)
- *Alyssum* being developed as commercial crop for phytomining and remediation by USDA (Chaney 1985)
- Mechanisms of metal tolerance as well as metal ion uptake, transport, and storage are being studied to improve hyperaccumulation.

***Alyssum murale* (yellowtuft)**

Alyssum murale in ebb-flow hydroponics

A. murale exposed to mixed metal (Ni, Co, Zn) systems

Uptake of Ni and Co by *A. murale* using ICP-OES

Ni-Co-Zn treatment	Bulk metal concentration in shoot tissue		
	Ni	Co	Zn
µM		µg/g	
50-0-0	1609 a	—	60 a
50-10-0	1417 a	404 a	57 a
50-50-0	1653 a	1569 b	69 a
50-50-50	1407 a	2065 c	129 b

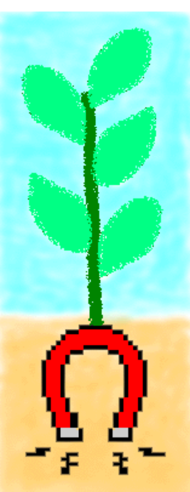

NOTE: 50 µM ~ 3 ppm solution

Internal metal localization in *A.m.* roots using fCMT

- Root tips (and root hairs) are important to absorption of Ni and Co
- In *A.m.* roots, Ni and Co localization patterns are nearly identical

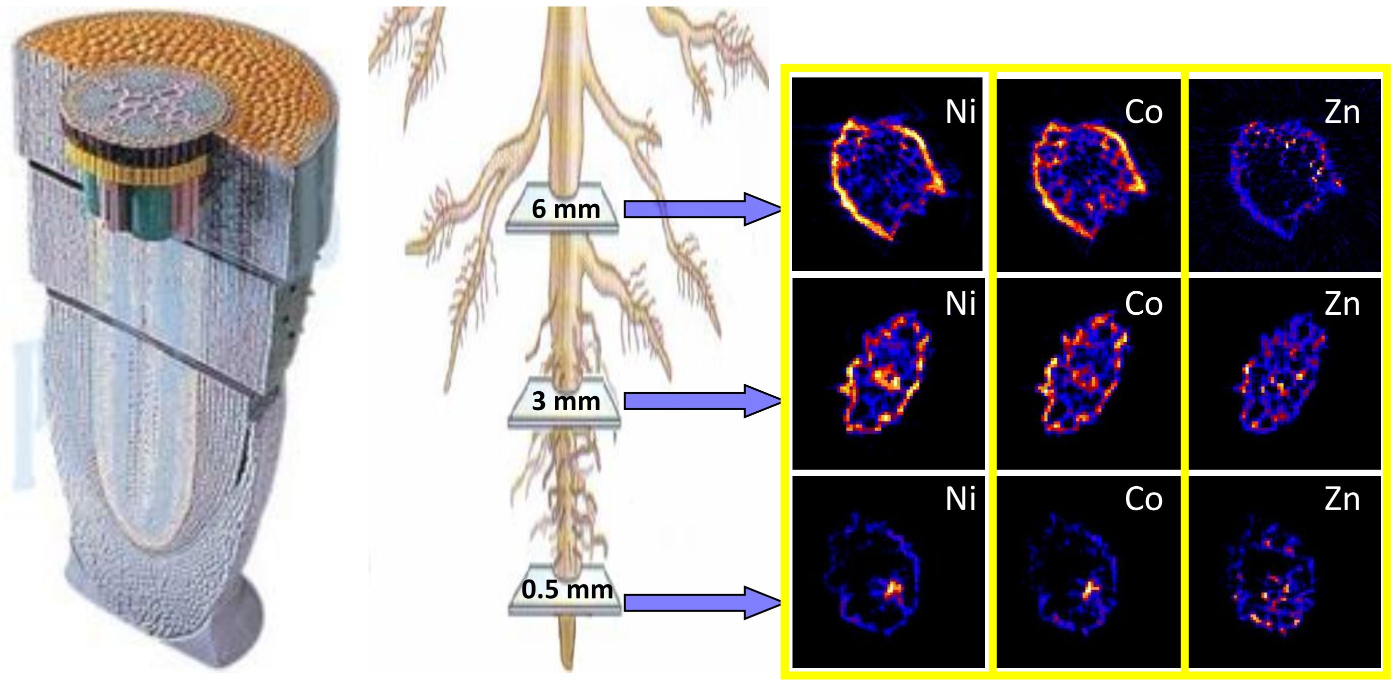

fCMT images showing metal localization in a hydrated *A.m.* root from 50-50-50 treatment

Metal localization in *A.m.* leaf using SXRF

- Nickel distribution is relatively uniform
- Cobalt is localized at leaf tips/margins !!!

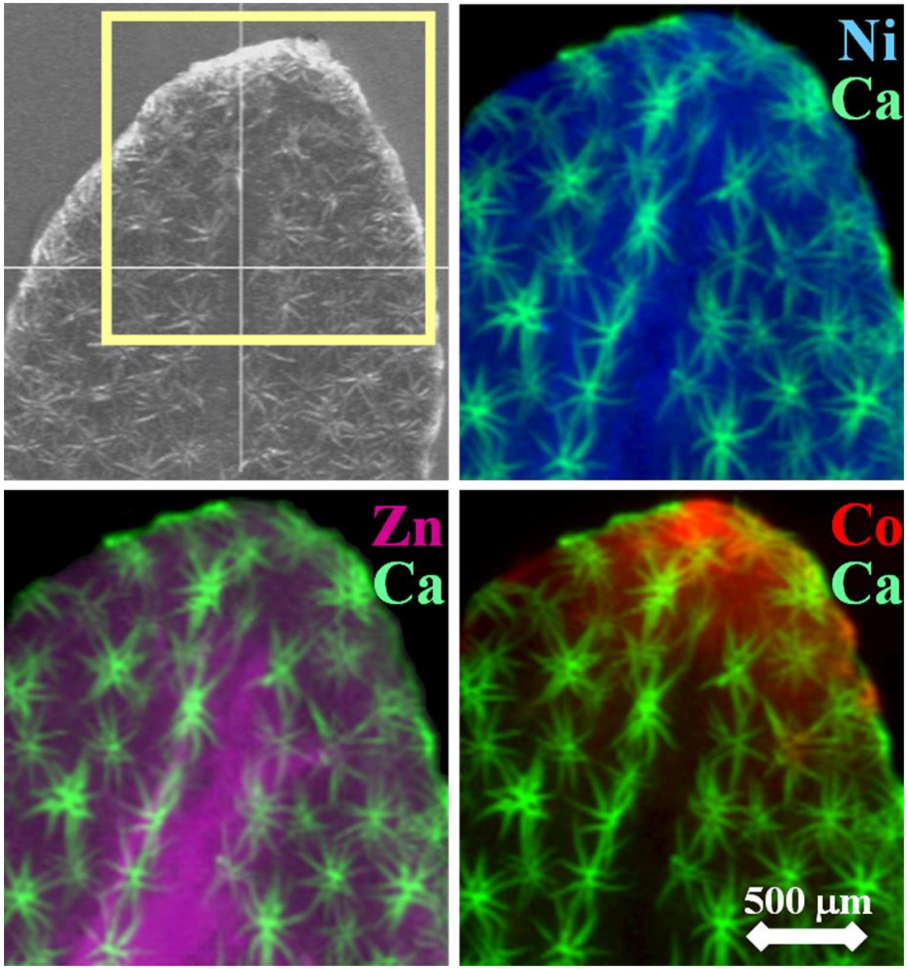

SXRF images showing metal localization in a hydrated *A.m.* leaf from 50-50-50 treatment

Hard X-rays are deeply penetrating…

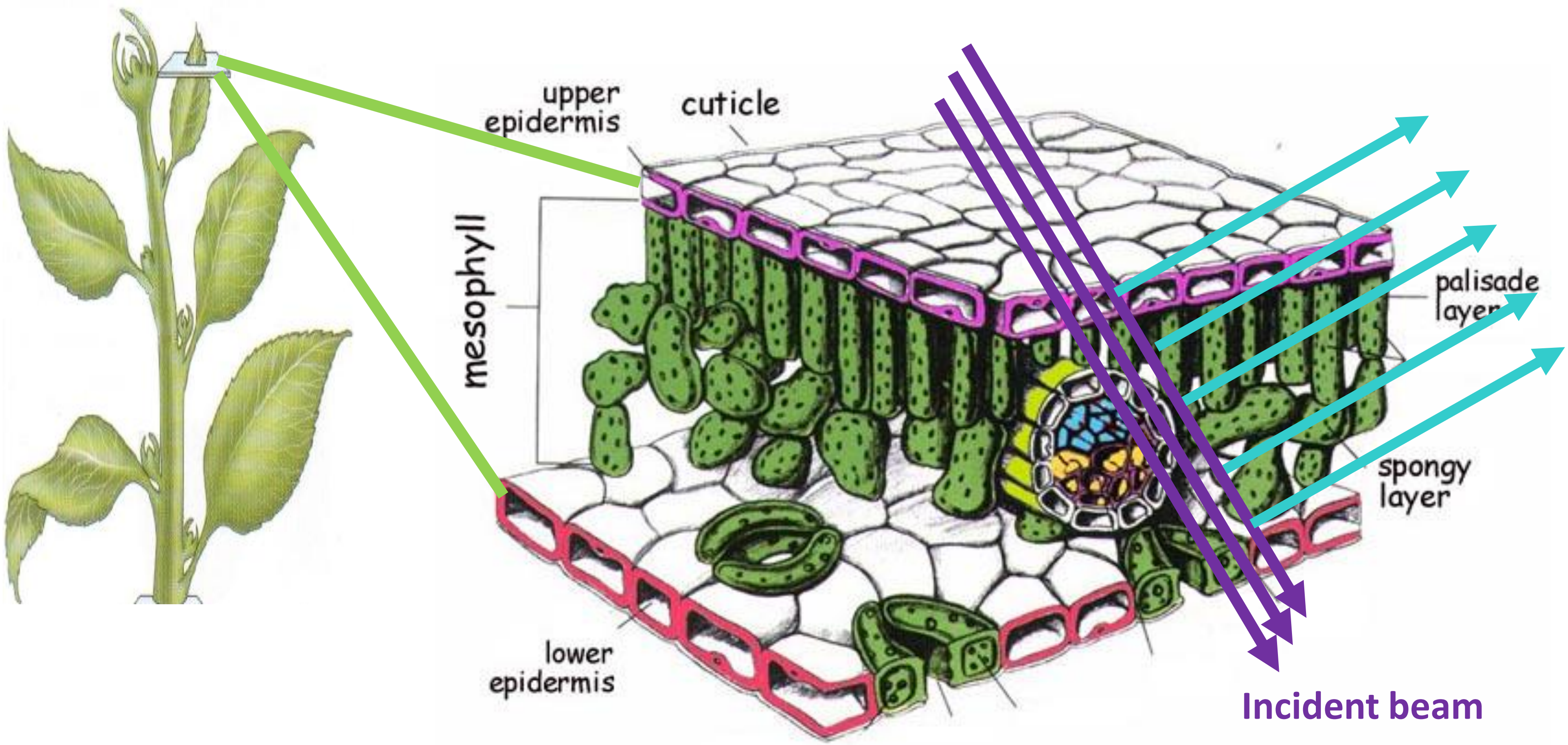

…fluorescence computed microtomography (fCMT)

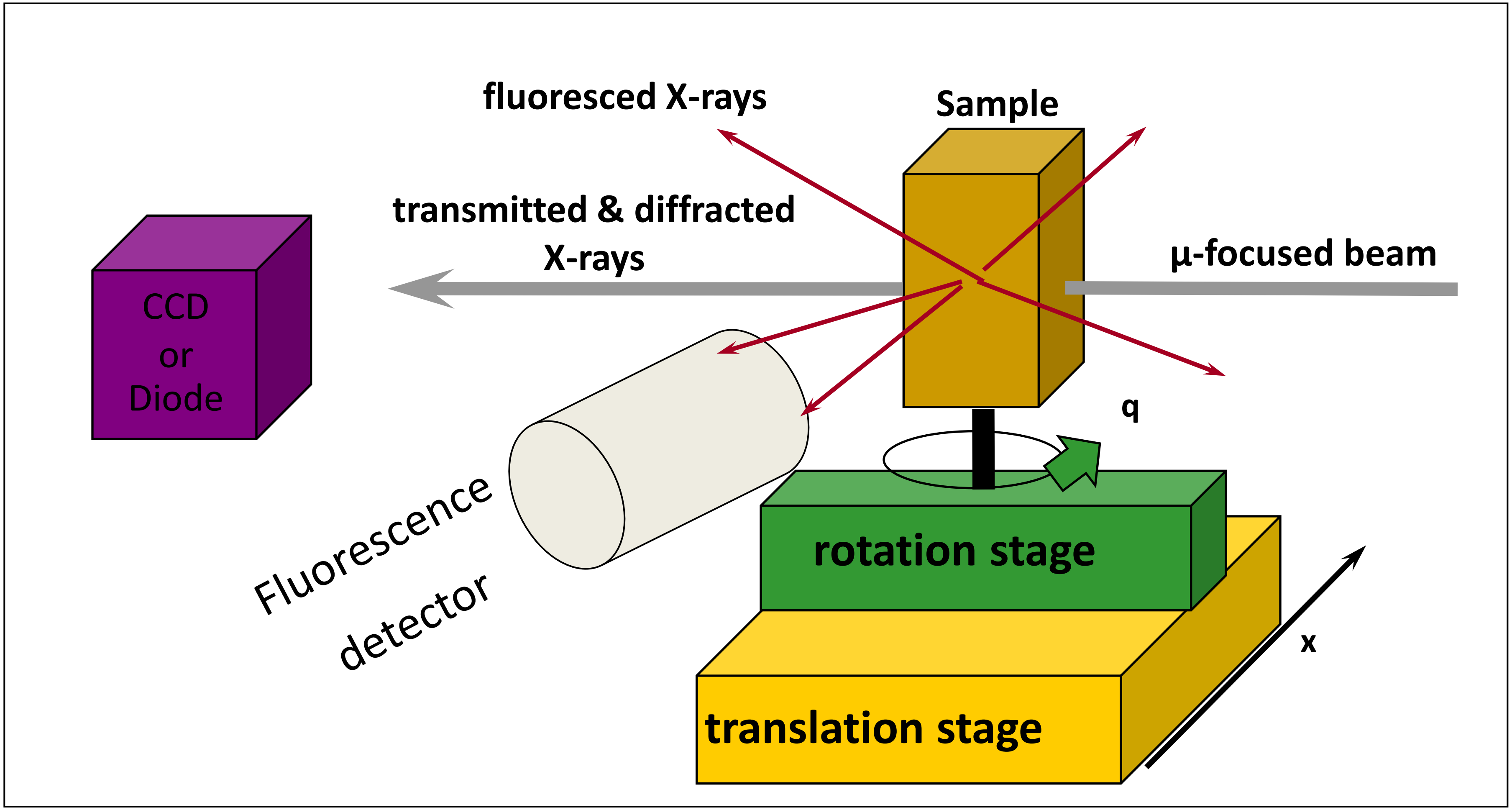

Cobalt localization in *A.m.* leaf using microtomography

- Cobalt is localized on leaf exterior near tips/ margins
- Cobalt is excluded from epidermal cell layer

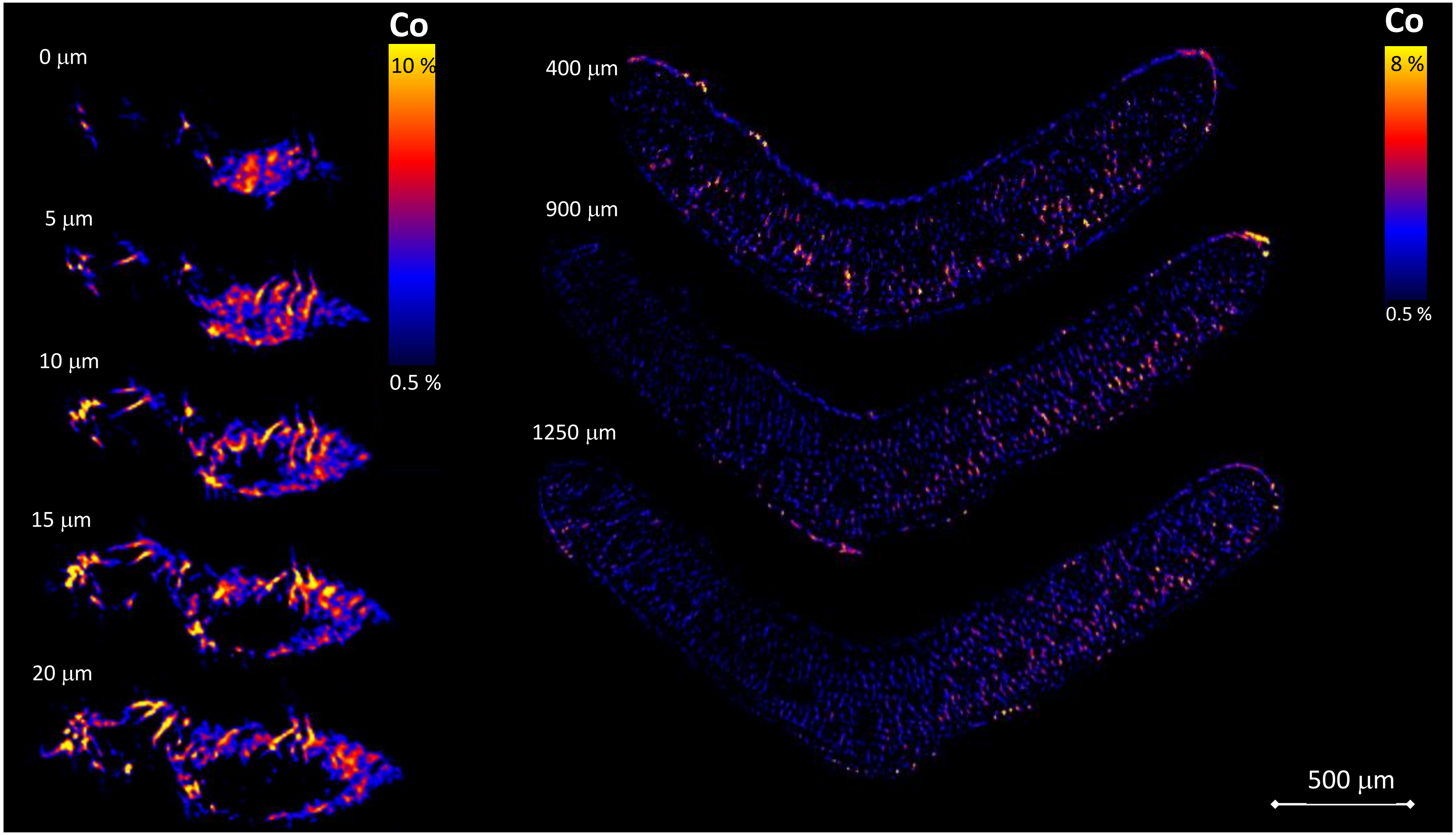

Cobalt localization in *A.m.* leaf using microtomography

- Co preferentially localized between cells (apoplastic fluid)

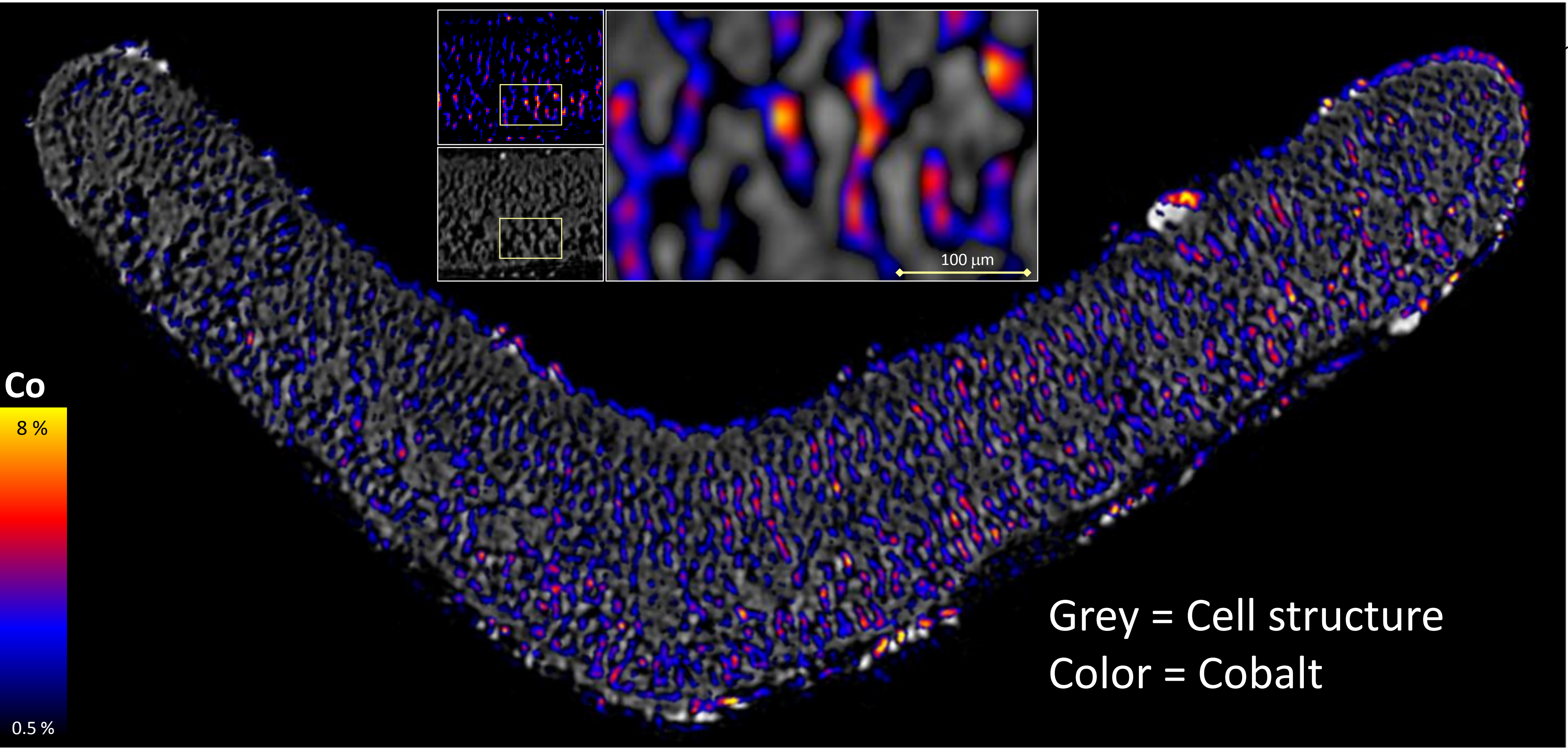

Organic acids in apoplastic fluid using HPLC

- Fumarate levels increase in response to increasing concentrations of Co in nutrient solution (Co = 0, 25, or 50 mM)

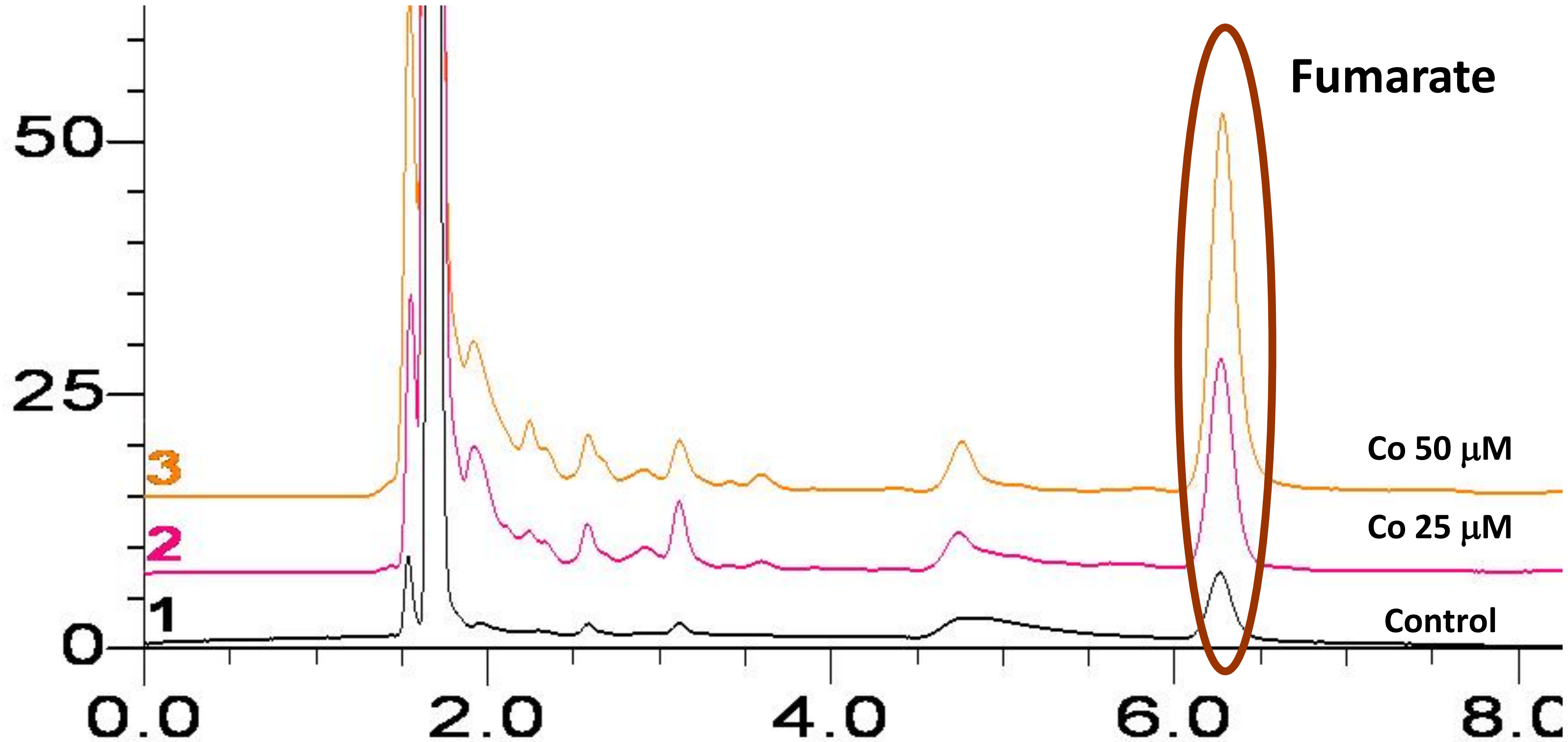

Cobalt speciation in *A.m.* leaf using bulk EXAFS

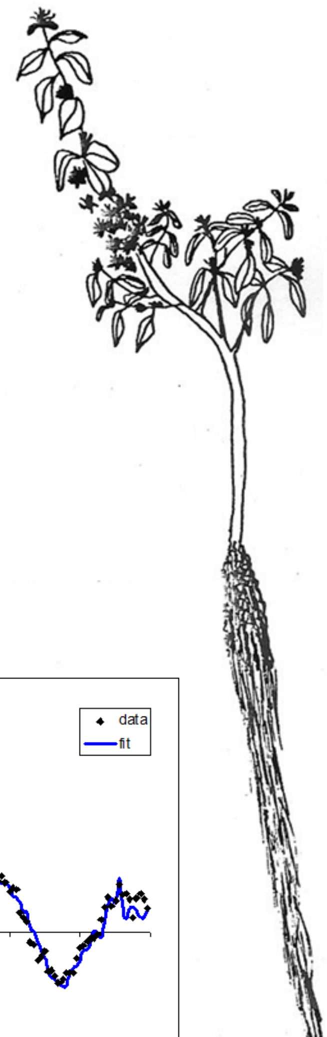

	Co-Histidine	Co-COOH
Leaf	40 % (1010 ug/g)	60% (1520 ug/g)
Stem	50% (206 ug/g)	50% (206 ug/g)
Root	60% (523 ug/g)	40% (348 ug/g)

Greatest proportion of histidine-bound Co found in roots; largest fraction of carboxylate-bound Co found in leaves

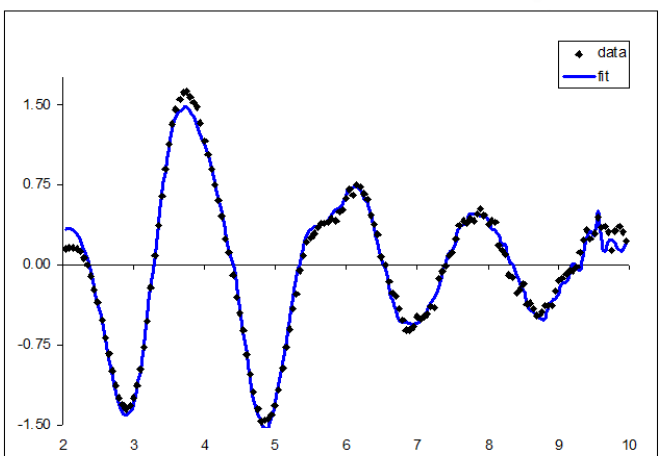

Cobalt speciation in *A.m.* leaf using μEXAFS

- Speciation varies between leaf-tip and bulk-leaf region

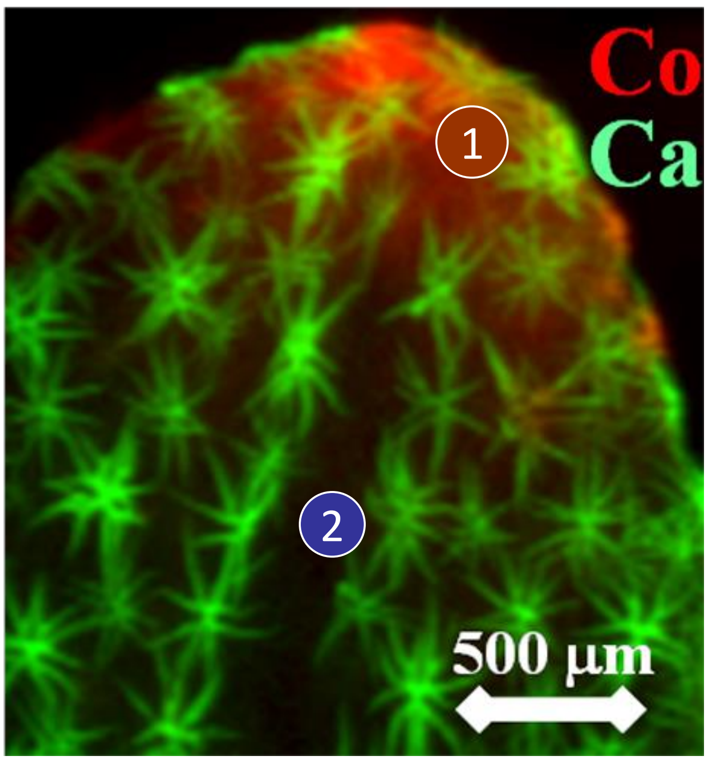

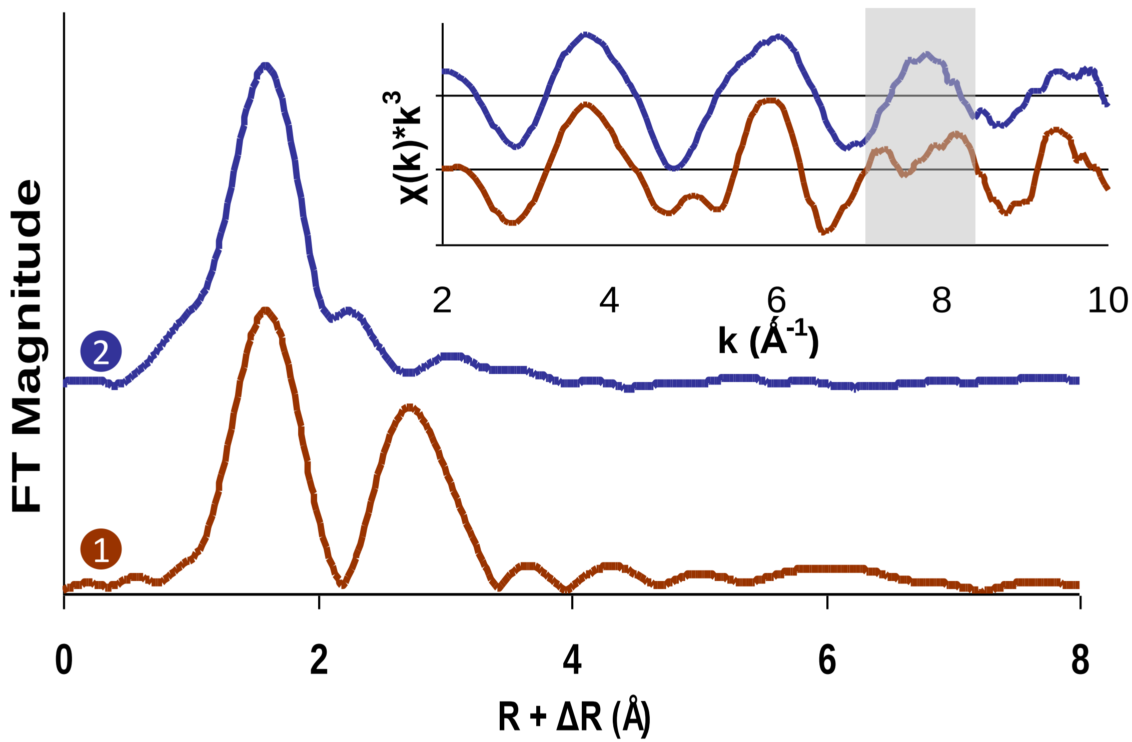

Cobalt speciation in *A.m.* leaf tip using μEXAFS

- Speciation at leaf-tip is poorly-ordered hydrous Co silicate

Shell	CN	R (Å)	σ^2 ($Å^{-2}$)	ΔE_0 (~eV)	Res.
Co - O	**5.8**	**2.08**	0.008	-3.17	1.55
Co - Co	**4.7**	**3.11**	0.010	-3.17	1.55
Co – Si	**3.3**	**3.27**	0.005	-3.17	1.55

CN = coordination number (1st shell +/- 20 %, 2nd shell +/- 40 %)

R = radial distance (1st shell +/- 0.03, 2nd shell +/- 0.06)

σ^2 = Debye-Waller factor (1st shell +/- 0.003, 2nd shell +/- 0.006)

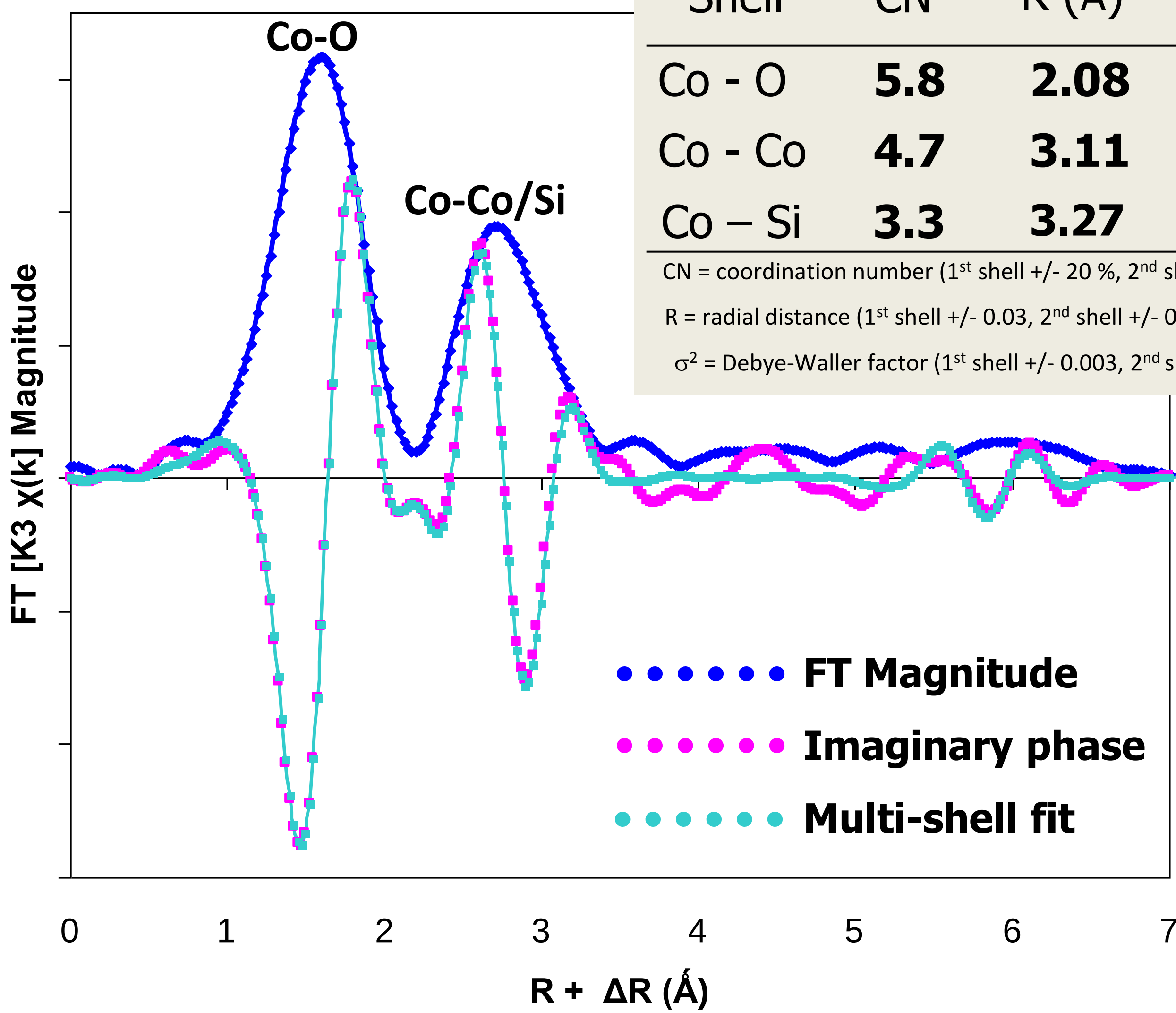

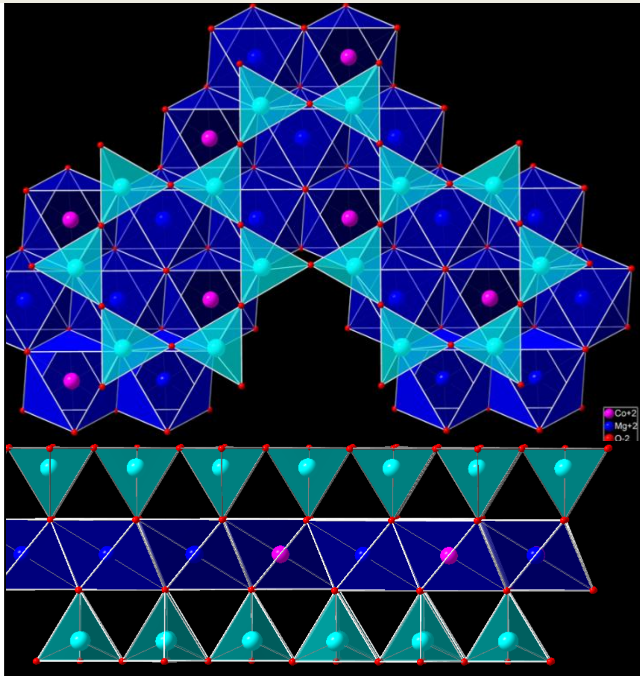

Light element imaging of *A.m.* leaf tip using SEM

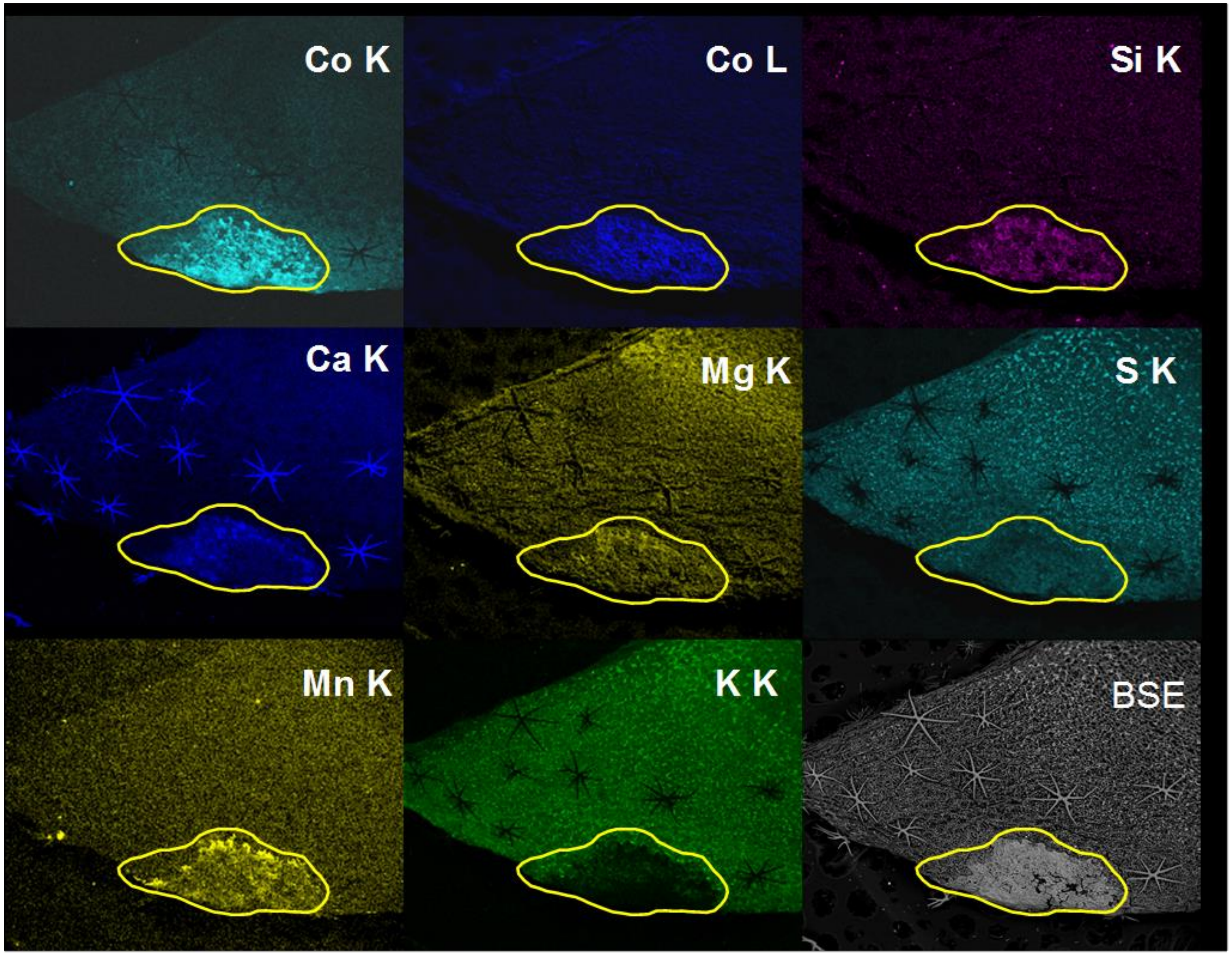

Light element imaging of *A.m.* leaf tip using SEM

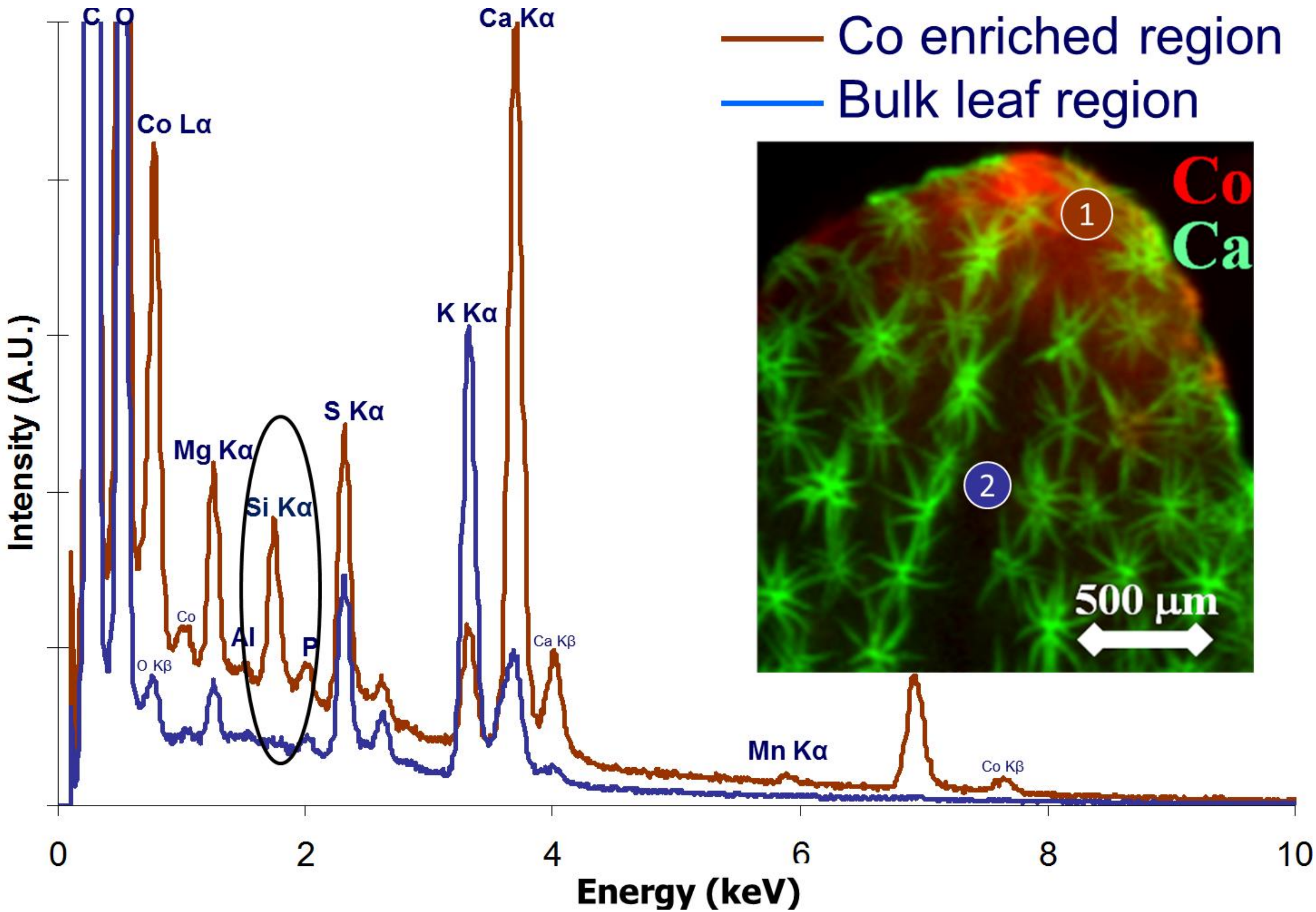

Summary: *Metal interaction study*

- Nickel hyperaccumulation is not compromised by the presence of Co and/or Zn at environmentally-relevant concentrations

- Nickel is bound to amino and organic acids for transport and storage, and is compartmentalized in leaf epidermal cells, thus “(hyper)tolerance”

- Cobalt is bound to amino and organic acids *in planta*, but is expelled from leaves and forms a hydrous Co silicate on the leaf exterior, thus “exocellular sequestration”

***A. murale* uses a different tolerance mechanism for Nickel than for Cobalt**

Biofortification Effort- Alfalfa

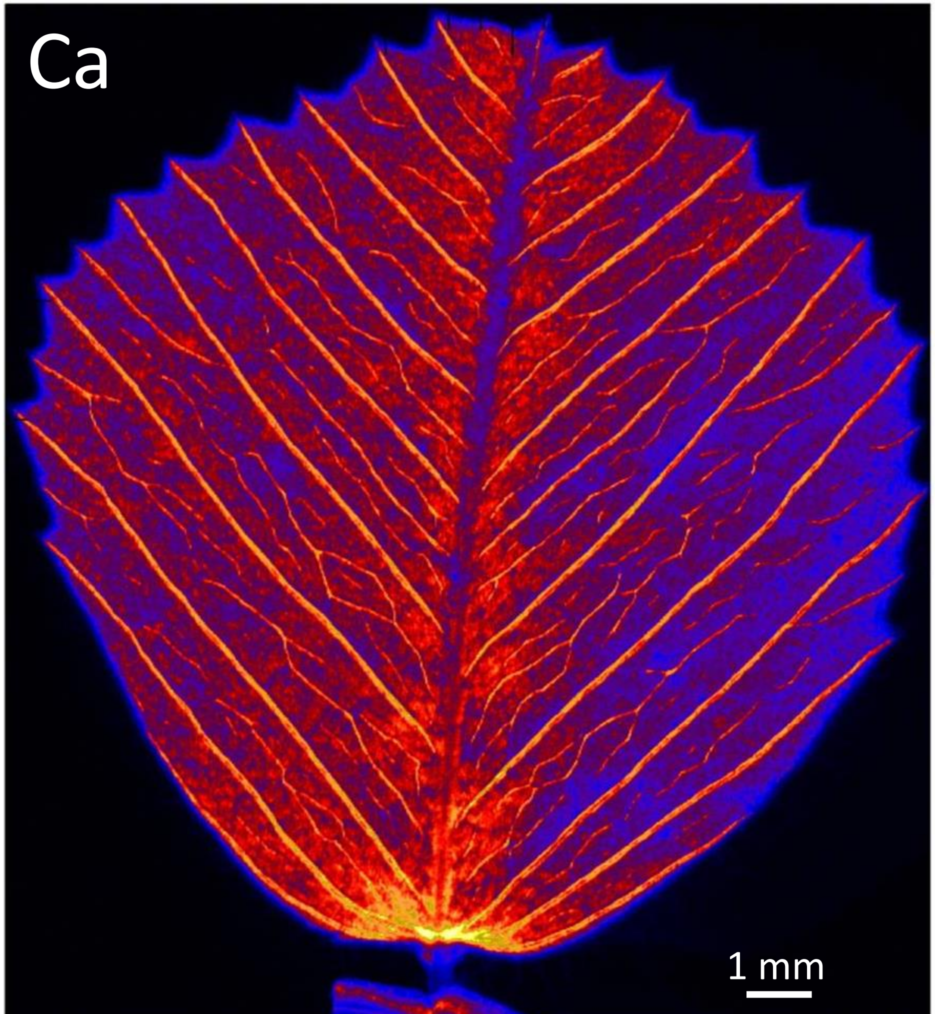

- Calcium (Ca) is an essential nutrient for humans, but excess Ca in plants is stored as mineral form not readily absorbed by humans
- Crop plants can be selected to contain more bioaccessible Ca (i.e. biofortification)
- At the X-ray microprobe, XRF, XAS & XRD were used to understand how CAX1 gene alters the storage form of Ca in alfalfa

Punshon, T., R. Tappero, F.K. Ricachenevsky, K. Hirschi, and P.A. Nakata. 2014. The Plant Journal 76:627-633.

Biofortification Effort- Alfalfa

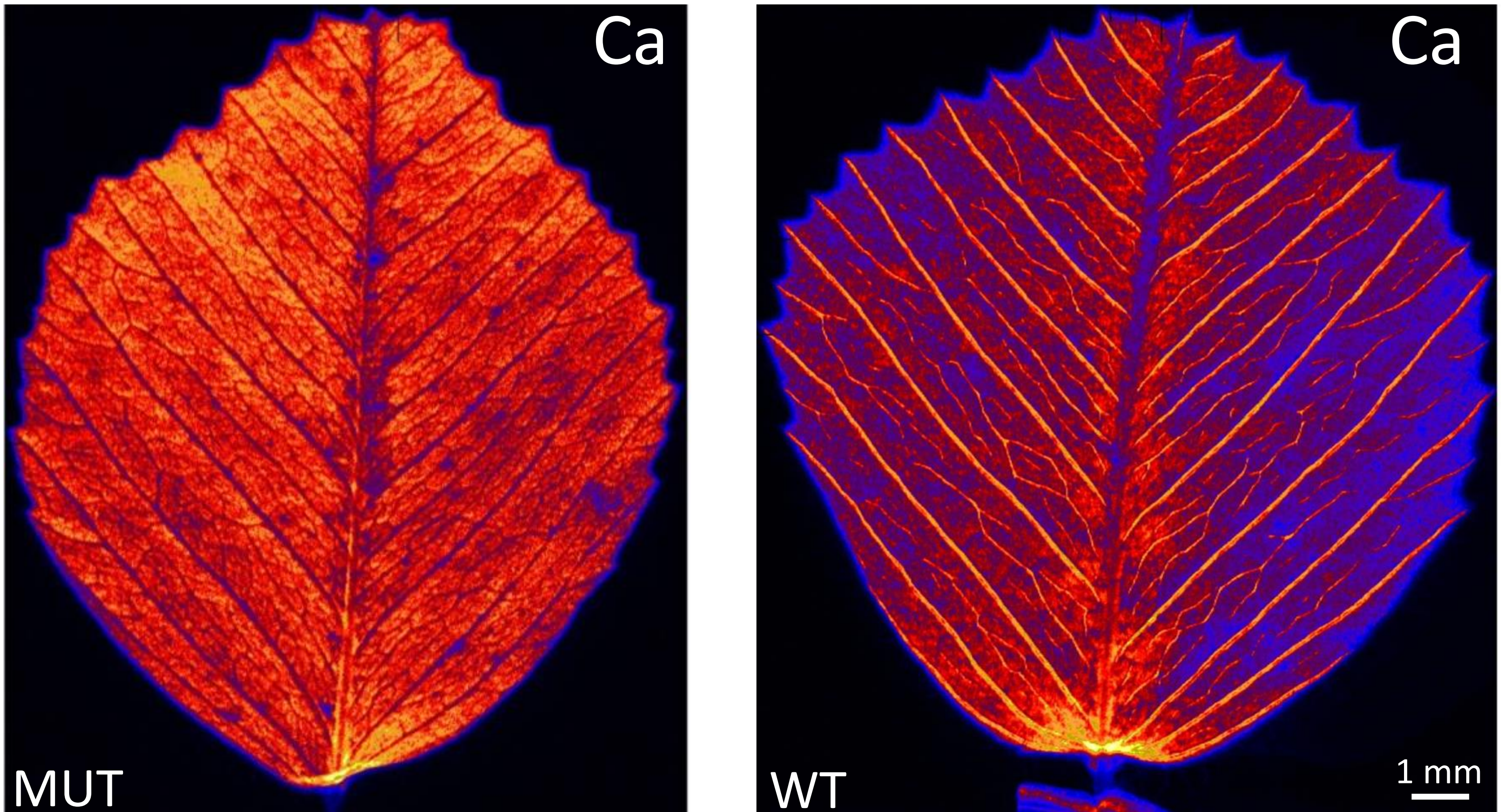

Punshon, T., R. Tappero, F.K. Ricachenevsky, K. Hirschi, and P.A. Nakata. 2014. The Plant Journal 76:627-633.

Biofortification Effort- Alfalfa

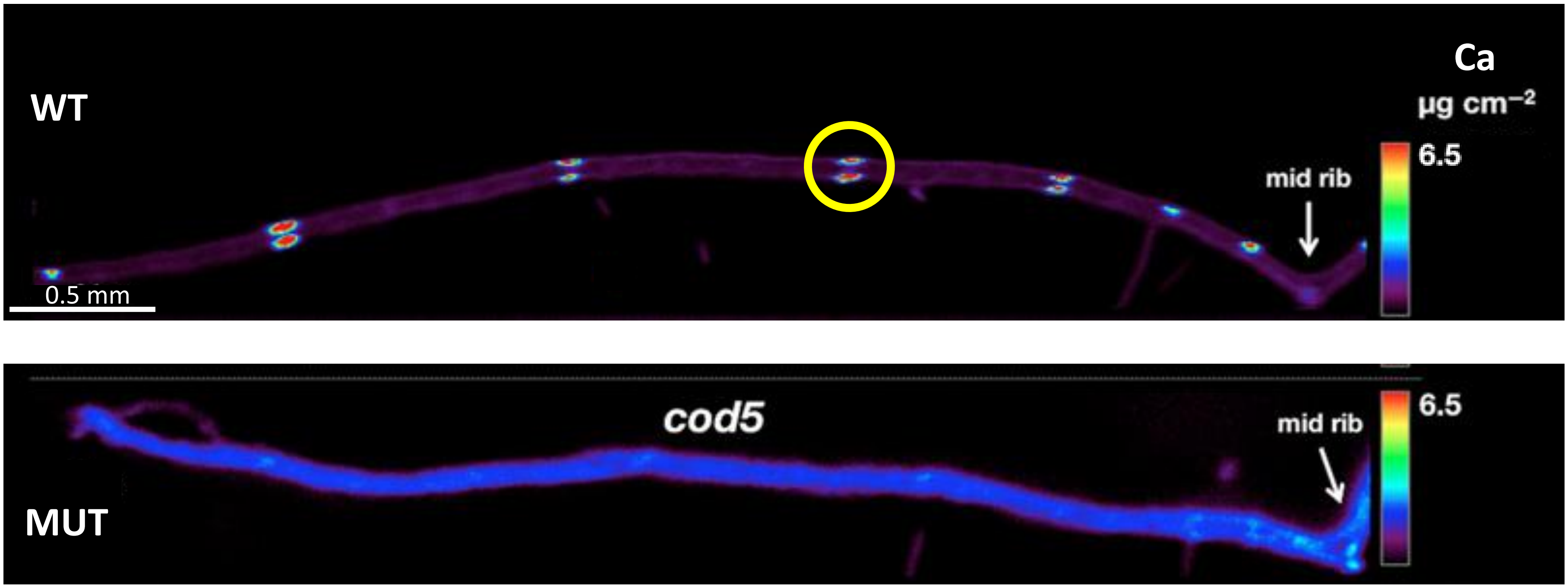

- Wildtype cultivars have preferential localization of Ca in discrete hotspots both above and below secondary veins, whereas mutant cultivars (cod5) do not.

Punshon, T., R. Tappero, F.K. Ricachenevsky, K. Hirschi, and P.A. Nakata. 2014. The Plant Journal 76:627-633.

Biofortification Effort- Alfalfa

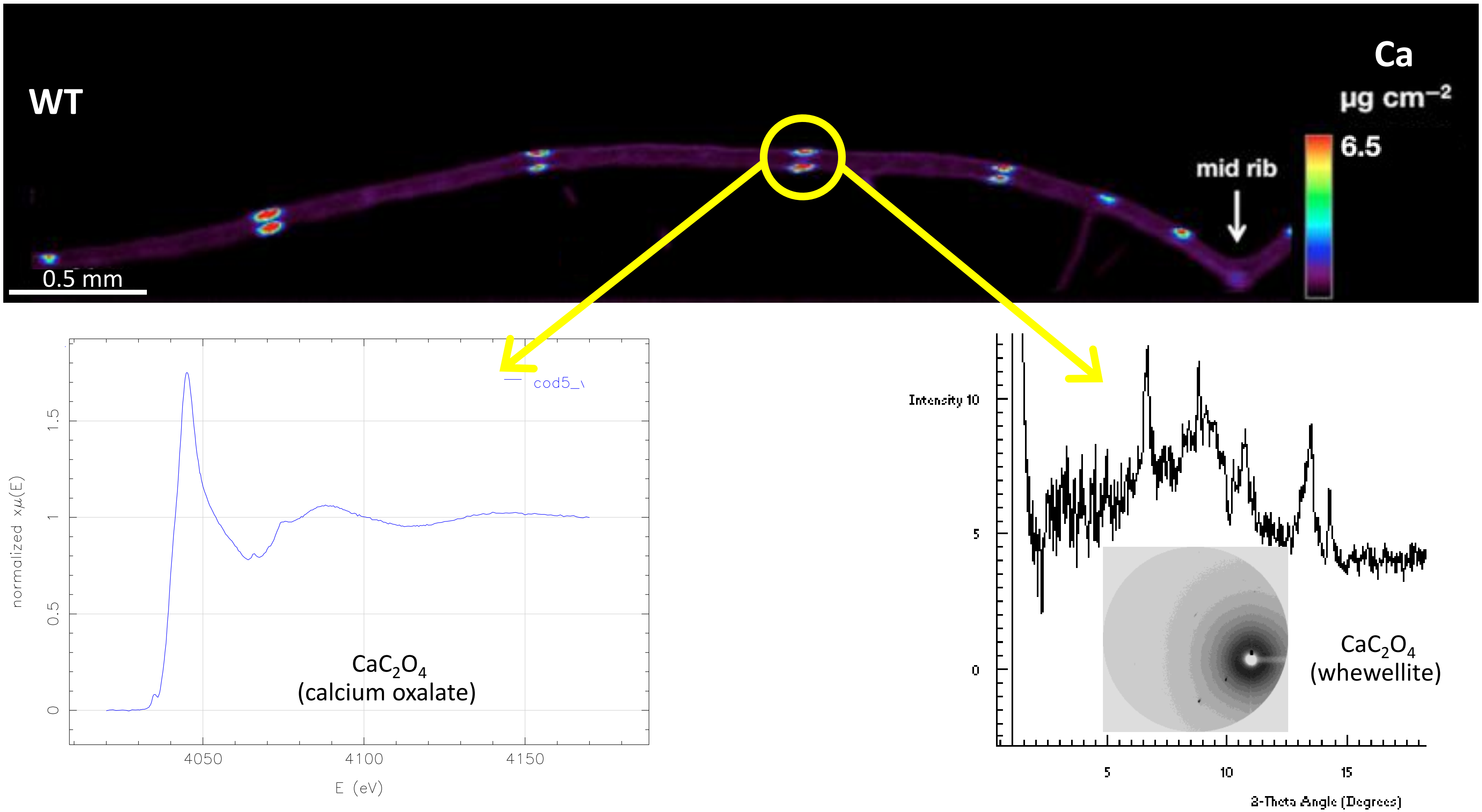

- XANES and XRD reveal Ca-oxalate (whewellite) in hotspots

Punshon, T., R. Tappero, F.K. Ricachenevsky, K. Hirschi, and P.A. Nakata. 2014. The Plant Journal 76:627-633.

Biofortification Effort- Alfalfa

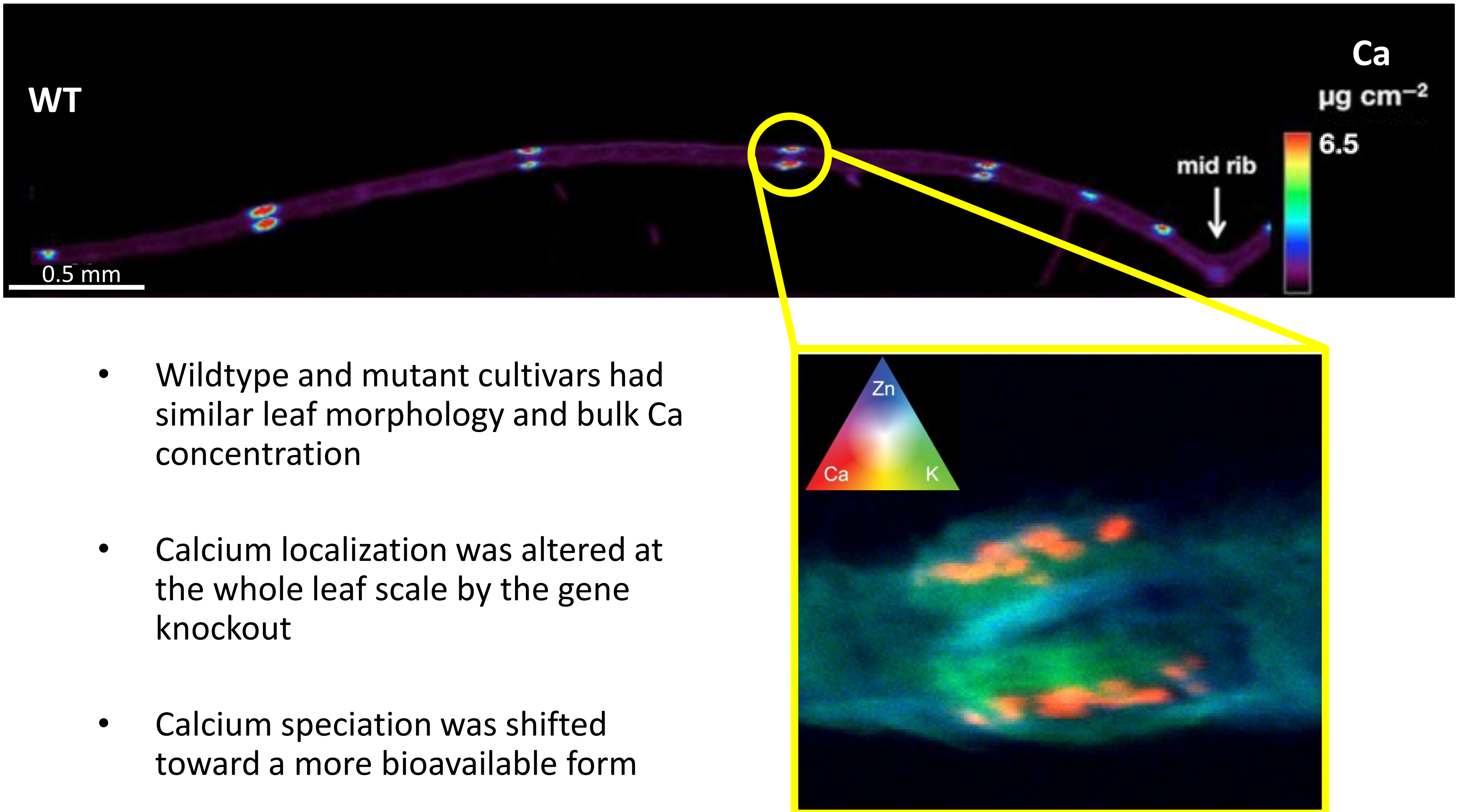

- Wildtype and mutant cultivars had similar leaf morphology and bulk Ca concentration
- Calcium localization was altered at the whole leaf scale by the gene knockout
- Calcium speciation was shifted toward a more bioavailable form

Punshon, T., R. Tappero, F.K. Ricachenevsky, K. Hirschi, and P.A. Nakata. 2014. The Plant Journal 76:627-633.

(Eco)toxicology of Cr- Mouse

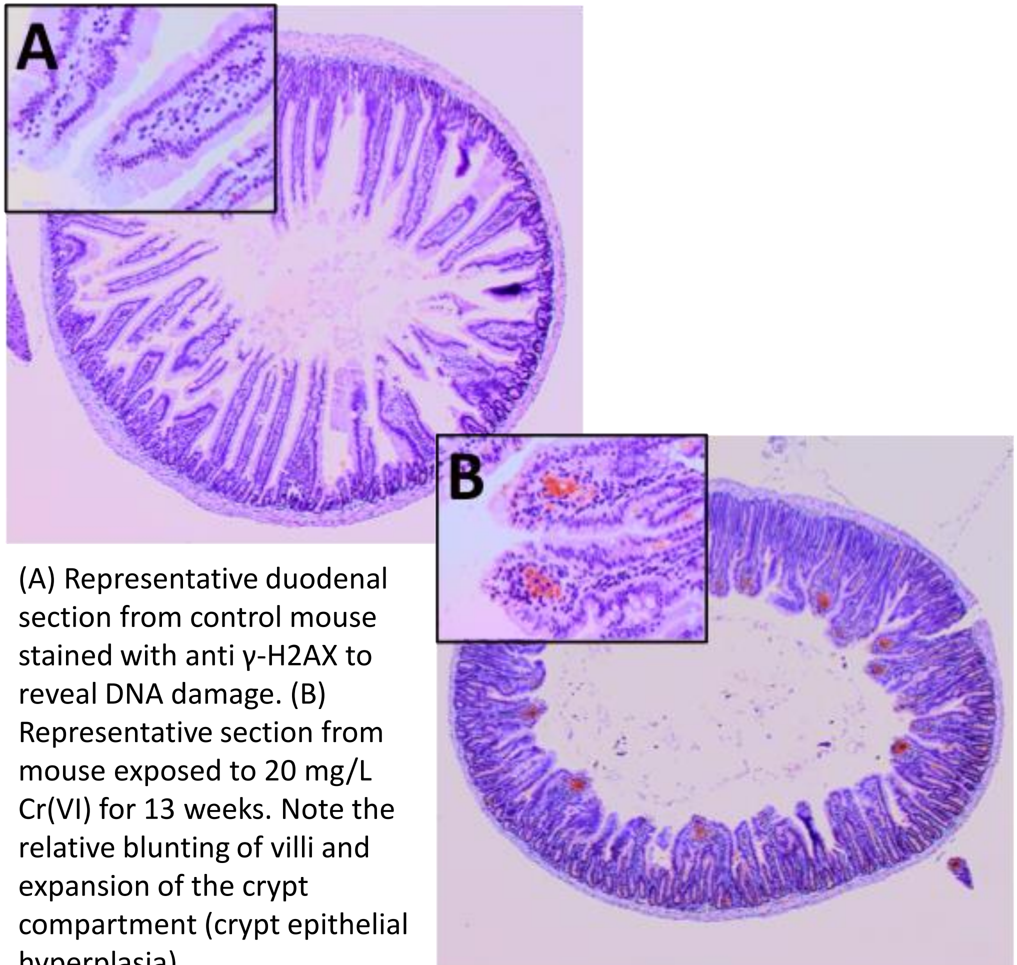

(A) Representative duodenal section from control mouse stained with anti γ-H2AX to reveal DNA damage. (B) Representative section from mouse exposed to 20 mg/L Cr(VI) for 13 weeks. Note the relative blunting of villi and expansion of the crypt compartment (crypt epithelial hyperplasia)

- Mice develop duodenal tumors upon chronic exposure (20 mg/L) of hexavalent chromium
- Critical to identify the mode of action (MOA) underlying the development of Cr(VI)-induced intestinal cancers
- At a super-micron X-ray probe, quantitative XRF and XAS were used to understand mechanisms of Cr toxicity in mouse model

Seiter, J., R. Tappero, C.M. Thompson et al.,. 2015. Toxicological Science (in review).

(Eco)toxicology of Cr- Mouse

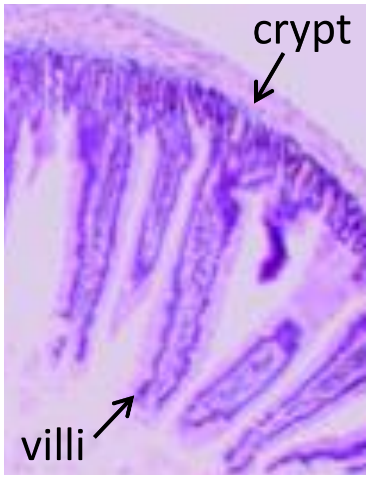

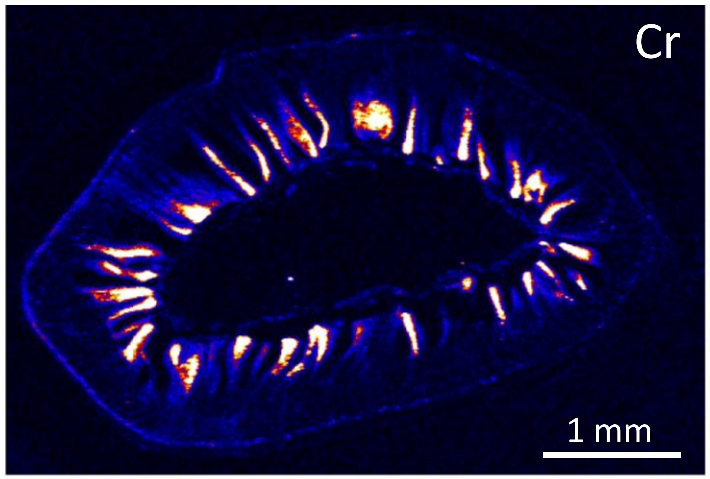

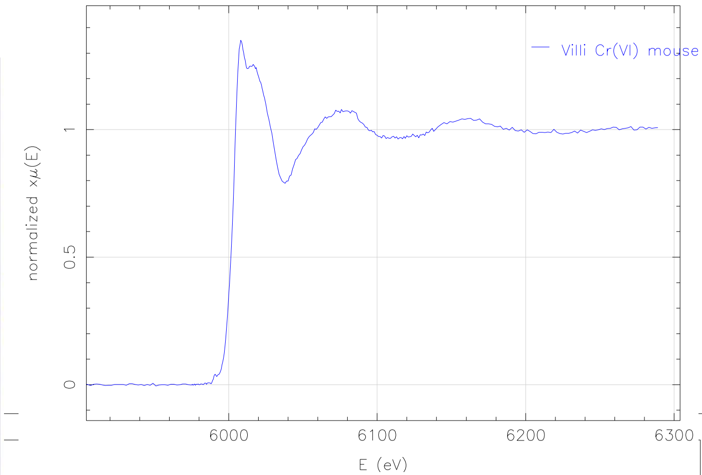

- Chromium accumulation up to 100 µg/g was observed in the duodenal villi, as trivalent Cr(III)
- Chromium did not accumulate in the duodenal crypts; crypt compartment is where stem cells reside

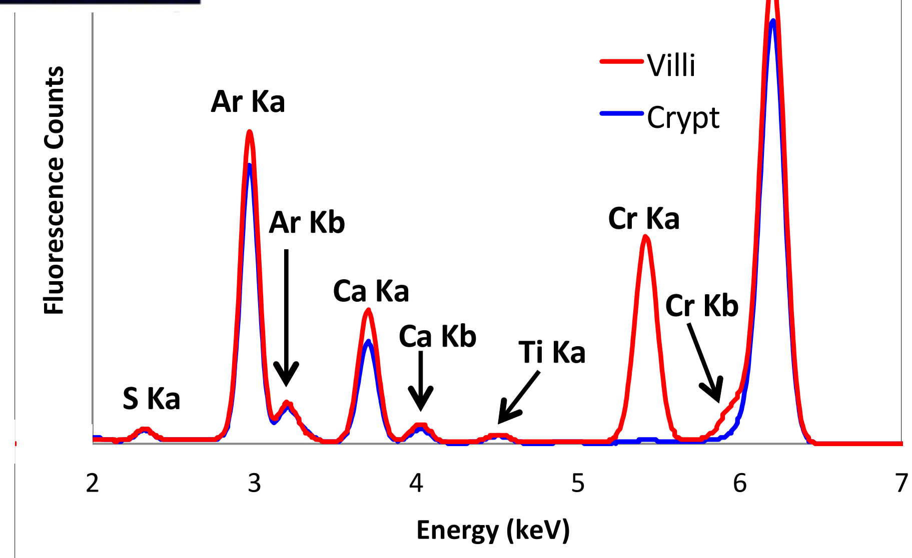

Seiter, J., R. Tappero, C.M. Thompson et al.,. 2015. Toxicological Science (in review).

(Eco)toxicology of Cr- Mouse

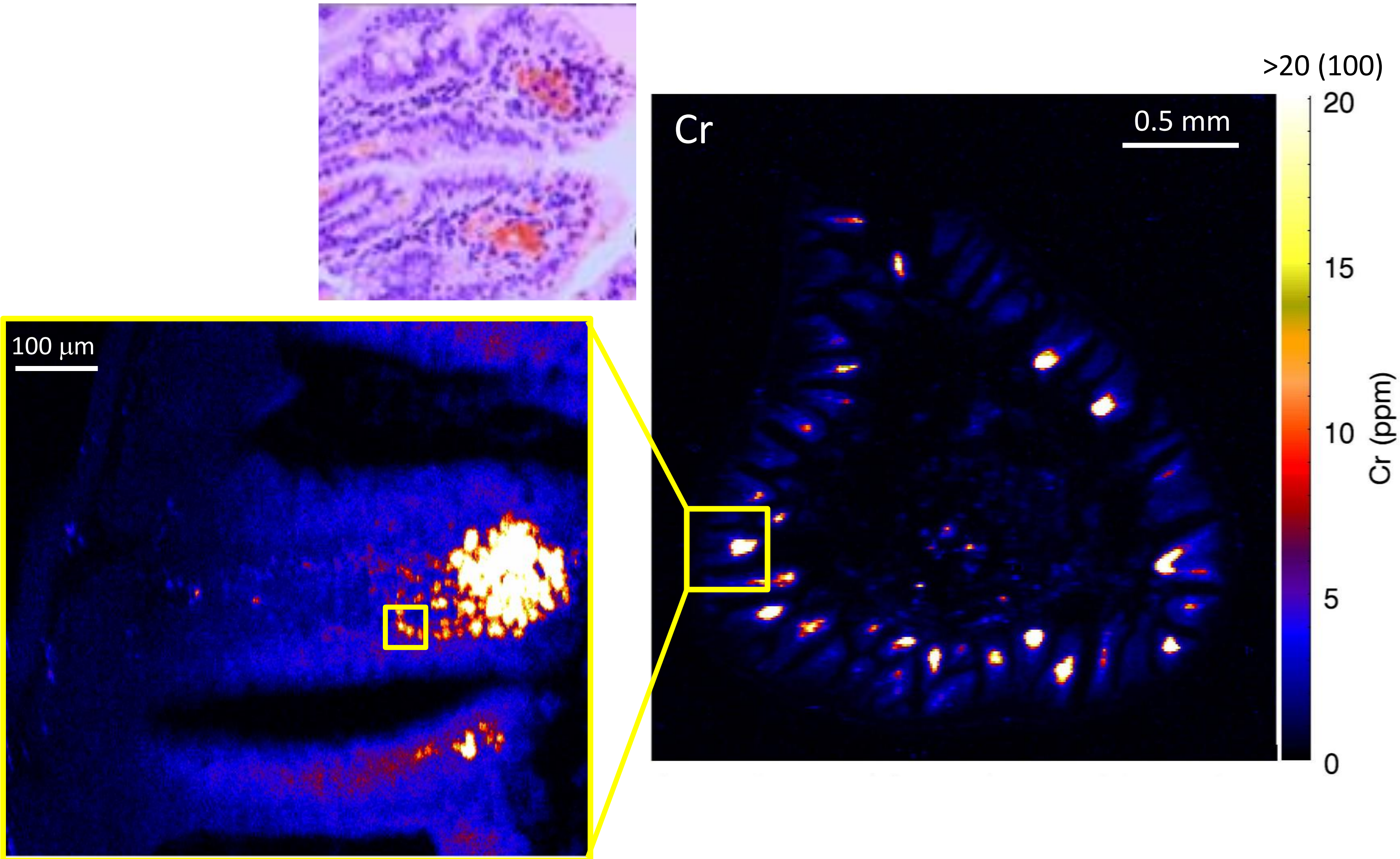

Seiter, J., R. Tappero, C.M. Thompson et al.,. 2015. ES&T (in review).

Cr chemistry in Chondritic Meteorite

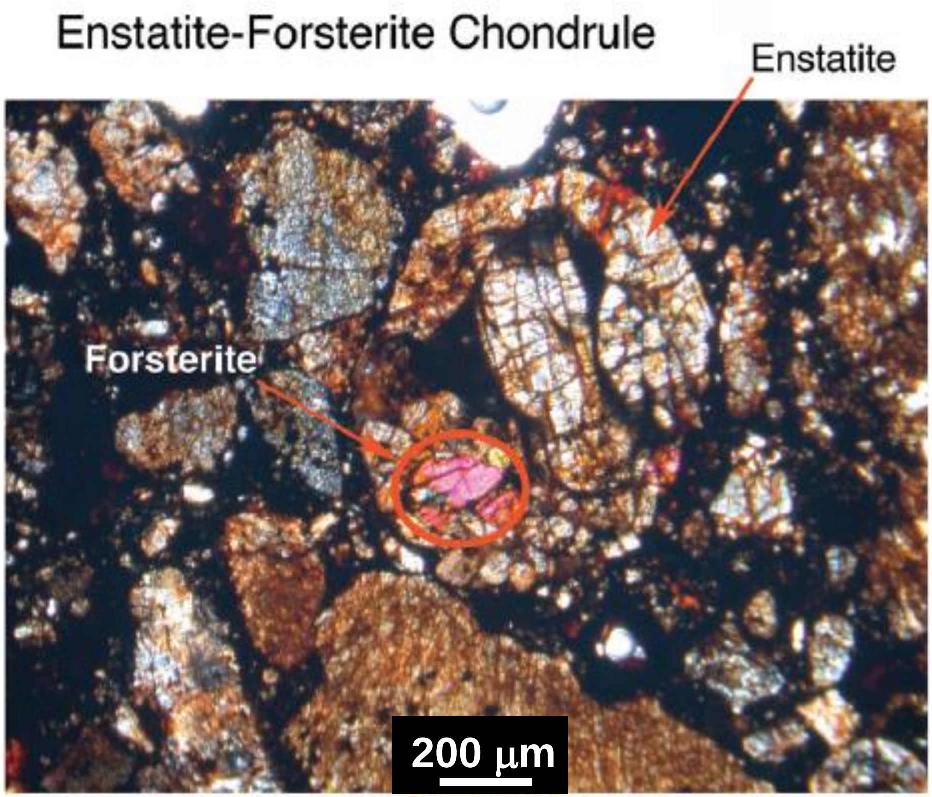

Photo-micrograph under cross-polarized transmitted light of meteorite MAC 88136 featuring a forsterite-enstatite chondrule.

- Understanding Cr valence states can shed light on the f_{O2} conditions of formation in meteorites
- Sample was a petrographic thin section with 50 – 200 micron size forsterite grains with ~0.13 wt% Cr.
- At a super-micron resolution X-ray probe, XANES and EXAFS were used to characterize Cr chemistry in forsterite-enstatite chondrule

McKeown, D.A., A.C. Buechele, R. Tappero, T.J. McCoy, and K.G. Gardner-Vandy. 2014. American Mineralogist 99:190-197.

Cr chemistry in Chondritic Meteorite

XANES: highly reduced Cr^{2+} species

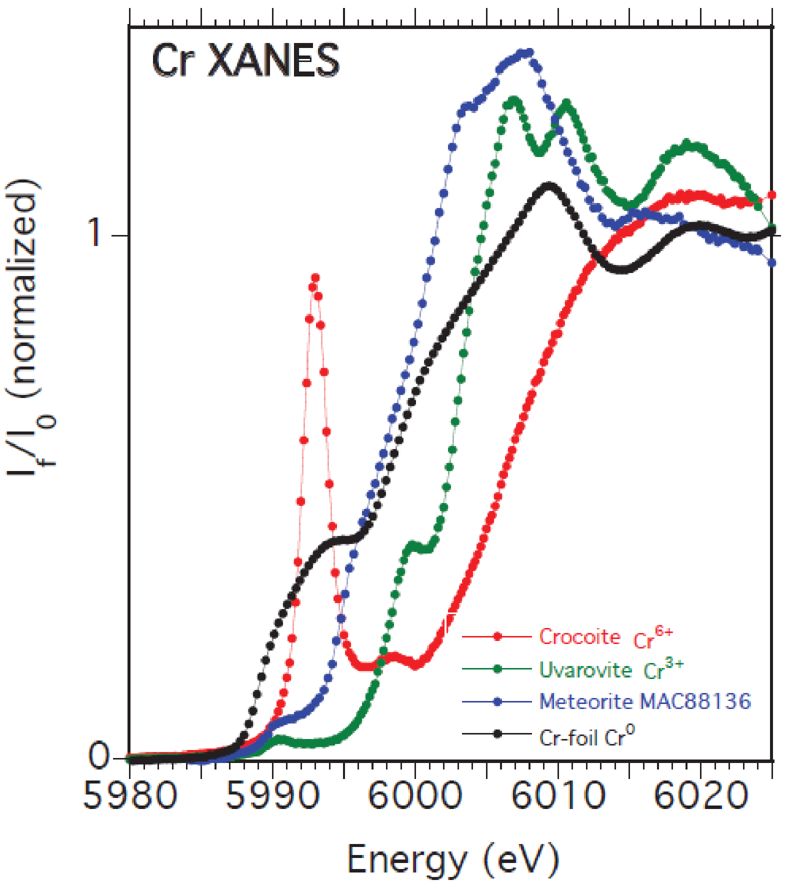

EXAFS: Cr^{2+} substituting for Mg^{2+} in the forsterite M(1) site

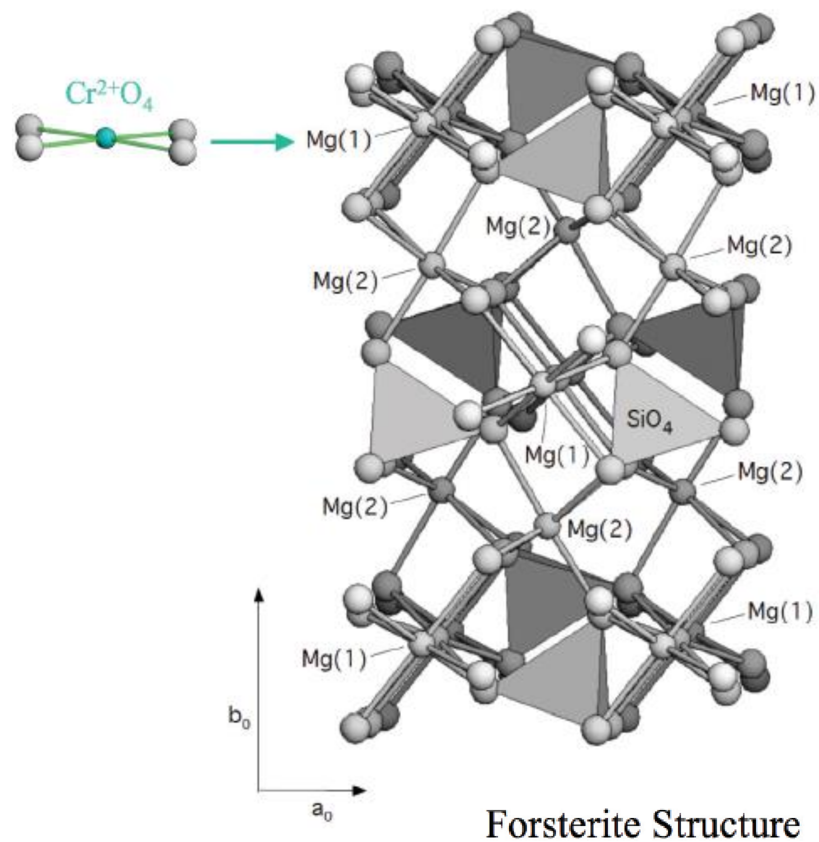

McKeown, D.A., A.C. Buechele, R. Tappero, T.J. McCoy, and K.G. Gardner-Vandy. 2014. American Mineralogist 99:190-197.

Chemistry of Depleted Uranium (DU) in Military Firing Range Soils

- DU munitions have been used by the US Army since the 1950's
- DU has been fired on military firing ranges all across the USA (Yuma, Aberdeen, Hawaii)
- Materials to replace DU in these rounds have been unsuccessful
- Current interest in cleanup and potential continued use – aim was to <u>characterize DU weathering products</u>

DU penetrator rods

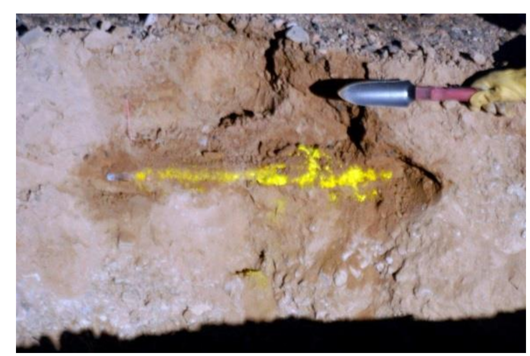

Lafferty, Seiter et al. (USACE)

Chemistry of Depleted Uranium (DU) in Military Firing Range Soils

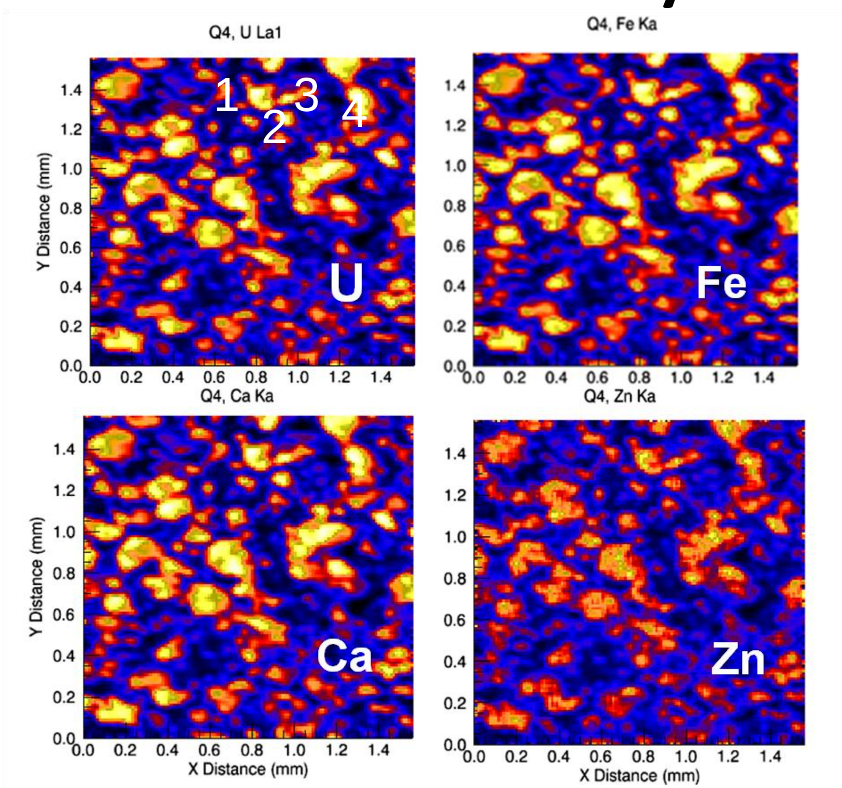

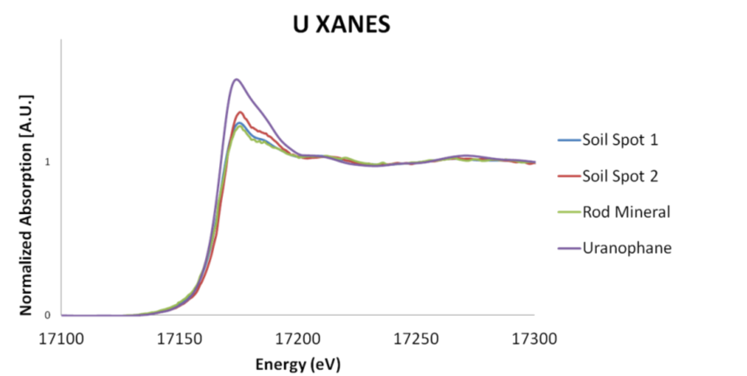

XANES spectra of the surface rod minerals, U(IV) Standard – Uranophane, and patterns for spots 1 and 2 from the maps at left

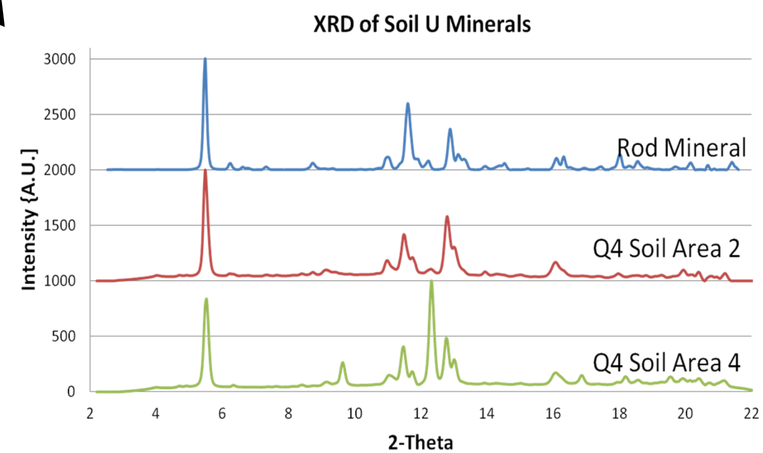

XRD patterns of the surface rod minerals (Bequerelite) and patterns for spots 2 and 4

- U found in the soil and around the rods is a mix of U(IV) and U(VI)
- A number of U minerals identified in soil and greater variety in the soils closely surrounding the rods

Chemistry of Depleted Uranium (DU) in Military Firing Range Soils

- DU penetration rods weather in arid environments
- U will migrate to some extent in soil in arid environments
- U species identified through XRD indicate that soil chemistry will influence U mineral formation
- High levels of Ca in the DU garden soils encouraged the formation of Becquerelite ($Ca(UO_2)_6O_4(OH)_6 \cdot 8(H_2O)$)

Ionomics study: Iron homeostasis in plants

- **XFM** is well-suited for evaluation of how specific genes influence the uptake of nutrients and contaminants in plants
- fCMT (3D XRF) provides non-destructive, three dimensional characterization of elemental distribution in plants *in vivo*.
- fCMT images of knockout and WT *Arabidopsis* seed confirmed localization of Fe requires vacuolar membrane transporter VIT1.

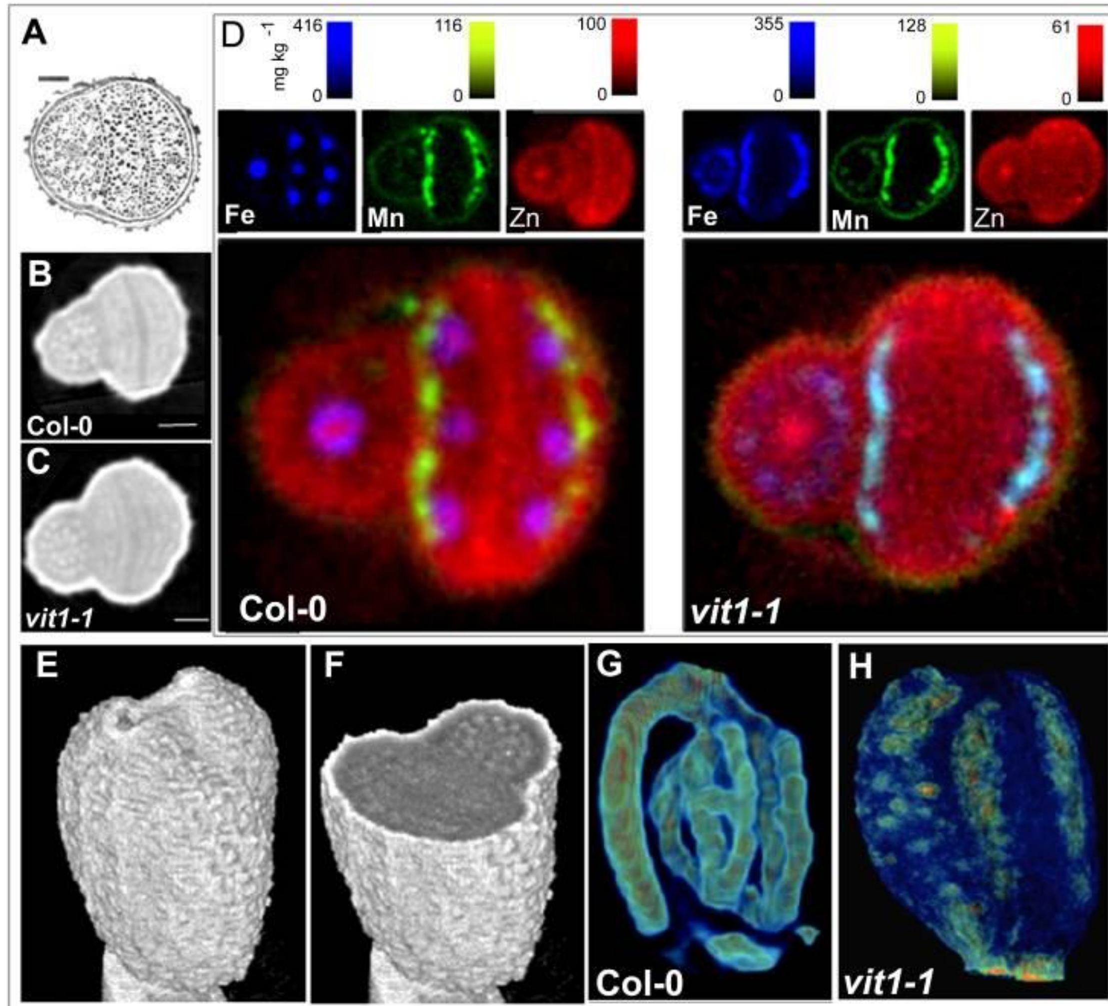

Kim, S.A., T. Punshon, A. Lanzirotti, L. Li, J.M. Alonso, J.R. Ecker, J. Kaplan, and M.L. Guerinot. 2005. Science 314:1295-1298.

Ionomics study: Iron homeostasis in plants

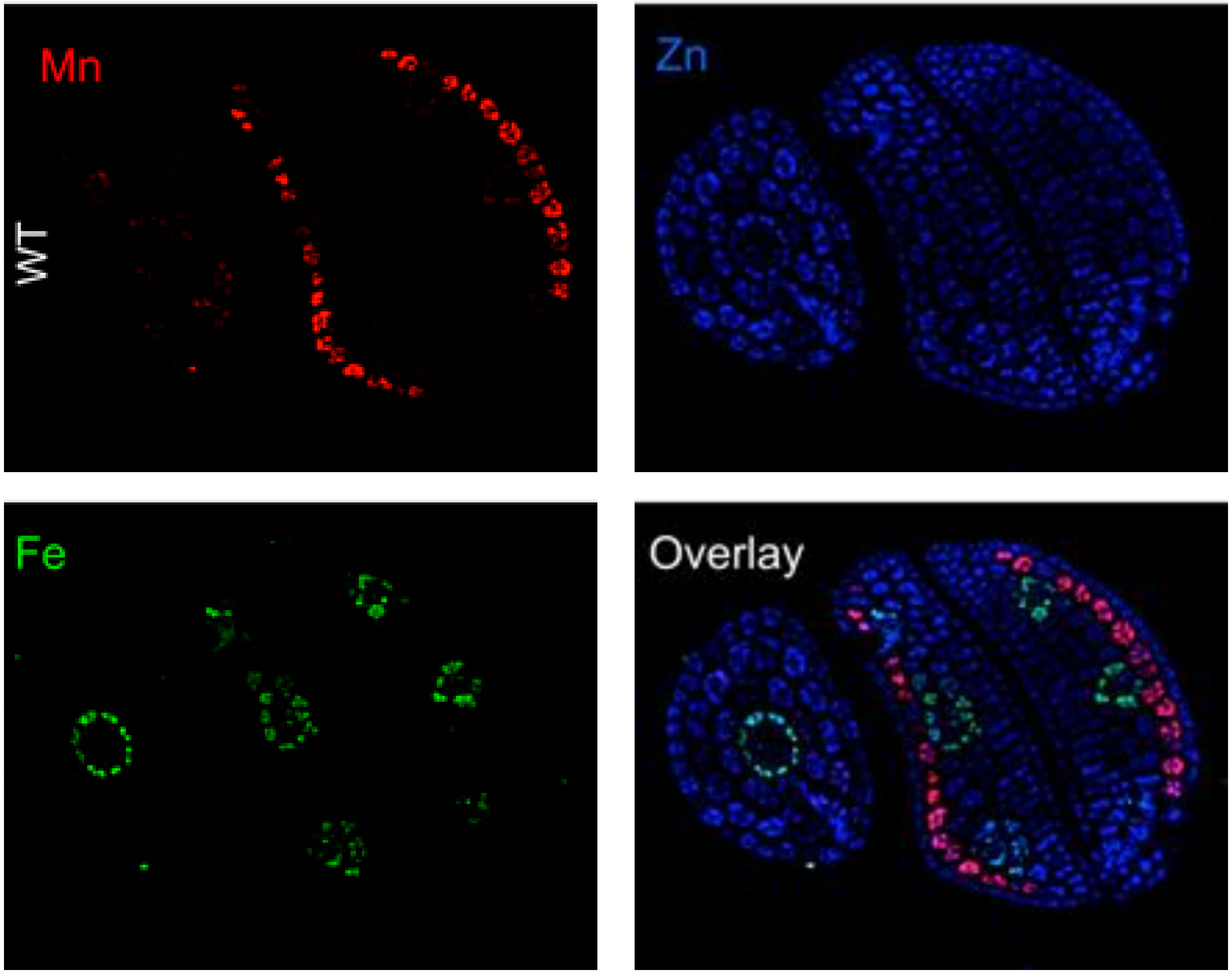

…Pushing to higher detection sensitivity and to better spatial and temporal resolution!

Punshon et al., 2012

Trace Element Chemistry in Diatoms

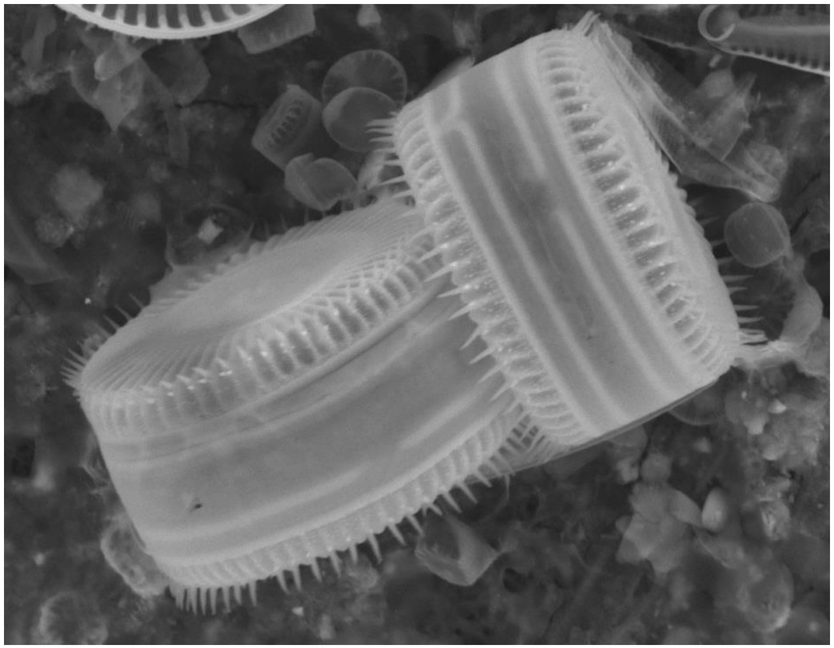

Cyclotella meneghiniana (diatom)

…and pushing to 3-D!

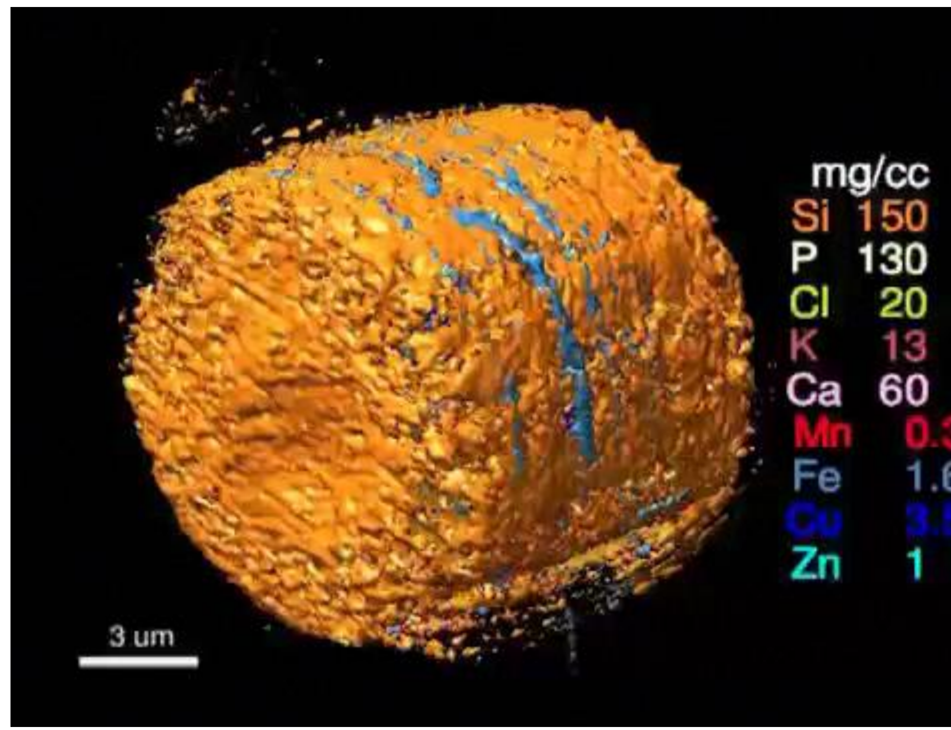

X-ray Fluorescence Microtomography (fCMT)

deJonge et al., 2010

Conclusions

- Synchrotron radiation sources are ideal for developing tunable, high-intensity, highly-focused X-ray fluorescence microscopes
- Useful for characterizing the speciation, transport, and reactions of chemical species in biological and inorganic systems
- No chemical pretreatment required, samples can be analyzed in an ‘as collected’ state.
- Detection sensitivities in the attogram range and spatial resolutions less than 50 nanometers

So in other words, we're hoping to discover what makes the nitty, gritty.

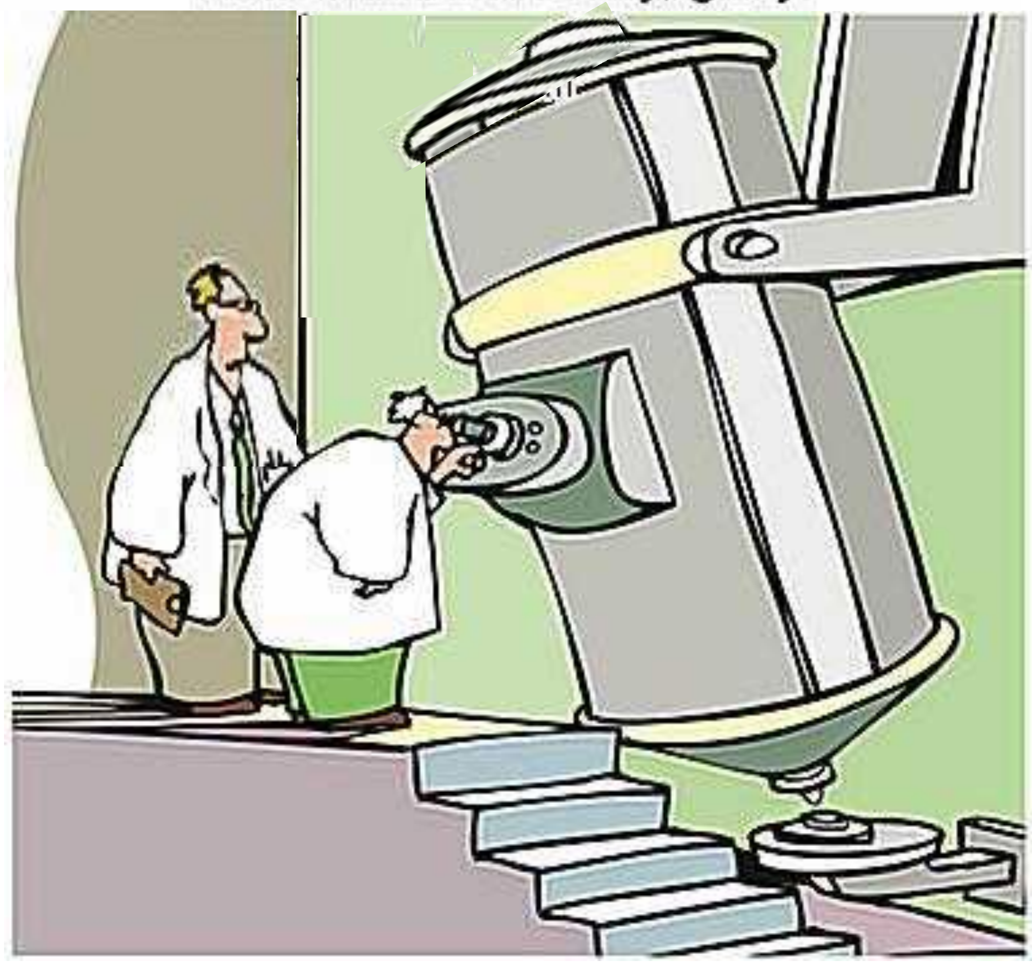

Thank you for your attention